AD NUMBER

AD432024

LIMITATION CHANGES

TO:

Approved for public release; distribution is unlimited.

FROM:

**Distribution authorized to U.S. Gov't. agencies and their contractors;
Administrative/Operational Use; JAN 1964. Other requests shall be referred to Aeronautical Systems Div., Wright-Patterson AFB, OH 45433.**

AUTHORITY

AFFDL ltr 2 May 1979

ASD-TDR-63-783

THERMAL STRESS DETERMINATION TECHNIQUES FOR SUPERSONIC TRANSPORT AIRCRAFT STRUCTURES

PART III - COMPUTER PROGRAMS FOR BEAM, PLATE, AND CYLINDRICAL SHELL ANALYSIS

TECHNICAL DOCUMENTARY REPORT NO. ASD-TDR-63-783, PART III

JANUARY 1964

Supersonic Transport Research Program
Sponsored by the
Federal Aviation Agency

Jointly Directed by: ASD, FAA and NASA

Flight Dynamics Laboratory
Aeronautical Systems Division
Air Force Systems Command
Wright-Patterson Air Force Base, Ohio

(Prepared under Contract AF33(657)-8936 by
R. H. Gallagher, J. Padlog and R. D. Huff of
Textron's Bell Aerosystems Company, Buffalo,
New York)

NOTICES

The information contained herein is a part of a national undertaking sponsored by the Federal Aviation Agency with administrative and technical support provided by the Department of Defense, Aeronautical Systems Division, Air Force Systems Command with contributing basic research and technical support provided by the National Aeronautics and Space Administration.

When Government drawings, specifications, or other data are used for any purpose other than in connection with a definitely related Government procurement operation, the United States Government thereby incurs no responsibility nor any obligation whatsoever; and the fact that the Government may have formulated furnished, or in any way supplied the said drawings, specifications, or other data, is not to be regarded by implication or otherwise as in any manner licensing the holder or any other person or corporation, or conveying any rights or permission to manufacture, use, or sell any patented invention that may in any way be related thereto.

Copies have been placed in the DDC collection. U.S. Government agencies may obtain copies from DDC. Other qualified DDC users may request through:

Office of the Deputy Administrator
for Supersonic Transport Development
Federal Aviation Agency
17th Street N.W. and Constitution Avenue
Washington 25, D.C.

DDC release to OTS not authorized.

This report must not be cited, abstracted, reprinted, or given further distribution without written approval of the above-named controlling office.

Copies of this report should not be returned to the Research and Technology Division, Wright-Patterson Air Force Base, Ohio, unless return is required by security considerations, contractual obligations, or notice on a specific document.

FOREWORD

This report was prepared by Textron's Bell Aerosystems Company, Buffalo, New York, under Contract AF33(657)-8936. The work was administered under the direction of the Flight Dynamics Laboratory, Aeronautical Systems Division, by Mr. G.E. Maddux, Project Engineer. The work was performed by the Structures Section of the Aerospace Engineering Department, Bell Aerosystems Company in the period of 15 June 1962 to 31 July 1963. Mr. Richard H. Gallagher was Technical Director of the study.

The authors wish to acknowledge, with deep appreciation, the efforts of Misses Beverly Dale and Monica Ostanski, members of the Bell Electronic Data Processing Department, who were responsible for the entire task of coding the computer programs described in this report. They are also appreciative of the cooperation given to these efforts by Mr. Raymond E. Carroll, Manager of Electronic Data Processing, and by Mr. Paul E. Murray, Supervisor, Technical Programming. Acknowledgement is due Mr. Walter A. Luberacki, who supervised checking out of the coded programs.

ABSTRACT

This report describes computer programs developed for the analysis of heated beams, plates, and stiffened cylindrical shells. The matrix displacement approach to structural analysis, which forms the theoretical basis of these programs, is developed in detail. Derivation of new relationships employed in these programs is also detailed. The capabilities and limitations of the respective programs are outlined and illustrative applications are presented.

PUBLICATION REVIEW

This report has been reviewed and is approved.

W. A. SLOAN, JR.
Colonel, USAF
Chief, Structures Division
Air Force Flight Dynamics Laboratory

TABLE OF CONTENTS

TABLE OF CONTENTS (CONT)

LIST OF ILLUSTRATIONS

LIST OF ILLUSTRATIONS (CONT)

LIST OF SYMBOLS

A	Cross-sectional area, $in.^2$
a_i	Arbitrary constant in an assumed stress or displacement function
B	Material behavior parameter in steady state creep law
b, d	Length dimension, in.
c	Buckling coefficient
D_X, D_Y, D_X, D_Q	Flexural and shear rigidities for orthotropic plates
E, E_X, E_Y	Modulus of Elasticity, $lb/in.^2$
e	Base of Natural Logarithms (2.718. . . . .)
F	Internal direct force, lb
G, G_X, G_Y	Modulus of rigidity, $lb/in.^2$
h	Plate thickness, in.
I	Area moment of inertia, $in.^4$
K	Stiffness coefficient for a complete structure, lb/in.
k	Element stiffness coefficient, lb/in.
L	Length dimension, in.
M	Externally applied bending moment, in. lb
M^{α}	Net thermal moment at a joint, in. lb
$\overline{M}$	Element (internal) node point bending moment, in. lb
$\overline{M}^{\alpha}$	Element net thermal moment at a node point, in. lb
M'	Bending moment per lineal inch, in. lb
$M^{\alpha'}$	Thermal moment per lineal inch, in. lb
m	Material behavior parameter in steady state creep law
N	Number of node points
N_X, N_Y, N_{XY}	Midplane direct forces, per inch, lb/in.
n	Material behavior parameter in stress-strain law for time-independent plastic strain
P	External direct force, lb
P_E	Euler critical load, lb

Q_X, Q_Y	Internal shear force per lineal inch, lb/in.
q	Shear load, lb/in.
T	Temperature change from the stress-free state, °F
t	Time, sec
u, v, w	Components of displacement in the x-, y-, and z-directions, in.
U	Strain energy, in. lb
V	Volume, $in.^3$
W	Work, in. lb
X, Y, Z	Rectangular coordinates
α	Coefficient of thermal expansion, in./in. °F
β	Material behavior parameter in steady state creep law
γ	Shear strain, rad/rad
Δ	Displacement, in.
ϵ	Direct strain, in./in.
θ	Angular displacement, rad
λ	Eigenvalue
μ	Poisson's ratio
ξ	"Local" coordinate, in.
σ	Direct stress, $lb/in.^2$
τ	Shear stress, $lb/in.^2$
ζ	Restraint coefficient, lb/in.
ψ	Material behavior parameter in stress-strain law for time independent plastic strain
ω	Material behavior parameter in steady state creep law

CHAPTER I

INTRODUCTION

The "Study of Thermal Stress Determination Techniques for Supersonic Transport Aircraft Structures" has consisted of three relatively independent efforts, directed towards the development of

(1) An annotated bibliography of literature pertinent to thermal stress analysis and related topics.

(2) Parametrically-presented design data for heated sandwich panels and cylinders.

(3) Three FORTRAN-coded computer programs for the solution of heated beam, plate, and cylindrical shell problems.

Items (1) and (2) are presented in references (1) and (2), respectively. A portion of item (3), in the form of a verbal description of the coded computer programs, is presented in this report.

Each of the three programs described in the present report is based on the "matrix displacement" or "stiffness" method for the analysis of structures which are idealized as systems of connected discrete elements. Programs described in the present report are available to participants in structural design activities related to the Supersonic Transport (SST) and to all others who are designated as being eligible by the Flight Dynamics Laboratory, Aeronautical Systems Division, USAF. The programs will be transmitted to eligible recipients by the latter agency. A transmitted program consists of punched cards, listings, detailed instructions with respect to input and output, and other information needed to make the program operative at a facility that will accept a program coded in conformity with the FORTRAN II Monitor System.

Many references have detailed the basis of the displacement method as it applies to the linear analysis of unheated elastic structures. (See, for example, references 3, 4, or 5). Phenomena which are not often considered in routine structural analysis are treated by the subject programs, however, and the approach to the analysis of these special phenomena by the matrix displacement method has not been described in any single reference. Hence, in the next chapter, the method is developed from fundamental principles and to an extent that includes all pertinent special phenomena, such as instability, thermal stress, and inelastic behavior.

The accuracy and efficiency of any solution performed by use of any computer program for matrix structural analysis is largely dependent upon the suitability of discrete element force-displacement equations employed. The techniques used in derivation of the element force-displacement equations contained in the subject

Manuscript released by authors in Jan. 1964 for publication as an ASD Technical Documentary Report.

programs are not well known and some of these techniques have, in fact, been formulated specifically for the requirements of this study. Consequently, in Chapter III a complete and detailed development of the techniques is presented. Chapter III also demonstrates how the techniques were applied to the derivation of element relationships appearing in the respective computer programs.

The three coded programs are as follows:

1. A program for the analysis of one-dimensional structural components.
2. A program for the analysis of flat plates,
3. A program for cylinder analysis.

Program (1) is described in Chapter IV. The objective of this program is to permit analyses of beam-type structures, i.e., structures whose cross-sectional dimensions are small with respect to their length and whose behavior is governed by the elementary concepts of beam flexure.

It often proves feasible in the analysis of airframes to isolate portions of major components and treat these as one-dimensional elements; i.e., as beams or beam-columns. The most common examples in modern constructional forms are spar caps, stringers, and longerons, but such idealizations may also be admissable in connection with trussed internal members (spars, ribs) and control surfaces. The objectives of the program described herein pertain to these types of elements.

With this program it is possible to analyze beams of nonuniform section over many supports for thermal stress, inelastic behavior, instability and other types of structural behavior. Chapter IV provides a detailed picture of these capabilities and also presents illustrative examples. Certain of the examples involve simple conditions with known solutions; these are performed to demonstrate the accuracy of the program. Another example, for which there is no complete alternative solution, is performed to demonstrate the capability of the program to deal with complex conditions.

Descriptions of Programs (2) and (3), which are presented in Chapters V and VI, are patterned after the description of Program (1). Program (2) is capable of performing analyses of irregularly shaped stiffened plates of nonuniform thicknesses for stresses and displacements due to applied loads, temperature gradients, and time-independent inelastic behavior, and for the prediction of buckling stresses. The use of the discrete element approach, rather than design charts, may be necessary even for isotropic rectangular plates of constant thickness where the temperature profile (and therefore the resulting stress distribution) is of a highly irregular form. Also, if the loadings on the plate have been developed through a matrix structural analysis, wherein the plate was employed as a single discrete element in a major component of the airframe (e.g., a wing or fuselage), the edge loadings will in general be nonuniform and it again may be desirable to utilize the

discrete element approach in the prediction of instability. The program is, of course, not limited in applicability to skin panels; it is directly useful for analyses of all types of planar structures -- stiffened bulkheads, plane trusses, beam grid-works, etc.

Program (3), the cylinder analysis program, can be employed to predict the stresses and displacements for heated cylindrical shells. The structure analyzed with this program need not be perfectly cylindrical. They may possess orthotropic skins and can be ring and longitudinally-stiffened. The temperature dependence of material properties can be taken into account.

CHAPTER II

PERTINENT CONCEPTS OF THE MATRIX DISPLACEMENT METHOD

A. GENERAL THEORY FOR LINEAR ELASTIC UNHEATED SYSTEMS

Most treatments of the displacement approach to the analysis of discrete element systems make extensive use of matrix notation and the concepts of matrix algebra. Matrices present an especially concise and convenient means of expressing algebraic procedures and are, in addition, the natural mathematical language of the digital computer. Because of this widespread use of matrix notation in the formulation of structural analysis programs, the topic of present interest is often referred to as "matrix structural analysis". For simplicity, the initial portion of the following development of the displacement method will be presented in detailed algebraic form; then, the formulation will be summarized with use of matrix algebra.

As already noted, this report is concerned with applications based on discrete element idealizations of the structures to be analyzed. Such discrete elements are usually defined by boundary or corner points which are sufficient in number to characterize the stress and deformational behavior of the element. A hypothetical discrete element, with four boundary points, is sketched below. For convenience, this section deals with relationships in two dimensions; in all cases, however, the approach to three-dimensional problems is readily apparent.

Relationships between the forces acting at the corner points and the displacements of the corner points are derived in detail in Chapter III. Generally, these relationships are first derived with reference to axes which are most convenient to the element itself. Then, by use of direction cosines, the relationsips are expressed as if the element were arbitrarily oriented in the complete structure. When this transformation has been accomplished, the equation for one of the forces shown in the sketch below, F_{x3} for example, would have the form

$$F_{x3} = k_{(x3)(u1)}\ u_1 + k_{(x3)(u2)}\ u_2 + \cdots\cdots\cdots\cdots k_{(x3)(v4)}\ v_4 \qquad \text{(II-1)}$$

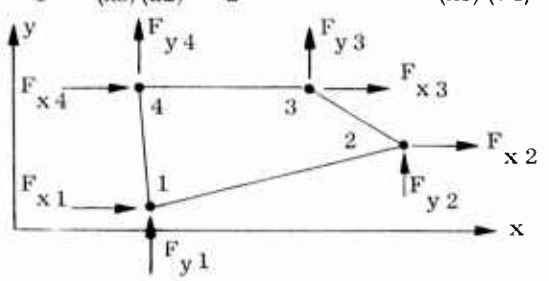

The coefficients $k_{(i)(j)}$ are functions of the geometry and material properties of the element and are known as element stiffness coefficients. In terms of physical meaning, a stiffness coefficient k_{ij} is the force at i necessary to produce a unit displacement of the degree of freedom j. The corner point forces may either be actual concentrated forces or the static equivalent of stresses acting upon the area subtended by the point; normally, they are the latter.

A complete set of force-displacement relationships for an element with n node points in two dimensions will appear as:

$$
\begin{aligned}
F_{(x1)} &= k_{(x1)(u1)}\, u_1 + \ldots . k_{(xl)\ (un)}\, u_n + k_{(x1)(v1)}\, v_2 + \ldots . k_{(x1)(vn)}\, v_n \\
F_{(xn)} &= k_{(xn)(u1)}\, u_1 + \ldots . k \qquad + k \qquad + \ldots . k \\
F_{(y1)} &= k_{(y1)(u1)}\, u_1 + \ldots . k \qquad + k \qquad + \ldots . k \qquad \text{(II-2)} \\
F_{(yn)} &= k_{(yn)(u1)}\, u_1 + \ldots . k \qquad + k \qquad + \ldots . k
\end{aligned}
$$

All degrees of freedom at the boundary points appear in Equation (II-2), i.e., the element is not fixed against displacement as a rigid body.

Once the element force-displacement relationships (Equation II-2) have been numerically evaluated for each element of the structure, they can be algebraically combined in a manner dictated by the requirements of juncture point equilibrium and compatibility. These operations produce a set of force-displacement equations for the element juncture points of the assembled structure. To illustrate how this is accomplished, consider the development of the force-displacement equation at point i in the x-direction in the assembled analytical model sketched below.

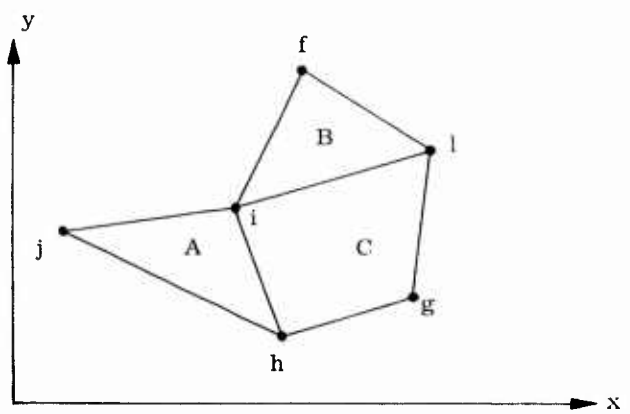

The theoretical basis for the establishment of the desired relationships is the explicit requirement of juncture point equilibrium. This condition states that the applied load (P_{xi}) is equal to the sum of the internal forces acting upon the respective elements common to the point

$$P_{xi} = F_{xi}^{A} + F_{xi}^{B} + F_{xi}^{C} \qquad \text{(II-3)}$$

where F_{xi}^{A} is the x-direction (internal) force on element A, etc. The force-displacement equations for each of the elements will have been previously evaluated so that expressions for F_{xi}^{A}, etc. in terms of the displacements are available. Substitution of these into Equation II-3 yields:

$$\begin{aligned} P_{xi} = {} & (k^{A}_{(xi)(uj)} u_j + \ldots\ldots\ldots\ldots k^{A}_{(xi)(ui)} u_i + \ldots.) \\ & + (k^{B}_{(xi)(uf)} u_f + \ldots\ldots\ldots\ldots k^{B}_{(xi)(ui)} u_i + \ldots) \\ & + (k^{C}_{(xi)(ug)} u_g + \ldots\ldots\ldots\ldots k^{C}_{(xi)(ui)} u_i + \ldots) \end{aligned} \qquad \text{(II-3a)}$$

and, since the displacement u_i is the same for A, B, and C at point i (the condition of compatibility) we have:

$$P_{xi} = k^{A}_{(xi)(uj)} u_j + \ldots. (k^{A}_{(xi)(ui)} + k^{B}_{(xi)(ui)} + k^{C}_{(xi)(ui)}) u_i + \ldots \qquad \text{(II-3b)}$$

This is the final form of the desired equation.

It is important to note that each of the three elements meeting at the indicated juncture point possess stiffness coefficients with common subscripts (e.g. $k^{A}_{(xi)(ui)}$, $k^{B}_{(xi)(ui)}$). These correspond to the common juncture of certain points on the element. Point i is of course a common juncture of all three elements, but two elements also meet at points h and l. Some coefficients associated with an element will not have a counterpart coefficient in the relationships for the other elements. These will pertain to points such as g, f, and j which are connected to only one of the elements meeting at i.

In view of the above reasoning, the following "automatic" approach to calculating the applied load-versus-displacement equations for the complete structure suggests itself:

(1) Each element stiffness coefficient is assigned a double subscript--the first is the force to which it is equated and the second is the displacement it multiplies.

(2) Provision is made for an equation for each force in every degree of freedom in the complete system, and for the possibility that each force will be related to every displacement in the system. The result is a rectangular array of spaces, each designated by two subscripts--the first pertains to the force equation, the second to the displacement in question.

(3) The numerical formulation of the equations can begin with point 1 in the x-direction. First, a search is made through the list of elements, which are designated by their corner points. When an element is reached whose designation contains a 1, the F_{x1} equation is selected and each coefficient of the equation is placed in the space reserved for its second subscript (each of the first subscripts is, of course, x1).

(4) The procedure of item (3) is continued for point 1 in the x-direction until the list of elements is exhausted. Each time the stiffness coefficient from a subsequent element is placed in a location where a value has already been placed, it is added to that value. The only locations that will be occupied as a result of these operations are those relating to the point in question and points that exist on elements meeting at the point in question. Thus, if the structure is large with many element juncture points, there will be many zeros in each equation. This is an advantageous feature in terms of the effort needed to solve the complete set of equations.

(5) The process of steps (3) and (4) is repeated for all other points in the x-direction and then for each of the other directions. The result will be a complete set of equations for the entire structure, but with no recognition of support conditions.

(6) The support conditions are accounted for by first noting which displacements are zero and then removing the stiffness coefficients multiplying these displacements from the equations, resulting in more equations than unknowns. To provide for an equality of equations and unknowns the equations which pertain to the external loads (reactions) at the support points, are removed. The general solution to the remaining set of equations gives the displacement influence coefficients; multiplication of the general solution by specific values for the loadings yields specific values for the displacements.

(7) By substituting the displacement values back into the element force-displacement equations the internal forces acting on the element - the corner point forces - can be determined. These may require retransformation from "system" to "local" coordinates, and finally a transformation into stress (σ_x, σ_y, τ_{xy}, etc.).

B. MATRIX FORMULATION

The foregoing can now be reviewed in the interests of obtaining a matrix formulation and a clearer picture of the computer operations in a practical program. First, any complete set of element force-displacement relationships (Equation II-2) can be written in matrix notation as

$$\{F_e\} = [k] \{\Delta_e\} \qquad \text{(II-2a)}$$

where $[k]$, the "element stiffness matrix", is composed entirely of the element stiffness coefficients $k_{(x1)(ul)}$, etc. The subscript e denotes that the indicated quantities refer to the node points of the element.

Once the element relationships have been evaluated, the elements are assembled to form the complete analytical model of the structure by joining all elements at their respective juncture points and applying in the process the requirements of juncture point equilibrium and compatibility. Thus, the components of internal loads $\{F\}$ and external loads $\{P\}$ at each point are related by equilibrium requirements; i.e., $\Sigma F_x = P_x$, etc. The respective coordinate displacements of the corner points of all elements meeting at a point are equal, a requirement that satisfies compatibility. It follows that the stiffness matrix $[K]$ for the complete structure can be assembled by merely adding element stiffness coefficients having identical subscripts. This results in a set of equations:

$$\{P\} = [K] \{\Delta\} \qquad \text{(II-4a)}$$

The matrix $[K]$ will henceforth be referred to as the "master" stiffness matrix. Displacement boundary conditions can be readily imposed by assigning the pertinent Δ's their known values (usually zero). The matrix $[K]$ will be altered in the process, and, taking note of this by utilizing the subscript R, the solution to the altered Equation (II-4a) becomes (if matrix inversion is utilized).

$$\{\Delta_R\} = [K_R]^{-1} \{P_R\} = [\delta] \{P_R\} \qquad \text{(II-5)}$$

where $[\delta]$ represents the set of displacement influence coefficients.

The subject computer programs, in their present form, are restricted to the use of a matrix inversion procedure for the solution of Equation (II-5). One advantage of the use of matrix inversion is that the analysis for load conditions additional to the first is accomplished at small additional expense. Thus, the respective programs each allow the solution for many load conditions in one computational cycle when linear elastic analyses for applied load are attempted. It is to be recognized, however, that the direct solution of Equation II-5 (e.g., through Gaussian elimination procedures or by iterative techniques) may prove more advantageous under many circumstances. In such cases it is possible to replace

the inversion subroutine used in the program with whatever direct solution subroutine may be available.

To obtain the stresses from the displacement solution there can first be selected, from the total column of displacements, the displacement vectors for the respective elements $\left(\left\{\Delta_e\right\}\right)$. Then, each vector can be multiplied into the stiffness matrix (Equation II-2a) to determine the node point forces $\left(\left\{F_e\right\}\right)$ and in an additional step, the node point forces can be transformed into the corresponding stresses. It is believed to be more efficient, however, to form, at the outset, direct relationships between the element stresses and the node point displacements, as follows

$$\left\{\sigma_e\right\} = \left[S\right] \quad \left\{\Delta_e\right\} \tag{II-6}$$

where $\left\{\sigma_e\right\}$ are the stress values which describe the distribution of stress within an element and $\left[S\right]$ is known as the "element stress matrix". The procedure followed, therefore, is to establish first the stress matrices at the start of a computation. When the displacement vectors for the respective elements $\left(\left\{\Delta_e\right\}\right)$ are evaluated, they are premultiplied by the corresponding element stress matrices to obtain the solutions for stress.

C. INITIAL STRAIN PROBLEMS

Problems associated with thermal and plastic strain can be classed as "initial strain" problems since they can exist prior to the imposition (or, in the case of plasticity, reimposition) of applied load. If a discrete element is in the state of initial strain, the element force-displacement relationships take the following form

$$\left\{ F_e \right\} = \left[K \right] \left\{ \Delta_e \right\} - \left\{ F_e^i \right\} \tag{II-7}$$

where $\left\{ F_e^i \right\}$ signifies the system of "initial forces" at the element node points. Physically, these values represent the forces required to impose, at the node points, displacements which are equal and opposite to those accruing from the initial strains. In other words, they are the forces required to suppress the node point displacements due to initial strain. A procedure for the derivation of element initial forces will be presented in the next chapter.

Upon assembly of Equations (II-7) to form the master set of stiffness equations, and reduction in cognizance of boundary conditions, there is obtained

$$\left\{ P \right\} = \left[K \right] \left\{ \Delta \right\} - \left\{ P^i \right\} \tag{II-8}$$

where now the values $\left\{ P^i \right\}$ are the "net thermal forces at the node points. The solution to (II-8) is given by

$$\left\{ \Delta \right\} = \left[K \right]^{-1} \left\{ \left\{ P \right\} + \left\{ P^i \right\} \right\} \tag{II-9}$$

To obtain the solution for stress the adopted approach is to formulate stress-displacement equations, i.e. "element stress matrices". In the presence of initial strain these take the form

$$\left\{ \sigma_e \right\} = \left[S \right] \left\{ \Delta_e \right\} - \left\{ \sigma_e^i \right\} \tag{III-10}$$

where $\left\{ \sigma_e^i \right\}$ represents the stresses required to obviate the initial strains.

D. ELASTIC INSTABILITY ANALYSIS

The concepts of elastic instability pertain to conditions in prismatic or thin walled structures, where the behavior across the thickness can be subdivided into "flexural" and "midplane" behavior. By virtue of displacements normal to the midplane the midplane forces have components which tend to enhance these displacements. When their magnitude is sufficiently large they produce infinitely large displacements, whatever the magnitude of the loads applied normal to the midplane. The values of midplane load which cause this elastic instability are the "critical loads."

In two of the developed computer programs - the one-dimensional and plate programs - it is possible to separate completely the midplane and out-of-plane

(flexural) behaviors. When considering elastic instability, the determination of the midplane stresses and displacements is unaffected with respect to the procedures discussed previously. However, element stiffness for out-of-plane behavior, $\left[k_{e_z}\right]$, now becomes the sum of two component stiffnesses:

$$\left[k_{e_z} \right] = \left[k_{e_f} \right] + \left[n \right] \qquad \text{(II-11)}$$

where $\left[k_{e_f} \right]$ is the stiffness for conventional flexural behavior and $\left[n \right]$ represents the effects of the midplane forces throughout the element on the out-of-plane behavior. The terms of $\left[n \right]$ consist of the dimensions of the element and the values of midplane force, as determined in the (independent) midplane analysis. Material properties do not appear in the $\left[n \right]$ matrix. Techniques for formulating Equation (II-11) for beam and plate elements were delineated in Reference 6 and are discussed in the next chapter.

Due to the segregation of midplane and out-of-plane behavior, two separate sets of master stiffness equations would be formed in an instability problem. The midplane equations would appear as (excluding initial strain effects)

$$\left\{ P_{xy} \right\} = \left[K_{xy} \right] \left\{ \Delta_{xy} \right\} \qquad \text{(II-12)}$$

while the out-of-plane equations would take the form

$$\left\{ P_z \right\} = \left[\left[K_z \right] + \left[N \right] \right] \left\{ \Delta_z \right\} \qquad \text{(II-13)}$$

To solve Equation (II-13) it is of course first necessary to solve Equation (II-12) and determine the associated midplane forces so that the matrix $\left[N\right]$ can be formed. In the form indicated, Equation (II-13) can be solved, under certain conditions, to obtain an "equilibrium" solution for out-of-plane behavior in the presence of given midplane forces. These conditions dictate that the midplane forces be of less than critical value. When they are of critical value or greater, the matrix to be inverted will be singular.

In practice, the solution of these equations as an instability problem involves the determination of the value of the midplane forces to cause instability. It is assumed that all midplane forces are at a fixed ratio to one another at all levels of applied load, from the onset of loading to the achievement of instability. (Correspondingly, the shape of a midplane temperature distribution causing midplane forces remains constant up through instability). Thus, the midplane analysis is performed for any convenient magnitude of the applied loads and it is assumed that at instability the actual intensity is a scalar, λ, times such magnitude. Equation (II-13) can then be written as

$$\left\{ P_z \right\} = \left[K_z \right] \left\{ \Delta_z \right\} + \lambda \left[N \right] \left\{ \Delta_z \right\} \qquad \text{(II-14)}$$

Also, it has been stated that elastic instability is independent of the value of the applied midplane loads. Hence, setting $\left\{ P_z \right\} = 0$

$$0 = \left[K_z \right] \left\{ \Delta_z \right\} + \lambda \left[N \right] \left\{ \Delta_z \right\} \tag{II-15}$$

$$\frac{1}{\lambda} \left\{ \Delta_z \right\} = - \left[K_z \right]^{-1} \left[N \right] \left\{ \Delta_z \right\} \tag{II-16}$$

Using matrix iteration, the above can be solved for the eigenvalues $1/\lambda_i$ and the associated eigenvectors $\left\{ \Delta_z \right\}_i$. There will be as many such eigenvalues as there are equations in (II-15), but the only eigenvalue of interest is the largest value of $\frac{1}{\lambda_i}$ representing the smallest λ_i and therefore the lowest magnitude of midplane load at which elastic instability will be experienced.

CHAPTER III

DISCRETE ELEMENT FORCE-DISPLACEMENT RELATIONSHIPS

A. DERIVATION PROCEDURES

1. Linear Elastic Stiffness

The force-displacement properties of discrete elements, of the form required for use in matrix displacement analyses, can be formulated by application of one of three general approaches. These approaches are outlined in Reference 7 and developed in detail in Reference 5 . In the derivation of relationships for the subject group of three matrix displacement computer programs it proved convenient and sufficiently accurate to employ only one of these three approaches. The selected approach is based on Castigliano's First Theorem, Part I, and is formulated from fundamental principles in this chapter of the report.

To formulate this approach for the case of linear elastic stiffness alone (initial strain and instability effects being temporarily disregarded--these are examined in later sections) consider the discrete element free body diagram, sketched below (Figure III-1). The element is

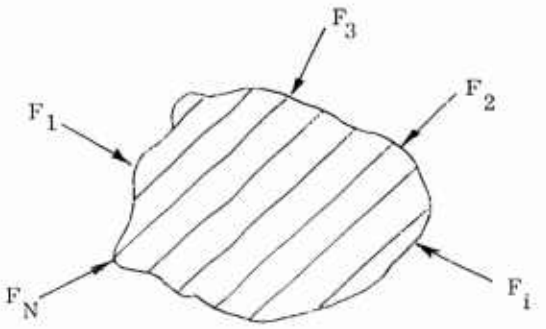

Figure III-1. Discrete Element

subjected to the indicated node point loads $F_1, F_2, \ldots F_i, \ldots F_N$, which include both applied and reactive forces. The corresponding node point displacements are $\Delta_1, \Delta_2, \ldots \Delta_i \ldots \Delta_N$. An amount of elastic strain energy (U) is stored in the structure as a consequence of the loading and displacements.

If the structure is restrained against displacements at all points of load application except at and in the direction of the i th load, F_i, an infinitesmal increase in the load F_i to $F_i + \delta F_i$ will result in an incremental displacement

$\delta\Delta_i$. In accordance with the principle of conservation of energy, the change in external work (δW) done by the infinitesmal force change must equal the change in the stored elastic strain energy, δU. Hence,

$$\delta W = \delta U \tag{III-1}$$

and, since $\delta W = (F_i + \delta F_i)\ \delta\Delta_i \approx \left(F_i\right)\left(\delta\Delta_i\right)$, Equation III-1 can be written as:

$$\left(F_i\right)\left(\delta\Delta_i\right) = \delta W = \delta U \tag{III-2}$$

when $\delta\Delta \longrightarrow 0$

$$F_i = \frac{\partial W}{\partial \Delta_i} = \frac{\partial U}{\partial \Delta_i} \tag{III-3}$$

which is a statement of Castigliano's Theorem, Part I.

For purposes of later developments, it should be emphasized that the strain energy in Equation III-3, although given in terms of displacements, could have originally been expressed in terms of the stresses and strains in the element, which are in turn a function of the displacements.

The condition employed in the derivation of Equation III-3 -- restraint of all displacement components except the one of interest -- is the condition associated with the definition of a stiffness coefficient. Thus, if the strain energy of a discrete element can be expressed in terms of the element node point displacements, application of Equation III-3 would result in the direct determination of the element stiffnesses.

In general, it is not possible or convenient to determine the elastic strain energy explicity in terms of the node point displacements, and the approach taken is as follows.
An assumed displacement component for the element can be written in the form

$$\Delta = a_1 f_1 (x, y, z) + a_2 f_2 (x, y, z) + \ldots\ldots a_N f_N (x, y, z) \tag{III-4}$$

Here, attention is restricted to developments where the number (N) of undetermined coefficients $a_1, a_2 \ldots a_N$, is equal to the total number of node point degrees of freedom. The expressions $f_1 (x, y, z)$, $f_2 (x, y, z)$ may be polynomials (e.g., xy^2, y^3, etc.), trigonometric functions (e.g., sinx, cos y, etc.) or may take other forms.

Once the displacement functions are chosen, or established as will be the case when stresses or strains are first assumed and then integrated to obtain the corresponding displacements, they can be evaluated at each node point, resulting in algebraic relationships between the node point displacements and the constants $a_1, a_2, \ldots a_N$. The complete set of such relationships for all node points of an element can be expressed as

$$\{\Delta\} = [B]\{a\} \tag{III-5}$$

where

$\{\Delta\}$ is a column matrix of N node point displacements.
$\{a\}$ is a column matrix of the constants $a_1, \ldots a_N$.
$\{B\}$ the square matrix of coefficients in the relationships between $\{\Delta\}$ and $\{a\}$.

Solving Equation III-5 through inversion of $[B]$, one obtains

$$\{a\} = [B]^{-1}\{\Delta\} \tag{III-6}$$

Since relationships between the element node point forces ($\{F\}$) and the displacements $\{\Delta\}$ are desired, the remaining steps in this development pertain to the establishment of relationships between $\{F\}$ and $\{a\}$. For this purpose consider Equation III-3 which, for a particular node point force F_i, can be written as

$$F_i = \frac{\partial U}{\partial \Delta_i} = \frac{\partial U}{\partial a_1}\frac{\partial a_1}{\partial \Delta_i} + \frac{\partial U}{\partial a_2}\frac{\partial a_2}{\partial \Delta_i} + \ldots \frac{\partial U}{\partial a_N}\frac{\partial a_N}{\partial \Delta_i} \tag{III-7}$$

Application of III-7 to all node point forces results in N relationships; these can be summarized in matrix form as

$$\{F_i\} = \left[\frac{\partial a_j}{\partial \Delta_i}\right]\left\{\frac{\partial U}{\partial a_j}\right\} \tag{III-8}$$

and, as shown in Reference 5 ,

$$\left[\frac{\partial a_j}{\partial \Delta_i}\right] = \left([B]^{-1}\right)^T \tag{III-9}$$

Also, the strain energy (U) is a quadratic form in the stresses, strains, or displacement derivatives and is therefore a quadratic form in the displacements $a_1, a_2 \ldots a_N$. i.e.,

$$U = g\,(a_i \times a_j) \tag{III-10}$$

Thus, when the strain energy is differentiated with respect to a particular constant, say a_j, the resulting expression is a linear function of the constants $a_1, \ldots a_n, \ldots a_N$, and can be written in matrix form as

$$\frac{\partial U}{\partial a_j} = \left[C_j \right] \left\{ a \right\} \qquad (j = 1, \ldots N) \tag{III-11}$$

and for the complete set of derivatives of U, one obtains

$$\left\{ \frac{\partial U}{\partial a_j} \right\} = \left[C \right] \left\{ a \right\} \tag{III-12}$$

Now, by combination of Equations II-6, -8, -9, and -12, there results

$$\left\{ F \right\} = \left(\left[B \right]^{-1} \right)^T \left[C \right] \left[B \right]^{-1} \left\{ \Delta \right\} \tag{III-13}$$

or

$$\left\{ F \right\} = \left[k \right] \left\{ \Delta \right\} \tag{III-14}$$

with

$$\left[k \right] = \left(\left[B \right]^{-1} \right)^T \left[C \right] \left[B \right]^{-1} \tag{III-15}$$

where, in recapitulation

$\left[B \right]$ = a matrix relating the node point displacements to the undetermined constants of the assumed displacement functions.

$\left[C \right]$ = a square matrix, each row of which contains the coefficients of the constants $a_1, \ldots a_N$ in equations which represent derivatives of the strain energy with respect to $a_1, \ldots a_N$.

Note that the subscript E, used in the previous chapter to designate element stiffness, displacements, etc., is discarded in the present chapter.

2. Derivation of Terms Representing Initial Strain Effects

Initial strains can be defined, for present purposes, as strains that exist in a structure prior to the imposition of applied loads. Only initial strain due to temperature change and prior inelastic deformation are of interest to this report.

The total value of a strain component at a point can be written in the form

$$\epsilon_T = \epsilon_e + \epsilon^i \tag{III-16}$$

where ϵ_T is the total strain, ϵ_e is the strain due to stress, and ϵ^i is the initial strain. For temperature change

$$\epsilon^i = \epsilon^\alpha = \alpha T \tag{III-17}$$

and for accumulated inelastic strain

$$\epsilon^i = \epsilon_p \tag{III-18}$$

The development of a procedure for deriving terms representing initial strain effects requires a re-examination of the expressions for strain energy. The strain energy to be employed is the elastic strain energy, but the strains appearing in the related formulation must be total strains since it is these which correspond to the displacements of the element stiffness equations.
Thus, the strain energy, U, can be written as

$$U = \frac{1}{2} \int^{V} \epsilon_e \quad \sigma d\ V \tag{III-19}$$

and by substitution of the expression for elastic strain (Equation III-16)

$$U = \frac{1}{2} \int^{V} (\epsilon_T - \epsilon^i) \quad \sigma d\ V \tag{III-20}$$

The significance of these factors will be shown in the development to follow.

If the formulation of element properties is to be based on assumed displacements, the relationship between the undetermined constants and the displacements is simply that given by Equations III-4 and III-5. The corresponding total strains are derived by differentiation of the displacement expression and the stresses are obtained by use of Hooke's Law (Equation III-16a). From equation III-20, the strain energy is

$$U = \frac{E'}{2} \int^{V} (\epsilon_T - \epsilon^i)^2\, dV \tag{III-21}$$

or, in expanded form

$$U = \frac{E'}{2} \int^{V} (\epsilon_T^2 - 2\ \epsilon_T\ \epsilon^i + \epsilon^{i2}) dV \tag{III-22}$$

and, as was noted earlier, this leads to a quadratic expression in the a's when the assumed displacement function is substituted and the integration performed i.e.,

$$U = g(a_i \times a_j) + h(a_j \times \epsilon^i) + j(\epsilon^{i2}) \tag{III-23}$$

From Equation III-8 and III-9

$$\left\{ F_i \right\} = \left(\left[B \right]^{-1} \right)^T \left\{ \frac{\partial U}{\partial a_j} \right\} \tag{III-24}$$

$\left[B \right]$ is unchanged by the presence of initial strain but U is now given by Equation (III-10a), rather than by Equation (III-10). Therefore

Therefore $$\frac{\partial U}{\partial a_j} = \lfloor C_j \rfloor \{ a \} + \frac{\partial h}{\partial a_j} \quad \text{(III-25)}$$

where $\lfloor C_j \rfloor$ results from the indicated differentiation of $g(a_i \times a_j)$ and ∂h is is intended to indicate differentiation of $h(a_j \times \epsilon^i)$.
For the complete set of derivatives of U , one obtains

$$\left\{ \frac{\partial U}{\partial a_j} \right\} = [C] \{ a \} + \left\{ \frac{\partial h}{\partial a_j} \right\} \quad \text{(III-26)}$$

Thus, by combination of (III-12a, -8a and -5)

$$\{F\} = \left([B]^{-1} \right)^T [C] [B]^{-1} \{ \Delta \} + \left([B]^{-1} \right)^T \left\{ \frac{\partial h}{\partial a_j} \right\} \quad \text{(III-27)}$$

which can be expressed in a form indentical to Equation (III-26), except that now

$$\{ F \} = [k] \{ \Delta \} - \{ F^i \} \quad \text{(III-28)}$$

where $$\{ F^i \} = - \left([B]^{-1} \right)^T \left\{ \frac{\partial h}{\partial a_j} \right\} \quad \text{(III-29)}$$

3. Incremental Stiffness

When midplane stresses or forces influence the behavior of plates and beams in bending, their effect on the analytical formulation of flexural stiffness relationships is in the form of an "incremental" stiffness, i.e., as an addition to the usual flexural stiffness. The purpose of this section is to extend the preceeding formulations to include techniques for incremental stiffness derivation. This development applies only to beams and plates in flexure which are subjected to a previously applied and equilibrated known axial or midplane force system.

For beams and plates under the conditions of interest, the following relationships exist between the work (W) done by the lateral and midplane loads during bending deformation and the strain energy of bending (U_f) (see Reference 10).

$$W = W_v + W_h = U_f \quad \text{(III-30)}$$

where

W_v = work done by the lateral loads ($F_1, F_2 \ldots F_i \ldots F_N$) during flexure.

W_h = work done by the midplane loads during the displacement of the structure caused by the lateral loads.

Furthermore, the change in W_v with respect to the displacement Δ_i can be obtained directly from Equation (III-30) as

$$\frac{\partial W_v}{\partial \Delta_i} = \frac{\partial \left(U_f - W_h\right)}{\partial \Delta_i} \qquad \text{(III-31)}$$

Now, if the restraint condition employed in the formulation of Equation III-3 is considered, it follows that

$$W = W_v$$

and

$$\frac{\partial W}{\partial \Delta_i} = \frac{\partial W_v}{\partial \Delta_i} \qquad \text{(III-32)}$$

Consequently, from Equations III-3, -31 and -32

$$F_i = \frac{\partial \left(U_f - W_h\right)}{\partial \Delta_i} \qquad \text{(III-33)}$$

The transformation of Equation III-33 into a matrix formulation of the desired element stiffness matrix could be accomplished rigorously through application of the same procedures that led to Equation III-15. For brevity, however, the already-developed Equation III-15 will be used as a basis. First, it must be noted that W_h can be expressed in terms of the lateral displacements. This is also the form taken by U_f. Hence, $(U_f - W_h)$ can be defined as an "effective" strain energy, U', and Equation III-3 can be written as

$$F_i = \frac{\partial U'}{\partial \Delta_i} \qquad \text{(III-34)}$$

Equation III-34 is of similar appearance to Equation III-3, which provided the basis for the development of Equation III-15. To use Equation III-34 in the same way, one must note that of the two matrices making up Equation III-15, only the matrix $[C]$ pertains to strain energy. Each row of $[C]$ represents an equation for the derivative of the strain energy. Since now the strain U' is composed of two parts one can write

$$[C] = [C_f] - [C_h] \qquad \text{(III-35)}$$

in which $[C_f]$ and $[C_h]$ result from the required operations on U_f and W, respectively. Equation III-15 therefore becomes

$$[k] = [k_f] - [k_h] = \left([B]^{-1}\right)^T [C_f] [B]^{-1} - \left([B]^{-1}\right)^T [C_h] [B]^{-1} \qquad \text{(III-36)}$$

It is pertinent to note that for beam segments

$$W_h = -\frac{F_x}{2} \int_0^L \left(\frac{dw}{dx}\right)^2 dx \qquad \text{(III-37)}$$

and, for plates of constant thickness

$$W_h = -1/2 \int_A \left[N_x \left(\frac{\partial w}{\partial}\right)^2 + N_y \left(\frac{\partial w}{\partial y}\right)^2 + 2N_{xy} \left(\frac{\partial w}{\partial x}\right)\left(\frac{\partial w}{\partial y}\right)\right] dA \qquad \text{(III-38)}$$

4. Stress-Displacement Relationships

It is possible, in theory, to determine the stresses in a matrix displacement analysis by utilizing the solved-for displacements and the element stiffness matrices to evaluate the node point forces. Then, these forces are transformed into stresses. It is believed more convenient, however, to form directly a set of relationships between the element stresses and node point displacements, Such relationships are termed "stress-displacement" equations in this report and are written in the form

$$\{\sigma\} = [S]\{\Delta\} \qquad \text{(III-39)}$$

The procedures used to determine these equations take one of two forms, dependent on whether the derivation of the element stiffness properties was based on assumed stress or assumed displacement behavior. Consider first the case of assumed stress patterns. Here, the development of element properties begins with expressions of the form

$$\{\sigma\} = [D]\{a\} \qquad \text{(III-40)}$$

Eliminating the column of constants from III-40 by use of III-24 results in

$$\{\sigma\} = [D][B]^{-1}\{\Delta\} - [D][B]^{-1}\{\Delta^i\} \qquad \text{(III-41)}$$

or

$$\{\sigma\} = [S]\{\Delta\} - \{\sigma^i\} \qquad \text{(III-42)}$$

where

$$[S] = [D][B]^{-1} \qquad \text{(III-43)}$$

$$\{\sigma^i\} = [D][B]^{-1}\{\Delta^i\} \qquad \text{(III-44)}$$

The initial stresses $\{\sigma^i\}$ correspond to the stresses that occur when the node point displacements are zero.

When the derivation of element properties is based on assumed displacement behavior, the starting point is

$$\{a\} = [B]^{-1} \{\Delta\} \tag{III-6}$$

The strains must be derived from the displacements through application of the strain-displacement derivatives. When this differentiation is applied to the basic assumptions, one obtains

$$\{\epsilon\} = [H] \{a\} \tag{III-45}$$

and, from Hooke's Law

$$\{\sigma\} = [E] \{\epsilon\} - \{\sigma^i\} \tag{III-46}$$

Hence, by combination of III-6, - 45 and - 46

$$\{\sigma\} = [E][H][B]^{-1}\{\Delta\} - \{\sigma^i\} \tag{III-47}$$

thus, in the present case

$$[S] = [E] [H] [B]^{-1} \tag{III-48}$$

B. BEAM-AXIAL FORCE ELEMENT

1. Basic Considerations

The beam-axial force element, shown in Figures III-2 and III-3, appears in each of the three computer programs described in Chapters IV-VI. It is the only major element in the One-Dimensional Structure Program (Chapter IV), where detailed attention is given to the variation of temperature, etc., on the cross-section of the element; only the gross effects on element cross-sections are treated in the other two programs. In developing the relationships for this element, the expressions employed in the One-Dimensional Structure Program will be established. By introducing the simplifications pertinent to the other two programs, the derived relationships can be reduced to the forms of interest.

This development is based on the following assumptions:

(1) Cross-sections originally plane remain plane.

(2) The geometry and temperatures on a cross-section are symmetric about one axis; the bending moments act only in the plane of symmetry.

(3) The cross-sectional geometry and temperatures do not vary along the axis of the element.

(4) Plastic strains are constant over the length of the element and are dependent only on the stress conditions on a cross-section midway between the ends of the element.

(5) Lateral deflections are relatively small.

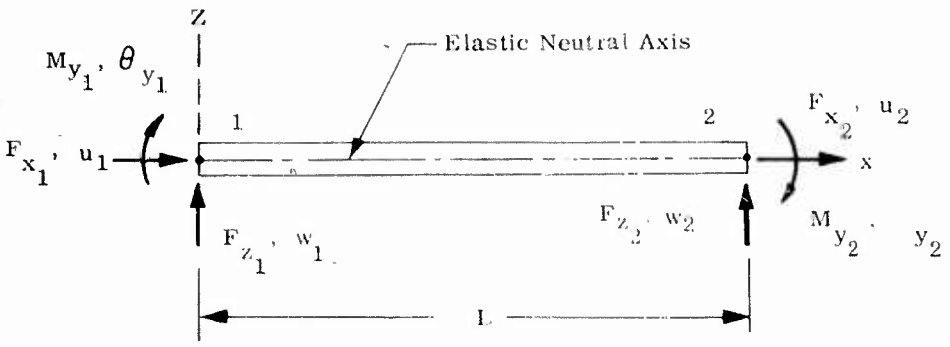

Figure III-2. One-Dimensional Element

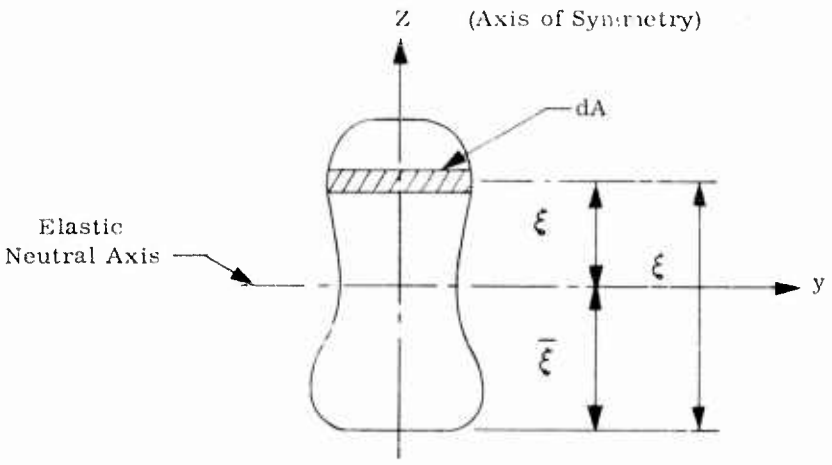

Figure III-3. Typical Cross-Section of One-Dimensional Element

Consider a typical symmetrical cross-section of the element as shown in Figure III-3. In accordance with assumption (1), the total axial displacement (u_T) of an arbitrary point on the cross-section can be written as

$$u_T = \bar{u}_T - \theta_T \xi \tag{III-49}$$

where ξ is the distance to the point in the direction of the axis of symmetry measured from an arbitrarily chosen reference line and θ_T is both the angular displacement of the cross section and the slope of each fiber of the beam at the cross-section under study. "Barred" values for u and ϵ represent quantities associated with pure translation of the cross-section. By definition:

$$\theta_T = \frac{dw_T}{dx} \tag{III-50}$$

Since the total axial strain, $\epsilon_{x_T} = \frac{du_T}{dx}$

$$\epsilon_{x_T} = \frac{d\bar{u}_T}{dx} - \xi \frac{d^2 w_T}{dx^2} = \bar{\epsilon}_{x_T} - \frac{\xi}{\rho_T} \tag{III-51}$$

The term ξ / ρ_T represents the component of the total strain resulting from the relative rotation of the cross-section, where ρ_T is the total curvature.

The total strain, ϵ_{x_T} is composed of two components: (1) an elastic strain $\frac{\sigma_x}{E}$ and (2) an initial strain ϵ_x^i. Replacement of the total strain in Equation III-49 by the sum of its components results in

$$\frac{\sigma_x}{E} + \epsilon_x^i = \bar{\epsilon}_{x_T} - \frac{\xi}{\rho_T}$$

or

$$\sigma_x = E \left[\bar{\epsilon}_{x_T} - \frac{\xi}{\rho_T} - \epsilon_x^i \right] \tag{III-51}$$

It is now necessary to relate the stresses to forces and moments or "stress-resultants". The axial stress resultant, F_x, and the bending stress resultant, $\bar{M}_y$, are related to the stresses on the cross-section through equilibrium as follows

$$F_x = \int^A \sigma_x \, dA$$
$$\bar{M}_y = \int^A \sigma_x \, \xi \, dA \tag{III-53}$$

(The "bar" over M_y signifies an internal moment. See Chap. II), and, by use of Equation III-52.

$$F_x = \bar{\epsilon}_{x_T} \int^A E dA - \int^A \frac{E\xi}{\rho_T} dA - \int^A E \epsilon_x^i dA$$

$$\bar{M}_y = \bar{\epsilon}_{x_T} \int^A E\xi \, dA - \int^A \frac{E\xi^2}{\rho_T} dA - \int^A \xi E \epsilon_x^i dA \qquad \text{(III-53a)}$$

These equations can be simplified by referring the integrations to the elastic neutral axis location, $\bar{\xi}$, defined as

$$\bar{\xi} = \frac{\int^A \xi E \, dA}{\int^A E \, dA} \qquad \text{(III-54)}$$

Hence, if the variable ξ in Equations (III-53a) is replaced by $\xi' = \xi - \bar{\xi}$ (i.e., the origin of coordinates is now placed at the neutral axis), $\int^A E\xi' dA = 0$ and the equations reduce to

$$F_x = \bar{\epsilon}_{x_T} \overline{EA} - F_x^i$$

$$\bar{M}_y = -\frac{\overline{EI}}{\rho_T} - \bar{M}_y^i \qquad \text{(III-53b)}$$

or

$$\epsilon_{x_T} = \frac{F_x + F_x^i}{\overline{EA}} = \frac{F_x}{EA} + \frac{F_x^i}{\overline{EA}} = \bar{\epsilon}_{x_e} + \frac{F_x^i}{\overline{EA}}$$

$$\frac{1}{\rho_T} = -\frac{(\bar{M}_y + \bar{M}_y^i)}{\overline{EI}} = -\frac{\bar{M}_y}{\overline{EI}} - \frac{\bar{M}_y^i}{\overline{EI}} = -\frac{1}{\rho_x} - \frac{\bar{M}_y^i}{\overline{EI}} \qquad \text{(III-53c)}$$

where

$$\overline{EA} = \int^A EdA \text{ (elastic axial stiffness)}$$

$$\overline{EI} = \int^A E(\xi')^2 dA \text{ (elastic flexural stiffness)}$$

$$F_x^i = \int^A E \epsilon_x^i dA \text{ (initital axial force)} \qquad \text{(III-55)}$$

$$\bar{M}_y^i = \int^A E \epsilon_x^i \xi \, dA \text{ (initital moment)}$$

$\bar{\epsilon}_{x_e}$ Average elastic strain due to the axial stress resultant.

ρ_e curvature due to the bending stress resultant.

Thus, the integrals containing the initial strain terms are in the form of initial equivalent stress resultants. Note that in replacing ξ by ξ', the displacement u_T is now defined as being the displacement at the neutral axis. Also,

$$\bar{\epsilon}_{x_T} = \epsilon_{x_T} = \frac{d\bar{u}_T}{dx}$$

and, (from III-52)

$$\epsilon_{x_T} = \frac{\sigma_x}{E} + \epsilon_x^i$$

Use of Equations (III-53c) in Equation (III-52) results in

$$\sigma_x = E\left[\frac{(F_x + F_x^i)}{EA} + \frac{(\bar{M}_y + \bar{M}_y^i)}{\bar{EI}}\xi - \epsilon_x^i\right] \qquad \text{(III-52a)}$$

Equations III-52a and III-53 are the basic equations for this development. It is important to note that the location of the neutral axis as defined by Equation III-54 is independent of the magnitude or distribution of the initial strains; it depends only on the variation of Young's Modulus (E) which in turn is only a function of temperature. Thus, the axial stiffness $\bar{EA}$ and the flexural stiffness $\bar{EI}$ only depend on the cross-sectional geometry and the temperature and if E is a constant the neutral axis will pass through the centroid of the cross-section. It should also be noted that the axial force F_x is an axial-stress resultant with its point of application at the neutral axis on the axis of symmetry. Correspondingly, the bending-stress resultant (M_y) acts about the neutral axis. Thus, externally applied axial forces are presumed to act through the neutral axis of the cross-section.

2. Axial Behavior

Since the conditions associated with axial load (see Figure III-2) produce a state of constant strain in the axial direction, the axial displacements are a linear function of the axial coordinate and points on the neutral axis can be expressed as

$$u_T = a_1 + a_2 x$$

Thus

$$\begin{Bmatrix} u_1 \\ u_2 \end{Bmatrix} = \begin{bmatrix} 1 & O \\ 1 & L \end{bmatrix} \begin{Bmatrix} a_1 \\ a_2 \end{Bmatrix} = [B] \begin{Bmatrix} a_1 \\ a_2 \end{Bmatrix} \qquad \text{(III-57)}$$

The total strain energy is given by

$$U = \frac{1}{2} \int_2^L \bar{\epsilon}_{x_e} F_x \, dx \qquad \text{(III-58)}$$

but, from (III-53c)

$$\bar{\epsilon}_{x_e} = \bar{\epsilon}_{x_T} - \frac{F_x^i}{\overline{EA}} \qquad \frac{d\bar{u}_T}{dx} + \frac{F_x^i}{\overline{EA}} \qquad \text{(III-59a)}$$

and

$$F_x = \overline{EA} \; \bar{\epsilon}_{x_e} = \overline{EA} \quad \frac{d\bar{u}_T}{dx} + F_x^i \qquad \text{(III-59b)}$$

For this element, the initial strains of interest are the thermal and accumulated inelastic strains. Thus,

$$F_x^i = F_x^{\alpha} + F_x^p \qquad \text{(III-60)}$$

where

F_x^{α} initial force due to temperature strain

F_x^p initial force due to accumulated plastic stains

Substitution of (III-59) and (III-60) into (III-58), with $\frac{dw_T}{dx} = a_1$ yields

$$U = \frac{1}{2} \int_o^L \left(a_1 - \frac{F_x^{\alpha} + F_x^p}{\overline{EA}}\right) \left(\overline{EA}\, a_1 - F_x^{\alpha} + F_x^p\right) dx \qquad \text{(III-58a)}$$

and expanding the product within the integral

$$U = \frac{\overline{EA}}{2} \int_o^L (a_1)^2 \, dx + \frac{1}{2}\int_o^L (a_1)\left(F_x^{\alpha} + F_x^p\right) dx \qquad \text{(III-58b)}$$

$$+ \frac{1}{2EA} \int_o^L \left(F_x^{\alpha} + F_x^p\right) dx$$

From Equation (III-12a), it follows that

$$\left\{\frac{\partial U}{\partial a_j}\right\} = \overline{EA}\begin{bmatrix}1 & 0\\ 0 & 0\end{bmatrix}\begin{Bmatrix}a_1\\ a_2\end{Bmatrix} + \frac{(F_x^{\alpha} + F_x^{p})}{2}\begin{Bmatrix}1\\ 0\end{Bmatrix} \qquad \text{(III-61)}$$

and from Equation (III-26) through (III-29)

$$[k] = \frac{\overline{EA}}{L}\begin{bmatrix}1 & -1\\ -1 & 1\end{bmatrix}, \left\{F_x^{i}\right\} = \begin{Bmatrix}-F_x^{\alpha}\\ F_x^{\alpha}\end{Bmatrix} + \begin{Bmatrix}-F_x^{p}\\ F_x^{p}\end{Bmatrix} \qquad \text{(III-62), (III-63)}$$

3. Force-Displacement Equations--Flexural Behavior

In the case of flexure (see Figures III-2 and III-4) a distinction must be made between the initial displacements associated with thermal and plastic strain and the initial displacements produced during fabrication. This is necessary because the latter are exempt from geometric boundary conditions, i.e., if it is specified that a node point displacement be zero, it is meant that only the displacement due to applied loads, temperatures and plastic strain is zero--the node point displacement due to fabrication remains. To retain this distinction, the total transverse displacement (w_T') is considered to be composed of three parts:

$$w_T' = w_e + w_i + w_f \qquad \text{(III-64)}$$

where

w_e = the transverse displacement due to elastic strain

w_i = the transverse displacement due to thermal and plastic strain

w_f = the fabricational transverse displacement

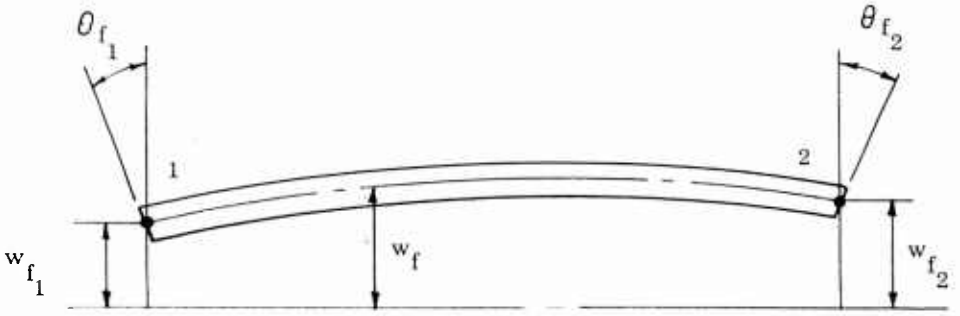

Figure III-4. Beam Segment with Fabricational Displacements

Generally w'_T (the total displacement from a reference axis) is employed in problems involving initial fabricational displacement. Here, however, it has been decided to employ the displacements corresponding to the difference between the total and fabricational displacements in the definition of the force-displacements relationships in the program. These displacements, w_T in this case, are therefore defined as

$$w_T = (w'_T - w_f) = (w_e + w_i) \tag{III-65}$$

To derive the equations of interest, the displacements are assumed to have the form

$$w_T = a_1 + a_2 x + a_3 x^2 + a_4 x^3 \tag{III-66}$$

so that

$$\theta_T = \frac{dw_T}{dx} = a_2 + 2a_3 x + 3a_4 x^2 \tag{III-67}$$

$$\frac{1}{\rho_T} = \frac{d^2 w_T}{dx^2} = 2a_3 + 6a_4 x \tag{III-68}$$

By evaluation of III-66 and -67 at the node points there is obtained

$$\begin{Bmatrix} w_{T_1} \\ w_{T_2} \\ \theta_{T_1} \\ \theta_{T_2} \end{Bmatrix} = \begin{bmatrix} 0 & -1 & 0 & 0 \\ 0 & -1 & -2L & -3L^2 \\ 1 & 0 & 0 & 0 \\ 1 & L & L & L \end{bmatrix} \begin{Bmatrix} a_1 \\ a_2 \\ a_3 \\ a_4 \end{Bmatrix} \quad \text{or} \quad [B] \begin{Bmatrix} a_1 \\ a_2 \\ a_3 \\ a_4 \end{Bmatrix} \tag{III-69}$$

Consider first the component associated with simple flexure, given in this case by

$$U_f = \frac{1}{2} \int_o^L \bar{M}_y \left(\frac{1}{\rho_e} \right) dx \tag{III-70}$$

By use of Equations III-53b and III-53c, and with $\bar{M}_y^{\,i} = \bar{M}_y^{\,\alpha} + \bar{M}_y^{\,p}$, this becomes

$$U_f = \frac{1}{2} \int_o^L \left(\frac{1}{\rho_T} + \frac{\overline{M}_y^{\alpha} + \overline{M}_y^{p}}{\overline{EI}} \right) \left(\frac{\overline{EI}}{\rho_T} + \overline{M}_y^{\alpha} + \overline{M}_y^{p} \right) dx \qquad \text{(III-70a)}$$

Using $\frac{1}{\rho_T}$ as given by (III-68)

$$U_f = \frac{\overline{EI}}{2} \int_o^L (2a_3 + 6a_4 x)^2 dx + \frac{1}{2} \int_o^L (2a_3 + 6a_4 x)(\overline{M}_y^{\alpha} + \overline{M}_y^{p}) dx$$

$$+ \frac{1}{2} \int_o^L \frac{(\overline{M}_y^{\alpha} + \overline{M}_y^{p})}{\overline{EI}} dx \qquad \text{(III-70b)}$$

and, by applying $\frac{\partial U_f}{\partial a_i}$ to this expression, for $i = 1, \cdots 4$, there results

$$\begin{Bmatrix} \frac{\partial U_f}{\partial a_1} \\ \frac{\partial U_f}{\partial a_2} \\ \frac{\partial U_f}{\partial a_3} \\ \frac{\partial U_f}{\partial a_4} \end{Bmatrix} = \begin{bmatrix} 0 & 0 & 0 & 0 \\ 0 & 0 & 0 & 0 \\ 0 & 0 & 2L & 3L^2 \\ 0 & 0 & 3L^2 & 6L^3 \end{bmatrix} \begin{Bmatrix} a_1 \\ a_2 \\ a_3 \\ a_4 \end{Bmatrix} - 2L \begin{Bmatrix} 0 \\ 0 \\ (\overline{M}^{\alpha} + \overline{M}^{p}) \\ \frac{2}{3} L (\overline{M}^{\alpha} + \overline{M}^{p}) \end{Bmatrix} \qquad \text{(III-71)}$$

or, symbolically

$$\left\{ \frac{\partial U_f}{\partial a_j} \right\} = \left[C_f \right] \left\{ a \right\} + \left\{ \frac{\partial h}{\partial a} \right\} \qquad \text{(III-71a)}$$

From Equations (III-36) and (III-29), and with use of (III-69), it follows that

$$\left[k_f \right] = \left(\left[B \right]^{-1} \right)^T \left[C_f \right] \left[B \right]^{-1} \qquad \text{(III-36a)}$$

$$\left\{ F_z^{\alpha} \right\} = - \left(\left[B \right]^{-1} \right)^T \left\{ \frac{\partial h}{\partial a} \right\}^{\alpha} \qquad \text{(III-29a)}$$

$$\left\{ F_z^{p} \right\} = - \left(\left[B \right]^{-1} \right)^T \left\{ \frac{\partial h}{\partial a} \right\}^{p} \qquad \text{(III-29b)}$$

The resulting matrices ($\left[k_f \right]$, $\left\{ F_z \right\}$, $\left\{ F_z^{p} \right\}$) are shown in Figure III-5, where the subscript T has been dropped from w and θ.

$$\begin{Bmatrix} \bar{M}_{y_1} \\ \bar{M}_{y_2} \\ F_{z_1} \\ F_{z_2} \end{Bmatrix} = \left[\left[k_f \right] + \left[n \right] \right] \begin{Bmatrix} \theta_{y_1} \\ \theta_{y_2} \\ w_1 \\ w_2 \end{Bmatrix} - \left\{ F^{\alpha} \right\} - \left\{ F^{p} \right\} - \left\{ F^{f} \right\}$$

$$\left[k_f \right] = \frac{2\bar{E}I}{L^3} \begin{bmatrix} 2L^2 & L^2 & -3L & 3L \\ L^2 & 2L^2 & -3L & 3L \\ -3L & -3L & 6 & -6 \\ 3L & 3L & -6 & 6 \end{bmatrix}, \quad \left[n \right] = \frac{F_x}{10L} \begin{bmatrix} \frac{4}{3}L^2 & -\frac{L^2}{3} & -L & L \\ \frac{-L^2}{3} & \frac{4}{3}L^2 & -L & L \\ -L & -L & 12 & -12 \\ L & L & -12 & 12 \end{bmatrix}$$

$$\left\{ F_z^{\alpha} \right\} = \begin{Bmatrix} \bar{M}_y^{\alpha} \\ -\bar{M}_y^{\alpha} \\ 0 \\ 0 \end{Bmatrix}, \quad \left\{ F_z^{p} \right\} = \begin{Bmatrix} M_y^{p} \\ -M_y^{p} \\ 0 \\ 0 \end{Bmatrix}, \quad \left\{ F_z^{f} \right\} = -\left[n \right] \begin{Bmatrix} \theta_{y_1}^{f} \\ \theta_{y_2}^{f} \\ w_1^{f} \\ w_2^{f} \end{Bmatrix}$$

Figure III-5. One Dimensional Element – Out-of-Plane Force-Displacement Relationships

The terms of the force-displacement relationships that arise from the work done by the axial force during flexure will now be developed. Here, the term representing work done by inplane forces is (see section III.A.3)

$$W_h = -\frac{F_x}{2}\int_o^L \left(\frac{dw'}{dx}T\right)^2 dx \qquad \text{(III-37a)}$$

where F_x is the axial stress resultant, which is a known value prior to the flexural analysis. Note that the slope due to the total displacement from the reference axis is employed in the above equation since Equation III-37a emanates from strictly geometric considerations. This total displacement is assumed to be of the form:

$$w'_T = a'_1 + a'_2\ x + a'_3\ x^2 + a'_4\ x^3 \qquad \text{(III-72)}$$

Together with Equation (III-66), this assumption implies that the initial fabricational displacements take the same form as the elastic displacements.

With use of the derivative of Equation (III-72) in (III-37a), there is obtained:

$$W_h = -\frac{F_x}{2}\left[\ (a'_2)^2 L + \frac{4}{3}(a'_3)^2 L^3 + \frac{9}{5}(a'_4)^2 L^5 + 2a'_2\, a'_3 L^2 + 2a'_2\, a'_4 L^3 + 3a'_3\, a'_4 L^4\ \right] \qquad \text{(III-37b)}$$

and, by establishing the derivatives of W_h with respect to each of the constants a'_1, a'_4 there is obtained.

$$\begin{Bmatrix} \frac{\partial W_h}{\partial a_1} \\ \frac{\partial W_h}{\partial a_2} \\ \frac{\partial W_h}{\partial a_3} \\ \frac{\partial W_h}{\partial a_4} \end{Bmatrix} = -F_x \begin{bmatrix} 0 & 0 & 0 & 0 \\ 0 & L & L^2 & L^3 \\ 0 & L^2 & \frac{4}{3}L^3 & \frac{3}{2}L^4 \\ 0 & L^3 & \frac{3}{2}L^4 & \frac{9}{5}L^5 \end{bmatrix} \begin{Bmatrix} a'_1 \\ a'_2 \\ a'_3 \\ a'_4 \end{Bmatrix} = \left[C_h\right]\left\{a'\right\} \qquad \text{(III-73)}$$

Since the stiffness relationships are given by $\left(\left[B\right]^{-1}\right)^T \left[C_h\right]\left[B\right]^{-1}$ this particular contribution to flexural stiffness (denoted by $\left[n\right]$) is given by

$$\left[n \right] = \left(\left[B \right]^{-1} \right)^{T} \left[C_h \right] \left[B \right]^{-1} \qquad \text{(III-74)}$$

The postmultiplier of the above incremental stiffness matrix is the column of displacements w'_T and θ_T'. As stated earlier, however, it is desired that all relationships be expressed in terms of the difference between w'_T and the fabricational displacements w_f, i.e., in terms of w_{Tf}. This is easily accomplished by making the substitutions $w'_T = w_T + w_f$, $\theta_T = \theta_T + \theta_f$, resulting in

$$\left[n \right] \begin{Bmatrix} \theta_{T_1} \\ \theta_{T_2} \\ w'_{T_1} \\ w'_{T_2} \end{Bmatrix} = \left[n \right] \begin{Bmatrix} \theta_{T_1} \\ \theta_{T_2} \\ w_{T_1} \\ w_{T_2} \end{Bmatrix} + \left[n \right] \begin{Bmatrix} \theta_{f_1} \\ \theta_{f_2} \\ w_{f_1} \\ w_{f_2} \end{Bmatrix} \qquad \text{(III-74a)}$$

also, since the fabricational displacements θ_f, w_f are known quantities in an analysis, the product of the incremental stiffness and the column of fabricational displacements (the second term on the right side of Equation III-74a) can be expressed as an initital force column $\left\{ F^f \right\}$, i.e.

$$\left\{ F_z^f \right\} = - \left[n \right] \begin{Bmatrix} \theta_{f_1} \\ \theta_{f_2} \\ w_{f_1} \\ w_{f_2} \end{Bmatrix} \qquad \text{(III-75)}$$

The explicit forms for $\left[n \right]$ and $\left\{ F_z^f \right\}$ appear in Figure (III-5), where they are included in the complete expression for the out-of-plane force-displacement equations for the one-dimensional element.

4. Stress-Displacement Equations

In general, the stresses will vary along the length of the element so that a presentation of the complete stress distribution would involve a voluminous amount

of information. Thus, only the stresses at the center of the element, which should suffice to define the significant stresses within the element and structure as a whole, are determined.

Equation (III-52a) gives the stress at a point on the cross-section of the one-dimensional element in terms of the stress resultants. The stress-resultants have been formulated in terms of the displacements in the preceding two sections. By combining these formulations with Equation (III-52a) and effecting an evaluation at the central cross-section of the element (i.e., at x = L/2) the following stress-displacement equation is obtained

$$\sigma_{x_{(x = L/2)}} = E\left[\frac{u_2 - u_1}{L} + \frac{\xi'}{L}(\theta_{y_1} - \theta_{y_2}) - (\alpha \Delta T + \epsilon_x^p)\right] \qquad \text{(III-76)}$$

C. PLATE ELEMENTS

1. Triangular Plate

A detailed development of all plate element relationships would be beyond the scope of this report. Their development is documented elsewhere (Reference 8). The present report simply outlines the bases for the derivation of the pertinent stiffness matrices, thermal forces, etc.

The stiffness matrix for the triangular plate element was originally derived by Turner, et al (Reference 3). By use of Castigliano's Theorem (Equation III-15) and the assumption of constant strains θ_x, θ_y, γ_{x_y}, the stiffness relationships were re-derived for orthotropic behavior. The element is shown in Figure III-6. Note that the element is arbitrarily oriented in the x-y plane; use is not made of one of the element edges as a local coordinate axis. The x-y axes are intended to be the axes of the complete structure. This is because it is expected that the axes of the complete structure will correspond to the principal axes of orthotropy. The inplane thermal and plastic forces were derived from Equation III-29 under the assumption that the thermal and plastic strains were constant throughout the element.

After extensive investigation, it was decided to base the development of the relationships for out-of-plane behavior on the following assumed displacement function.

$$w = a_1 + a_2x + a_3y^2 + a_4y + a_5x^2 + a_6x^3 + a_7y^3 + a_8xy + a_9xy^2 \qquad \text{(III-77)}$$

It is to be noted that this function is geometrically unsymmetric, i.e., the term a_ix^2y which is the counterpart of a_9xy^2 is absent. Attempts were made to remedy this situation but none succeeded. By operating on Equation (III-77) in the manner indicated by Equation III-36, the desired flexural and incremental stiffnesses were

derived. The thermal and plastic moment terms were obtained by means of a prorating of the "edge moments" to the corner points. Both the thermal and plastic moments were assumed constant throughout the plate.

2. Quadrilateral Plate

The quadrilateral plate element is shown in Figure III-7. The relationships for plane stress behavior are those adopted by Turner, et al, in Reference 3, i.e.

$$\sigma_x = a_1 + a_2 y$$

$$\sigma_y = a_3 + a_4 x$$

$$\tau_{xy} = a_5 \qquad \text{(III-78)}$$

There are, in fact, numerous alternatives to these assumptions. In the extensive evaluations of Reference 5, however, it has been found that there are unimportant differences in the results for these alternatives when other than a coarse gridwork of points is involved. By use of the above assumptions and Equation III-15, stiffness equations were formulated for the case of orthotropic material properties. With respect to thermal and plastic forces, it was decided to formulate the required expressions for condition of constant thermal and plastic strain.

A suitable basis for the derivation of the flexure stiffnesses was not to be found elsewhere. The approach adopted was first to assume the following displacement function:

$$w = a_1 x^3 + a_2 x^2 + a_3 x + a_4 y^3 + a_5 y^2 + a_6 y + a_7 x^3 y + a_8 x^2 y + a_9 xy + a_{10} xy^3 + a_{11} xy^2 + a_{12} \qquad \text{(III-79)}$$

Then, by means of Equation (III-36) the appropriate flexural and incremental stiffnesses were derived. Note that (III-79) is "geometrically symmetric", e.g., corresponding to the $a_8 x^2 y$ term there is an $a_{11} xy^2$ term. Also, (III-79) satisfies the appropriate differential equation of equilibrium. To obtain thermal moments, the temperature gradient across the thickness was assumed constant at all points on the surface and corner thermal moments were defined by prorating the distributed edge moments to the corners.

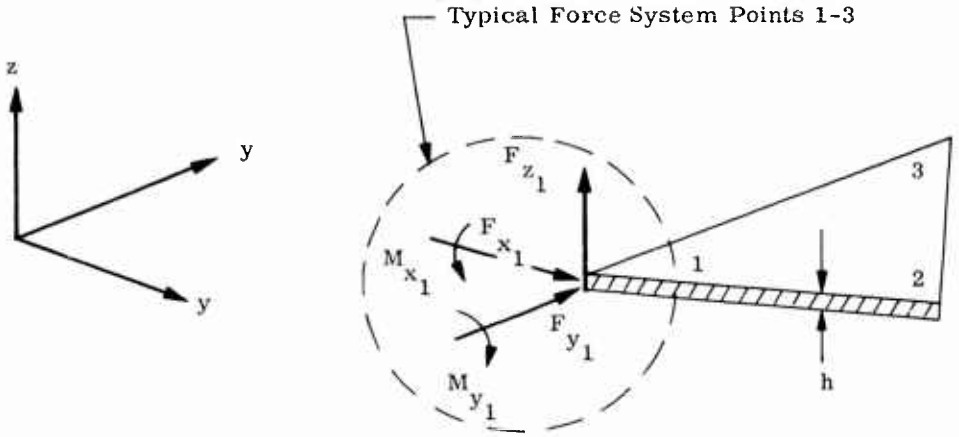

Figure III-6. Triangular Plate Element

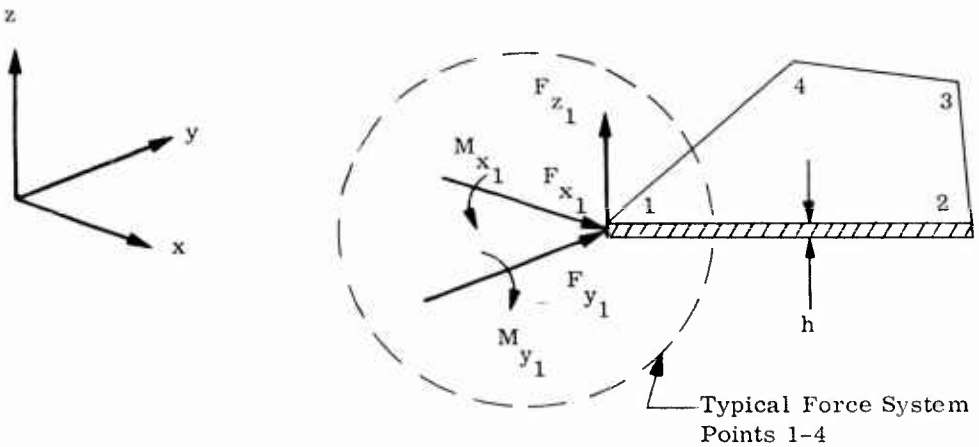

Figure III-7. Quadrilateral Plate Element

CHAPTER IV

PROGRAM FOR THE ANALYSIS OF ONE-DIMENSIONAL STRUCTURES

A. SCOPE

The computer program described in this chapter provides a means for the determination of the stresses, displacements, and instability of structures possessing, cross-sectional dimensions which are small with respect to the length dimension and where the deformational behavior on all cross-sections is governed by elementary beam theory, i.e., the assumption that plane sections remain plane under deformation. In addition to applied loads and thermal gradients, the effects of initial displacements and plasticity can be taken into account.

Figure IV-1 illustrates typical conditions which can be treated with use of the program. The "real" structure appears in Figure IV-1a, while the idealization appears beneath in Figure IV-1b. Each discrete element is a one-dimensional segment of constant cross-section (Figure IV-1c). Comparison of Figures IV-1a and IV-1b discloses the limitations and capabilities of this type of idealization. Lengthwise variations of cross-sectional geometry, as well as temperature conditions, are represented in a stepwise manner. Distributed loads must be defined in terms of statically equivalent concentrated forces at the element juncture points. Support conditions, including flexible support, can be imposed at each node point. The representation of a flexible support consists of "flexible support" (or "restraint") elements. To distinguish between such elements and usual elements (pictured in Figure IV-1c) whenever confusion is likely to result, the latter will be referred to as "conventional" elements.

The force-displacement behavior of a conventional element is segregated into inplane and out-of-plane behavior, respectively. Formulation of the detailed relationships for this element was accomplished in the previous chapter.

The maximum of fourteen conventional elements and four flexible support elements can be employed in the idealization of a structure. Initial displacements of the structure due to fabrication are taken into account by specifying the values of these displacements at the element juncture points.

In order to provide for an arbitrary (but symmetric) geometric and temperature condition on the cross-section of each element, provision is made for the cross-section of each element to be divided into as many as 30 differential areas $d A$. (See Section A-A of Figure IV-1c). A value of temperature can be assigned to each differential area, thereby defining the cross-sectional variation of temperature and also of material properties, since the latter can be defined as being temperature dependent.

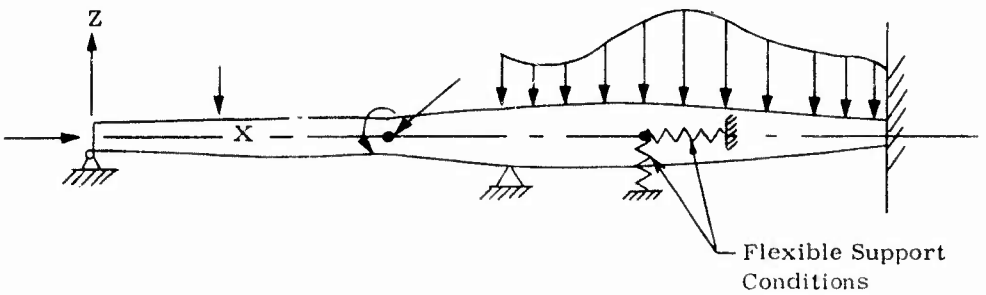

a. Actual Structure

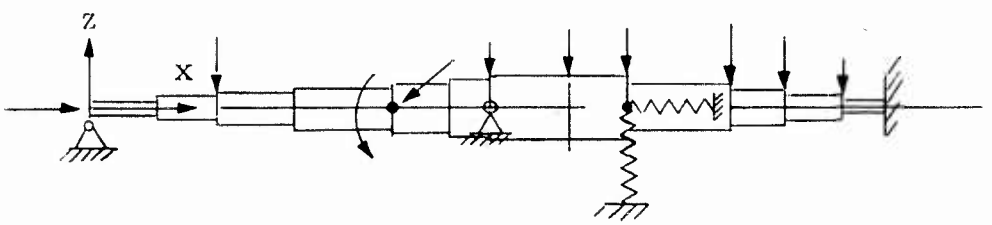

b. Analytical Idealization

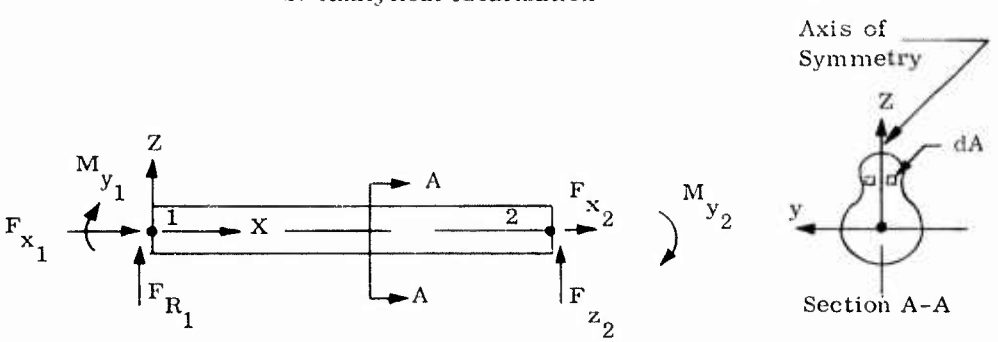

c. Individual Element

Figure IV-1. Conditions for One-Dimensional Analysis Program

Flexible support elements are described by their axial stiffness (ζ_u), lateral stiffness (ζ_w), and flexural (or torsional) stiffness (ζ_θ). These quantities will also be referred to as "restraint coefficients". Each flexible support element is associated with two node points and, in general, displacements of the node point of the restraint element which is not attached to the structure proper is considered as fixed. Support conditions at the other (attached) node point must be specified in conformity with the conditions of the problem at hand.

In general, the input must consist of the data for every element, including all differential areas and their corresponding temperatures. However there are many practical circumstances in which simplified conditions prevail and for certain of these a provision has been made for reduced input. These options are detailed in the report describing input data preparation for the program.

The capabilities for inelastic analysis permit solutions for either time-independent or time-dependent (creep) behavior, or both in combination. The relationships for such analyses are discussed in the next section, where the theoretical basis of the program is outlined. The computational process for inelastic analysis, which differs considerably from the process for elastic and instability analysis, is treated in a later separate section, however,

B. THEORETICAL BASIS

1. Elastic Analysis

The following is a description of the analysis procedure for conditions of linear elastic behavior, including thermal stress, initial displacements, and elastic instability. The terms for inelastic analysis are represented since the procedure for inelastic analysis is essentially a succession of elastic analyses. (The procedures for inelastic analysis are examined in the next section).

As shown in the preceding chapter (Section III.B) the force displacement relationships for the beam-axial force element are

For inplane behavior

$$\left\{F_x\right\} = \left[k_x\right]\left\{u\right\} + \left\{F_x\right\} + \left\{F_x^{\,p}\right\} \qquad \text{(IV-1)}$$

For out-of-plane behavior

$$\left\{\bar{M}_y,\ F_z\right\} = \left[\left[k_z\right] + \left[n_z\right]\right]\left\{\theta_y,\ w\right\} + \left\{\bar{M}_y^{\,\alpha},\ F_z^{\,\alpha}\right\} + \left\{M_y^p,\ F_z\right\} + \left\{M_y^f,\ F_z^f\right\} \qquad \text{(IV-2)}$$

Where

$\{ F_x \}, \{ \bar{M}_y, F_z \}$	are column vectors which list the forces acting upon the ends of the element,
$[k_x], [k_z]$	are the respective elastic stiffness matrices
$\{ u \}, \{ \theta_y, w \}$	are column vectors which list the displacements at the ends of the element.
$\{ F_x^{\alpha} \}, \{ \bar{M}_y^{\alpha}, F_z^{\alpha} \}$	are forces produced by complete restraint of the element against thermal deformations.
$\{ F_x^{p} \}, \{ \bar{M}_y^{p}, F_z^{p} \}$	are forces produced by complete restraint of the element against inelastic deformations.
$\{ \bar{M}_y^{f}, F_z^{f} \}$	are equivelent forces dependent on the presence of fabricational displacements at the ends of the element.
$[n_x]$	"Incremental Stiffness" - the influence of the axial loads on flexural behavior.

The detailed form of these matrices was presented in Chapter III. There, it was shown that each matrix on the right side of Equations (IV-1) and (IV-2) contains a scalar multiplier which is an integral to be evaluated over the area of the cross section. $[k_x]$, for example, contains the scalar $\frac{\int E \cdot dA}{\ell}$, while $[k_z]$ has the multiplier $\frac{2 \int \xi^2 E \cdot dA}{\ell^3}$.

The evaluation of the above integrals is accomplished through a subdivision of the cross section of each element into differential areas. As noted earlier, the element cross section can be subdivided into as many as thirty differential areas; the temperature variation on the cross section is represented by assigning an average temperature to these areas. Since the material properties are representable as a function of temperature, the computer selects for each differential area those properties which are consistent with the temperature of that differential area.

Based on geometric, load, temperature, and material property data of the problem and the selected analysis options the computer evaluates the pertinent portions of Equations (IV-1) and (IV-2) for each element. The individual element relationships are then assembled, in satisfaction of node point equilibrium and compatibility requirements (See Chapter II), and geometric boundary conditions are applied to yield a set of equations for the assembled "analytical model".

Once the stiffness equations have been formulated the analysis process can take one of many forms, dependent upon the exercise of available options, but in the following discussion it will be assumed that none of the possible analysis operations, except those pertaining to inelastic behavior, are to be eliminated. (Analysis for inelastic behavior is discussed in the next section). In such a case, the relationships for the complete structure can be written in matrix form as:

For axial behavior

$$\left\{P_x\right\} = \left[K_x\right]\left\{u\right\} + \left\{P_x^{\alpha}\right\} + \left\{P_x^{p}\right\} \qquad \text{(IV-3)}$$

For flexural behavior

$$\left\{M_y, P_z\right\} = \left[K_z\right]\left\{\theta_y, w\right\} + \left[N\right]\left\{\theta_y, w\right\} + \left\{M_y^{\alpha}, P_z^{\alpha}\right\} + \left\{M_y^{p}, P_z^{p}\right\} + \left\{M_y^{f}, P_z^{f}\right\} \qquad \text{(IV-4)}$$

These equations are presented in general form in Chapter III as Equations (II-12) and (II-13).

In the first step of the solution process the axial displacements, $\left\{u\right\}$, are determined by inversion of the $\left[K_x\right]$ matrix in Equation (IV-3).

Thus:

$$\left\{u\right\} = \left[K_x\right]^{-1}\left\{P_x - P_x^{\alpha} - P_x^{p}\right\} \qquad \text{(IV-5)}$$

These axial displacements ($\left\{u\right\}$) are substituted back into the element relationships (Equation IV-1) to yield the element node point forces ($\left\{F_x\right\}$), from which the axial stress resultants are obtained.

The influence of the axial forces is accounted for in the flexural analysis. The matrix $\left[N\right]$ is a function of the axial loads and can be evaluated after the inplane analysis is complete. The solution for the flexural displacements follows as:

$$\left\{\theta_y, w\right\} = \left[\left[K_z\right] + \left[N\right]\right]^{-1}\left\{\left\{M_y, P_z\right\} - \left\{M_y^{\alpha}, P_z^{\alpha}\right\} - \left\{M_y^{p}, P_z^{p}\right\} - \left\{M_y^{f}, P_z^{f}\right\}\right\} \qquad \text{(IV-6)}$$

These flexural displacements and the previously determined axial stress resultants are employed in the direct determination of the stresses on each of the differential areas of each structural element.

To accomplish a determination of a critical load it is first necessary to specify a Reference Critical Load Value-P_{ref}. All element axial loads are normalized on this value through the relation

$$F_n = \lambda_n \quad P_{ref} \tag{IV-7}$$

where F_n is the axial stress resultant on the nth structural element.

Equation (IV-4) then appears as:

$$\left\{M_y, P_z\right\} = \left[\ K_z\ \right] \left\{\theta_y, w\right\} + P_{ref}\left[N\right] \left\{\theta_y, w\right\} + \left\{M_y^a\ ,\ P_z^a\right\} + \left\{M_y^p\ ,\ P_z^p\right\} + \left\{M_y^f,\ P_z^f\right\} \tag{IV-8}$$

$\left[\ N\ \right]$ now contains the λ_n values, rather than the F_n values.

The condition of elastic instability derived from Equation IV-8 is

$$\frac{1}{P_{ref}} \left\{\theta_y, w\right\} = \left[\ K_z\ \right]^{-1}\left[N\right] \left\{\theta_y, w\right\} \tag{IV-9}$$

Application of matrix iteration to this condition yields the minimum P_{ref} and corresponding mode shape for instability.

With regard to the selection of the reference axial load, the program allows for two possibilities. In one, the reference axial load is automatically set equal to the axial force computed in a designated element. Alternatively, the value of the reference load can be designated.

Once the critical reference axial load, P_{ref} has been computed, the distribution of critical axial forces, as obtained from Equation (IV-7), is given by:

$$F_{n_{cr}} = \lambda_n \quad P_{ref_{cr}} \tag{IV-10}$$

Neither the foregoing discussion nor Chapter III has given explicit consideration to the treatment of flexible support elements. Flexible support conditions at a node point are simulated by means of this special type of element which, as in the case of the conventional element, is associated with two node points and three stiffnesses, one each in the direction of the three displacement degrees of freedom. These three stiffnesses (or "restraint coefficients"), ζ_u, ζ_w, and ζ_θ, are defined as follows:

For axial behavior:

$$\Delta F_x = (\zeta_u)\ \Delta u \tag{IV-11}$$

For lateral behavior

$$\Delta F_z = (\zeta_w)\,\Delta w \tag{IV-12}$$

and, for rotational behavior

$$\Delta M_y = (\zeta_\theta)\,\Delta\theta \tag{IV-13}$$

Note that the three restraint coefficients are independent of each other. It is left to the analyst to decide upon the values of these coefficients. By analogy with the stiffness matrices for a conventional element, the stiffness matrices for a restraint element are:

For axial behavior:

$$\left[k_x \right] = \begin{bmatrix} \zeta_u & -\zeta_u \\ -\zeta_u & \zeta_u \end{bmatrix} \tag{IV-14}$$

and, for flexure.

$$\left[k_z \right] = \begin{bmatrix} \zeta_\theta & -\zeta_\theta & 0 & 0 \\ -\zeta_\theta & \zeta_\theta & 0 & 0 \\ 0 & 0 & \zeta_w & -\zeta_w \\ 0 & 0 & -\zeta_w & \zeta_w \end{bmatrix} \tag{IV-15}$$

Effects of initial displacements due to fabricational inaccuracies accounted for by the inclusion of a column matrix, $\left\{ \theta^f, w^f \right\}$, composed of initial rotational (θ^f) and lateral (w^f) deflections determined at each node point. These initial deflections are measured relative to a straight line which passes through the x-axis of the one-dimensional structure. Total deflections are determined as the addition of the fabricational deflections and the deflections computed from Equation IV-6.

2. Inelastic Analysis

It is intended that this program be capable of solving inelastic problems wherein the loads and temperatures vary with time, as sketched below. For analytical purposes and to avoid the necessity of listing large quantities of time increments that may be required in the computations, points in a given load-temperature history are first specified. These points are illustrated by the heavily dashed lines in the sketch below; the distance between points are termed time intervals in this report. Each time interval may then be further subdivided into equal time increments which may differ for each interval.

In an earlier development of the matrix displacement method to permit inelastic analyses (Reference 9) the approach suggested was based on the selection of time increments small enough so that a single computation cycle for

(or pertaining to) the time increment would suffice to determine accurately inelastic strains, both time independent and creep strains. However, to afford greater flexibility and possibly more accuracy under certain conditions, it is proposed here that time-independent plastic strains be computed at the ends of each time increment (i.e., at specific times in the history) by either an accumulative step-by-step or iterative process. Creep strains, on the other hand, are computed within a time increment based on the assumption of constant stress and average temperature conditions. For creep determinations the stress is taken equal to the stress which prevails at the start of a time increment.

There are no limits on the number of time intervals and increments which can be used in an analysis; the number of accumulative steps or iterations performed at a given time in the load-temperature history in an inelastic analysis are limited, however, by a specified convergence criterion with regard to the stresses.

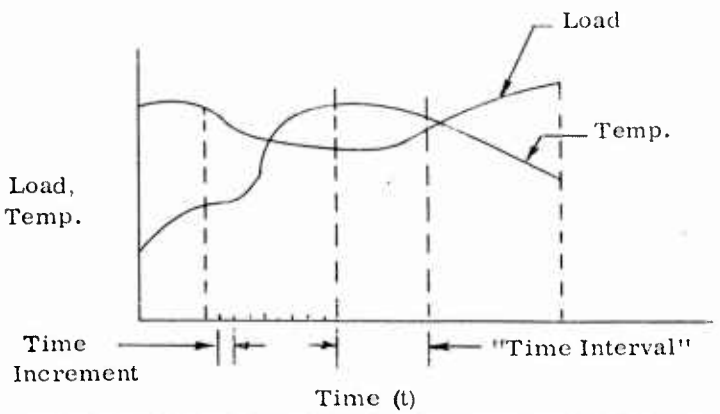

The time-independent plastic strain component of the total strain ϵ_e obtained in a conventional uniaxial specimen test is assumed representable by the following expression

$$\epsilon_{ep} = \left(\frac{\sigma}{\psi}\right)^n \qquad \text{(IV-16)}$$

where n and ψ are temperature dependent material properties, determined, in the analysis, from the pertinent material property versus temperature curve.

There are two options in the analytical procedure for determining plastic strains with the aid of Equation IV-16. These are designated as Methods A and B, respectively. Method A involves an accumulative step-by-step process and is based on the analytical assumption that the change in plastic strain induced at a point in the structure subject to the stress σ', can be approximated as $\Delta\epsilon'_{ep}$, shown in Figure IV-2a. In general, the plastic strain change determined in this manner will be an underestimation of the true plastic strain change and is considered as the first

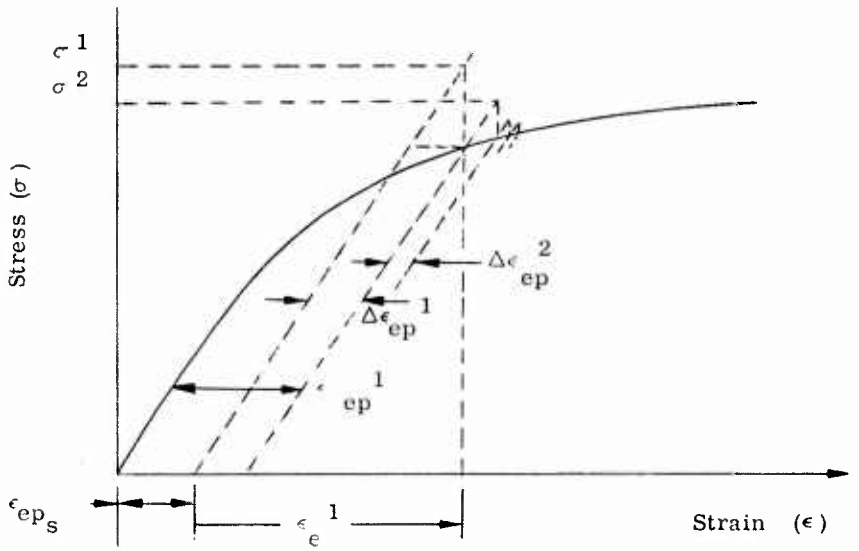

(a) Method A

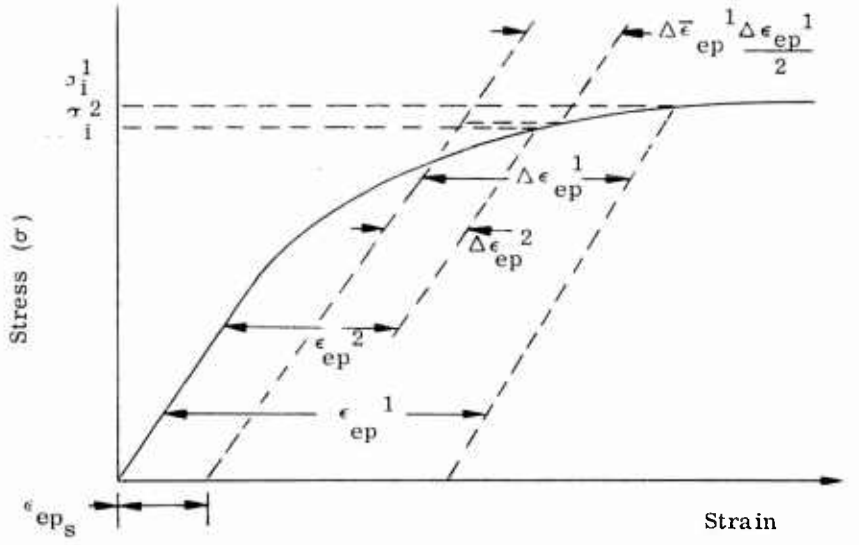

(b) Method B

Figure IV-2. Methods of Computation of Time-Independent Plastic Strains

step toward the computation of the actual plastic strains. The plastic strain is added to the previously determined total plastic strain (ϵ^{1}_{ep}) to determine new stresses σ^{2} for the same temperature and load condition. Additional plastic strain changes, $\Delta\epsilon^{2}_{ep}$, are computed and new stresses determined. This accumulative process is continued for either a specified number of approximations or until the stresses in successive approximations are in agreement to within a certain number of significant digits as specified by the analyst.

Method B is an iterative procedure for determining the plastic strain change and is shown in Figure IV-2b. As a first approximation, the plastic strain change, $\Delta\epsilon^{1}_{ep}$, is determined for the stress σ^{1}. In general, the plastic strain change so determined will be an overestimation of the true value in regions of higher stress in a given structural stress distribution. The strain change, $\Delta\epsilon^{1}_{ep}$, is then employed together with the previously determined value (which initially is zero) to compute an average strain change, $\Delta\epsilon^{1}_{ep}$, which is used to obtain the next approximation to the stress, σ^{2}. This iterative process is continued until convergence conditions specified on the stresses are satisfied. It will be noted that for Method B the plastic changes are replaced by new values with each computational cycle but for Method A, they are accumulated after each cycle.

The preferred method to employ in a particular plastic analysis will depend to a large extent on the stress strain curve and the details of the structural configuration and loading. For materials which exhibit ideally plastic characteristics (i.e. $n = \infty$) Method A must be adopted. For highly redundant or thermally strained structures, Method A is preferable, but for situations in which the stresses are somewhat linearly related to the external loading, Method B is recommended. However, it should be realized that either method should yield identical results in the limit.

The computational procedures employed to predict the accumulation of time-independent plastic strains will now be briefly outlined. Consideration is given to the ith time t_i in the load-temperature history condition under investigation for a given structure. Since, as discussed previously, several approximations are computed at time t_i a particular approximation to a quantity at time t_i will be denoted by the superscript j.

In Method A, the steps are as follows:

(1) The increment of plastic strain developed during the (j-1) th approximation is added to that previously accumulated to establish a total plastic strain ($\epsilon^{j}_{ep_{T_i}}$) pertinent to the jth approximation. Accumulated

strains associated with the strain hardening history are also evaluated.

(2) The total plastic strains ($\epsilon^{j}_{ep_{T_i}}$) are transformed into the related element plastic forces $\left\{ F_x^p \right\}$ and $\left\{ M_y^p, F_z^p \right\}$ and solutions for the associated stresses (σ^{j}_{i}) and elastic strain components ($\epsilon^{j}_{e_i}$) are effected with use of the matrix method discussed in the previous section.

(3) The signs (tension or compression) of the stresses in the (j-1)th and (j)th approximations are compared with each other. If the sign reverses the accumulated strain due to strain hardening is set equal to zero.

(4) Using Equation IV-16, the accumulated strain due to strain hardening, and the elastic strain component, a series of operations is performed which leads to the plastic strain change ($\Delta\epsilon^{j}_{ep_i}$) pertinent to the jth approximation.

The result of step (4) is employed in step (1) for the (j + 1)th approximation. The process is continued until the stresses of step (2) are in agreement with the stresses of the previous approximation in accordance with a specified criterion.

For Method B, the computational sequence is as follows:

(1) The average increment of plastic strain ($\Delta\epsilon_{ep}$) determined in the (j-1)th iteration is added to the total plastic strain as computed for the (i-1)th time increment to define a new approximation to the total plastic strain, $\epsilon^{j}_{ep_{T_i}}$.

(2) The new approximation to the total plastic strain is then used in the determination of the (j)th iteration stresses, in the same manner as step (2) of Method A.

(3) The magnitude of the plastic strain change for the (j)th iteration is developed with use of Equation (IV-16), the stresses determined in (2), and $\epsilon^{j}_{ep_{T_i}}$. This procedure for this determination differs from that of step (3) of Method A.

(4) The (j)th approximation to the average plastic strain change is computed and the process of steps (1)-(3) is repeated. The iterative sequence is continued until the specified convergence criteria on stress is satisfied.

The creep analysis capabilities of the subject program are based, in part, on the following assumptions regarding the mathematical representation of conventional uniaxial Constant Stress-Constant Temperature creep properties.

(1) The primary stage of the conventional creep curve is represented by the following relationship

$$\epsilon_c = \beta \ (e^{B\sigma} - 1)t^m \qquad \text{(IV-17)}$$

(where e is the base for natural logarithms)
whereas, in the secondary stage one has the minimum creep rate
$(\dot{\epsilon}_c = \frac{d\epsilon}{dt}_c)$ expressed as

$$\dot{\epsilon}_c = \omega \ (e^{B\sigma} - 1) \qquad \text{(IV-18)}$$

where β, B, m and ω are temperature dependent properties of the material. By equating the creep rate, as obtained by differentiation of Equation IV-17 with respect to time, to the creep rate of Equation IV-18, an expression for the transition time, $\bar{t}$, between primary and secondary creep is obtained as

$$\bar{t} = \left(\frac{\omega}{m\beta}\right)^{\frac{1}{m-1}} \qquad \text{(IV-19)}$$

Intrinsic in Equation IV-19 is the assumption that the transition time is only a function of the temperature and not the stress level.

(2) There exists a threshold temperature, $\bar{T}_c$, below which there is no creep strain, irrespective of the magnitude of the imposed stresses.

There are various methods available for predicting the accumulation of creep strains for the general condition of varying stresses and temperatures of interest here. The method adopted for the present program is referred to as the "strain hardening rule" which is fully explained in Reference 9. The overall computational procedure is outlined below for the ith time increment.

(1) Computations are initiated by the determination of the average temperature, $\overline{T}_i$, for the time increment, from

$$\overline{T}_i = \frac{T_i + T_{i-1}}{2} \qquad \text{(IV-20)}$$

where T_i and T_{i-1} are the temperatures obtained at times t_i and t_{i-1}, respectively, from the initially specified temperature-time curve. The average temperature is next compared with the creep threshold temperature, $\overline{T}_c$. If $\overline{T}_i > \overline{T}_c$ and there is no loss of creep strain hardening due to a stress reversal, there is a change in creep strain, $\Delta \epsilon_{c_i}$, for the time increment, Δt_i. This change is added to the total creep strain accumulated prior to the interval to yield a new total accumulated creep strain. If, on the other hand, $\overline{T}_i \leq \overline{T}_c$, the change in creep strain within the interval is zero and the total accumulated creep strain from the previous interval is carried on into the next interval.

(2) Next, the transition temperature $\overline{t}_i$ is computed from Equation IV-19 with material properties obtained for the average temperature, $\overline{T}_i$. The type of creep (primary or secondary) induced during the time increment is determined by comparing $\overline{t}_i$ with an equivalent creep time parameter $t_{c_{i-1}}$ computed from the following expression derived from Equation IV-17 (See Reference 9).

$$t_{c_{i-1}} \left[\frac{\left| \epsilon_{c_{s_{i-1}}} \right|}{\beta_i \left(e^{B \left| \sigma_{i-1} \right|} - 1 \right)} \right]^{\frac{1}{m}} \qquad \text{(IV-21)}$$

where $\epsilon_{c_{s_{i-1}}}$ is the creep strain accumulated by virtue of strain hardening (also computed in step (1)).

(3) If $t_{c_{i-1}} < \overline{t}_i$ primary creep prevails and the magnitude of the creep change, $\Delta \epsilon_{c_i}$ is given by

$$\Delta_{c_i} = \epsilon_{c_i} - \left| \epsilon_{c_{s_{i-1}}} \right| \qquad \text{(IV-22)}$$

where ϵ_{c_i} is obtained from Equation IV-17, written as follows

$$\epsilon_{c_i} = \beta_i \left(e^{B_i \left| \sigma_{i-1} \right|^{-1}} \right) \left(t_{c_{i-1}} + \Delta t_i \right)^m \qquad \text{(IV-17a)}$$

The creep change is then given the same sign as the stress, σ_{i-1}. If, on the other hand, $t_{c_{i-1}} > \bar{t}_i$ secondary creep is indicated and the change in creep strain is given by

$$\Delta \epsilon_i = \dot{\epsilon}_{c_i} \Delta t_i \qquad \text{(IV-23)}$$

where the creep rate $\dot{\epsilon}_{c_i}$ is obtained from Equation IV-18.

(f) Finally, the total creep strain, $\epsilon_{c_{T_i}}$, is determined as the sum of this change in creep strain and the prior total creep strain and employed in the determination of the inelastic node point forces and a stress analysis is performed in the manner described in the previous section.

C. ILLUSTRATIVE EXAMPLES

1. Comparison with Alternate Solutions

The objectives in presenting the following illustrative examples are to

(1) Outline the various types of results that can be obtained through exercise of the respective program options, and

(2) Demonstrate the level of accuracy of solutions achieved through use of the program.

To achieve the second objective it is necessary to effect comparisons with solutions obtained through alternate techniques. Since these other techniques are limited in applicability to relatively simple conditions the following comparative discrete element solutions are necessarily concerned with simple conditions. The capabilities of the program with respect to irregular geometry, nonuniform load, etc., are therefore not demonstrated in these analyses but, in the next section, a complicated problem for which only limited comparative results are available is presented.

The following analyses are performed in the present section

(1) Stress and Deflection Analyses

(a) Beam-column, elastic
(b) Beam-column, inelastic with initial displacements.

(2) Instability Analyses

(a) Elastically restrained column-thermal buckling
(b) Tapered column subjected to a distributed load.
(c) Column on four supports.

a. Stress and Deflection Analyses

(1) Beam-Column

Figure IV-3a illustrates the conditions for the analysis of a simple beam-column problem. The structure shown is loaded by an axial force (P_X) that is equal in value to three-fourths of the Euler critical load, P_E, i.e.

$$P_X = \frac{3}{4} P_E = \frac{3}{4} \frac{\pi^2 EI}{L^2} \qquad \text{(IV-24)}$$

The relationship between transverse applied loads (in this case a concentrated load (P_Z) at midspan) and displacement is linear in the presence of a fixed midplane force. Thus, the present results are representable in nondimensional form.

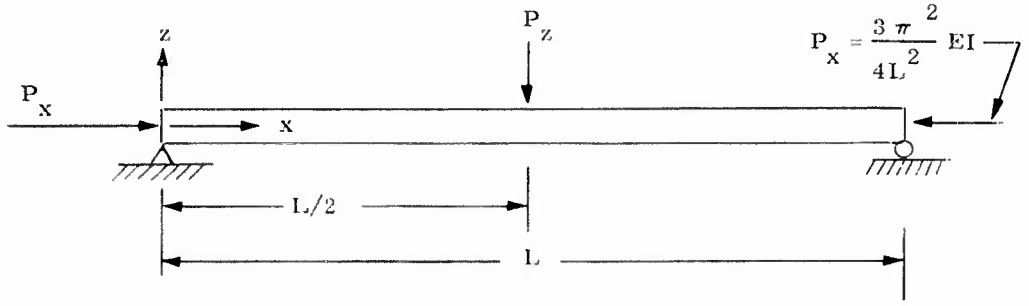

a. Conditions of Analysis

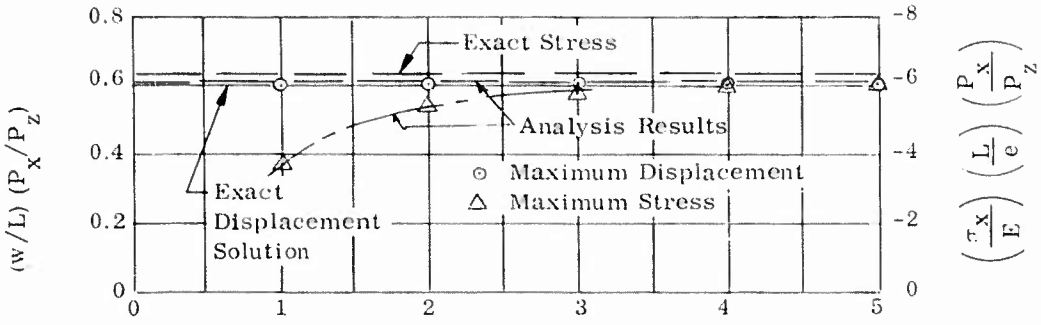

Number of Elements in Semispan

b. Comparison of Maximum Stresses and Deflections

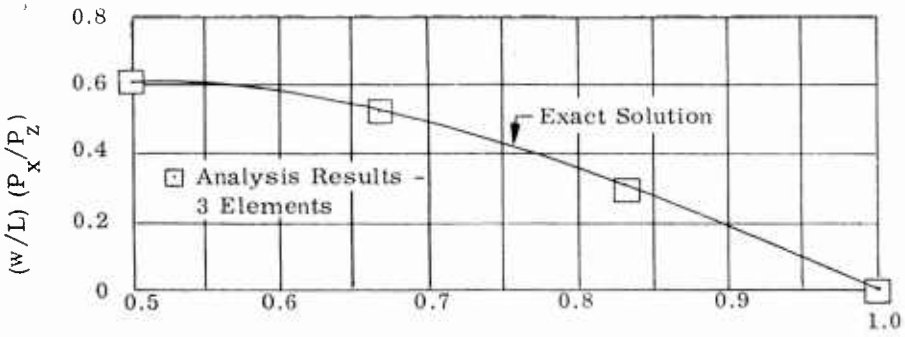

c. Comparison of Deflected Shapes

Figure IV-3. Analysis of Beam Column

Listed below are the values of maximum deflection (deflection at midspan) and of maximum bending stress at midspan as calculated for idealizations consisting of various numbers of elements. Due to symmetry it was possible to treat only one half the span. The parameters employed in defining these values were chosen in correspondence with the exact solutions, which can be written as follows:

$$\left(\frac{w}{L}\right)\left(\frac{P_x}{P_z}\right) = \frac{\left(\sin \frac{\pi}{2}\sqrt{\lambda}\right)\left(\sin \frac{\pi}{L}\sqrt{\lambda}\right)}{\pi\sqrt{\lambda}\ \sin \pi\sqrt{\lambda}} - \frac{x}{2L} \qquad \text{(IV-25)}$$

$$\left(\frac{\sigma_x}{E}\right)\left(\frac{L}{e}\right)\left(\frac{P_x}{P_z}\right) = \frac{\pi\sqrt{\lambda}\ \left(\sin \frac{\pi}{2}\sqrt{\lambda}\right)\left(\sin \frac{\pi x}{L}\sqrt{\lambda}\right)}{\sin \pi\sqrt{\lambda}} \qquad \text{(IV-26)}$$

where $\lambda = \dfrac{P_x}{P_E}$ (IV-27)

and e is the distance between the neutral axis and the extreme fiber in compression.

Also tabulated below are the percentages of error with respect to the exact solution. Figure IV-3b plots the degree of correspondence of the calculated and exact solutions as a function of the number of elements employed. There is extremely close agreement even for the crudest idealization. There is also excellent agreement between the deflected shapes computed using the exact solution and the solution based on three elements in the semispan, as illustrated in Figure III-3c.

No. of Elements Per Semispan	Max. Displacement $\left(\frac{w}{L}\right)\left(\frac{P_x}{P_z}\right)$	% Error	Max. Stress $\left(\frac{\sigma_x}{E}\right)\left(\frac{L}{e}\right)\left(\frac{P_x}{P_z}\right)$	% Error
1	-0.6006	1.72	-3.722	41.55
2	-0.6096	0.25	-5.437	14.62
3	-0.6102	0.15	-5.848	8.17
4	-0.6103	0.13	-6.017	5.51
5	-0.6103	0.13	-5.106	4.11

b. Beam-Column, Inelastic, with Initial Displacements

Sketched below is a simply supported axially loaded beam with initial displacements (w_o) of the form

$$w_o = 0.005 \sin \frac{\pi x}{20}$$

The beam is assumed to be heated instantaneously to a uniform temperature of 400°F. An axial load of 3750 pounds is then applied and sustained at this value. For simplicity, the cross-section of the beam is assumed to be composed of two area elements, each equal to 0.125 in.^{2}. Since there is symmetry, it is only necessary to consider half the beam, idealized as five elements of equal length. Numerical values used for the material constants are

$n = 12$	$\beta = 0.72 \times 10^{-6}$ in/in
$\omega = 0.158 \times 10^{-6}$	$B = 0.000238$ in/psi
$m = 0.72$	$\psi = 0.65 \times 10^5$ psi
$E = 9.1 \times 10^7$ psi	$\alpha = 13.25 \times 15^6$ in/in/°F

These values are representative of 2024-T4 Aluminum (See Reference 9).

Upon application of the axial load, the beam deflects elastically with a total theoretically-predicted deflection at the center (w_c) given by

$$w_c = \frac{(w_o)_{max}}{1 - P/P_E}$$

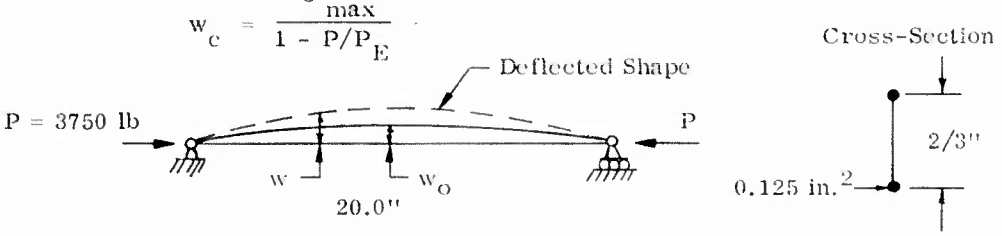

where $P_E = \pi^2 \frac{EI}{L^2}$. For the beam under consideration, with $(w_o)_{max} = 0.005$ in., the above expression gives a central deflection of $w_c = 0.012359$ in., whereas the program yielded a value $w_c = 0.012540$ in.

The applied load was selected small enough so that upon its initial application only elastic strains are experienced. With the passage of time, however, creep strains are sustained. These increase the deflections and bending moments and, therefore, the stresses. This eventually results in plastic strain.

Results of the application of the computer program to this problem are presented in Figures IV-4 and IV-5. Since the optimum time increment, Δt, was not known, computations were performed for decreasing time increments. Method B was employed in the computation of time-independent plastic strains and three-digit agreement on the corresponding stresses was specified.

Computed total lateral deflections at the center of the beam, presented as a function of time in Figure IV-4a, are similar to those obtained in various experiments (see, for example, Reference 11). Based on the results shown, it appears that the column becomes unstable at a critical time of 49 hours. As shown in Figure IV-4b, the cross-sectional area on the convex side of the column experiences a stress reversal at the critical time. Immediately prior to the critical time the lateral deflection is finite.

Inelastic strains computed for the center section of the beam are shown as a function of time in Figure IV-5. As indicated, time-independent plastic strains are induced only during the final stages of the deformation process.

b. Instability Analysis

(1) Elastically Restrained

The analysis condition is shown below in Figure IV-6a. The beam is simply supported at the left end but at the right end is elastically restrained by a torsional spring; transverse and axial deflections at the right end are prevented. The end restraint is assigned the following value.

$$\zeta_\theta = 77 \times 10^4 \text{ rad/lb in.}$$

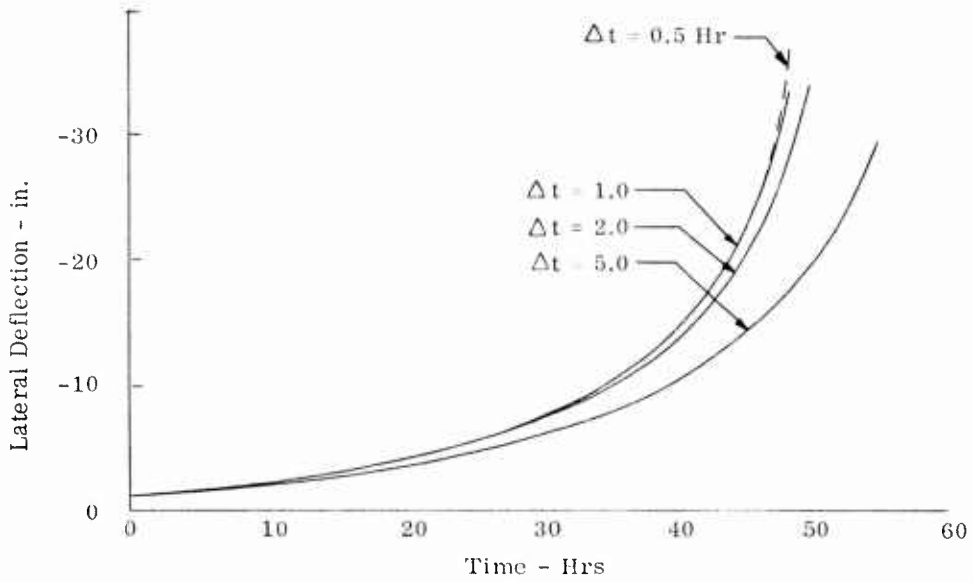

Figure IV-4. Total Lateral Deflection at Center of Beam

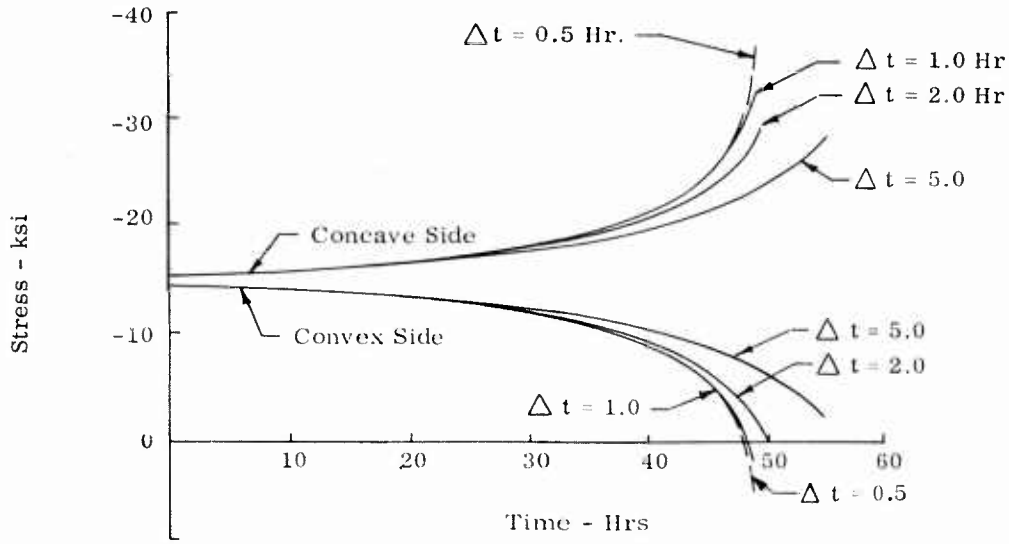

(a). Stresses at Center Section

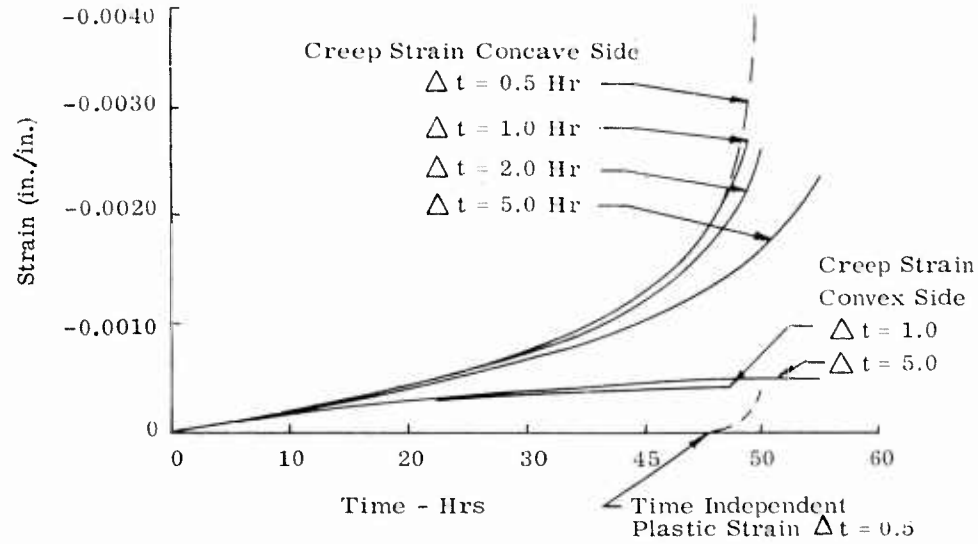

(b). Strains at Center Section

Figure IV-5. Axially Loaded Beam - Stress and Strain History

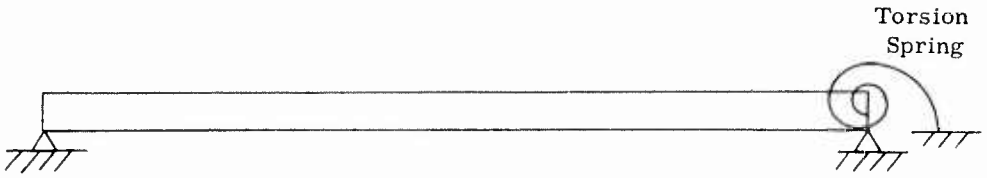

a. Condition of Analysis

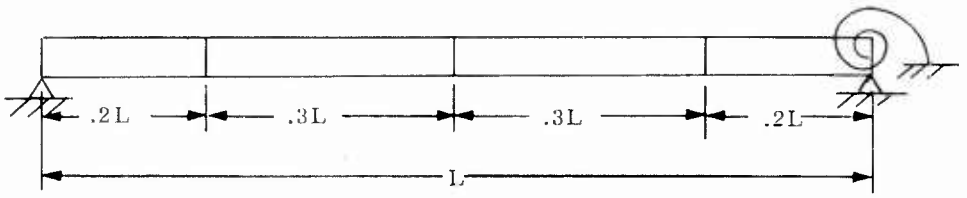

b. Structural Idealization

Figure IV-6. Elastically Restrained Column

The beam is assumed to undergo a temperature change (ΔT) from the stress free state. It is required to determine the value of ΔT for elastic instability.

The element spacing chosen for analysis is illustrated in Figure IV-6b; this spacing was selected in an entirely arbitrary manner. Based on these dimensions, the computations resulted in

$$\Delta T_{cr} \quad \frac{14.58\ I}{\alpha\ L^2} \tag{IV-28}$$

where α is coefficient of thermal expansion. By adapting a solution presented in Reference 12 , one can obtain a comparison solution of

$$\Delta T_{cr} = \frac{14.6\ I}{\alpha\ L^2} \tag{IV-29}$$

It is seen that the difference between the two solutions is insignificant, despite the arbitrary choice of element spacing.

(2) Tapered Column Subjected to Distributed Load.

A problem that represents a measure of complexity but which is nevertheless solvable in closed form is that which involves the prediction of the instability of a tapered cantilevered column subjected to a triangular distributed load (see Figure IV-7a). The moment of inertia varies in accordance with the expression.

$$I = I_o(1 - \frac{x}{L}) \tag{IV-30}$$

where I_o is the moment of inertia at the support. The expression for the variation of "shear load" (q) is

$$q = q_o\ (1 - \frac{x}{L}) \tag{IV-31}$$

The idealization for analysis is shown in Figure IV-7b. The distributed loading was replaced by a series of concentrated loads at the node points and for convenience the reference critical load (P_{ref}) was chosen as the axial load in the element adjacent to the support.

The significance of the approximation of the distributed load by a series of concentrated loads can be reduced by developing the relationship between q_o and the axial load in the element near the root. This relationship is

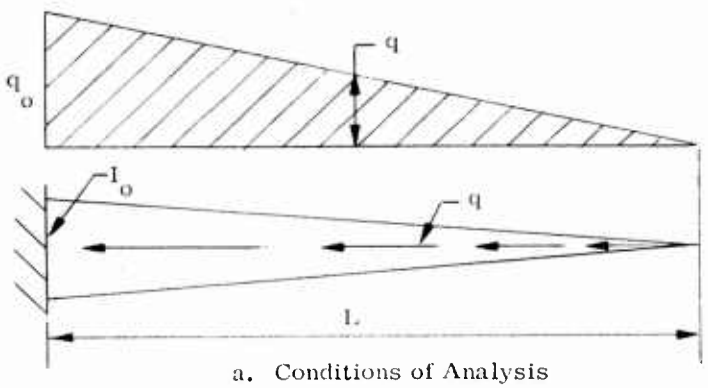

a. Conditions of Analysis

b. Analytical Idealization

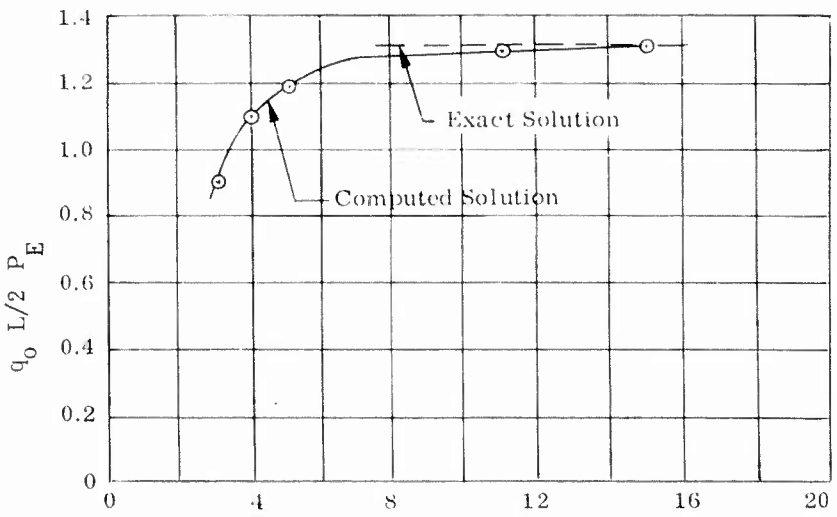

c. Results

Figure IV-7. Buckling of a Tapered Column Subjected to a Triangular Distributed Axial Load

$$\left(\frac{q_o L}{2}\right)_{cr} \quad P_{ref} \Big/ \left[1 - \frac{(3N-4)}{3(N-1)^2} \right]$$

where N is the number of node points in the idealization. Thus, the evaluated critical reference loads are divided in the indicated manner to obtain the calcualted critical value of distributed load. For purposes of comparison with the exact solution, the results of analyses for various numbers of node points are shown below. For purposes of comparison with the exact solution as given in Reference 12, pg 139, the results are presented in the form of the ratio between $(q_o L/2)_{cr}$ and the Euler critical load ($P_E = \frac{\pi^2 E I_o}{L^2}$) of a simply supported beam of the same length and moment of inertia I_o. The "exact" value of this ratio is 1.317. Figure IV-7c gives a graphical representation of the results. Note that in contrast with uniform load and geometry conditions, the present case requires 10 node points to reduce the error below engineering significance.

Number of Node Points	$\frac{q_o L}{2} \Big/ P_E$ (calculated)	% Error*
3	0.912	+30.7
4	1.117	+15.2
5	1.201	+ 9.7
11	1.299	+1.41
15	1.308	+ 0.7

$$*\% \text{ Error} = \frac{1.317 - \frac{q_o L}{2} \Big/ P_E}{1.317}$$

(3) Column on Four Supports

As an example of a more complicated instability problem, the case of the uniform section column, supported at four points, has been solved. The conditions of analysis are illustrated in Figure IV-8. The outer ends are simply supported while the two inner supports are elastically restrained. Solutions for this problem were developed by Klemperer and Gibbons (Reference 13) and described by Timoshenko in Reference 10, pg. 107.

In performing the present analyses, two gridworks were employed: a subdivision of each segment between supports into three elements, and also a subdivision into four elements. The rigidity of the supports is defined by the restraint coefficient, ζ_w. However, for purposes of data representation it is preferable to embody this consideration into a "support rigidity parameter", defined as $\frac{\zeta_w L}{P_E}$,

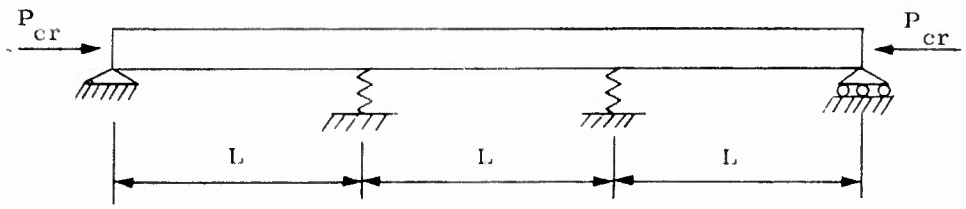

a. Problem Data

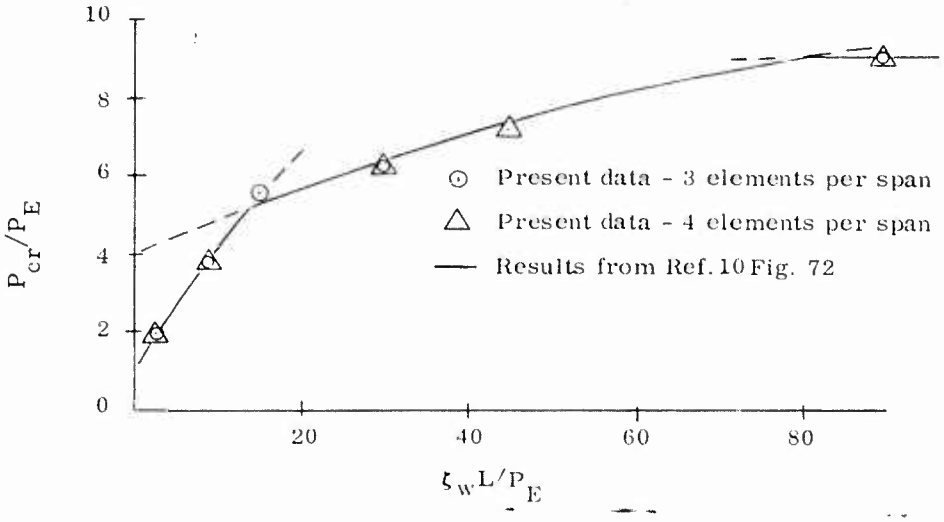

b. Critical Loads

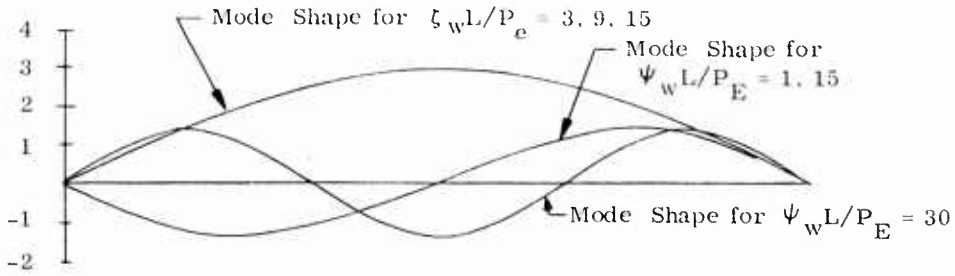

c. Mode Shapes

Figure IV-8. Instability Analysis of a Column on Four Supports

where P_E is the Euler critical load for a single span, $P_E = \frac{\pi^2 EI}{L^2}$. The results, expressed as the ratio between the critical value of the applied load, P_{cr}, and P_E are tabulated below for a wide range of support rigidity parameters and are plotted in Figure IV-8b.

Figure IV-8b also shows the results presented in Reference 10, Figure 72. There is extremely close agreement between the present results and those given in Reference 10. It is noteworthy that three distinct relationships between the parameters, P_{cr}/P_E, and $\zeta_w L/P_E$, governed by three different mode shapes, are involved. These mode shapes, as determined by the output of the present analyses, are shown in Figure IV-8c; their regions of occurance, as defined in Reference 10, are shown in Figure IV-8c. It is noteworthy that, for values of support rigidity parameters that lie within the center region and near the curve intersections it was difficult to obtain convergence to the lowest root. Support rigidity parameter values in excess of 80 required over 150 iterations for convergence.

Support Rigidity Parameter $\frac{\zeta_w L^3}{\pi^2 EI}$	$\frac{P_{cr}}{P_E}$	
	3 Elements Per Span	4 Elements Per Span
3	1.910	1.909
9	3.718	3.717
15	5.506	——
30	6.151	6.147
45	——	7.105
90	9.014	9.005

2. Analysis of Practical Complex Conditions

As an example of the analysis of a complex indeterminate one-dimensional structure for thermal stress and applied load, the conditions illustrated in Figure IV-9a are examined. The conditions shown were analyzed for support reactions in Reference 14. The present analysis considers not only the equilibrium solution for stress and displacement but also solves for one form of elastic instability.

The discrete element idealization employed appears in Figure IV-9 b and c. The entire length of the structure is divided into nine elements each of which is assigned 10 differential areas. In addition, there is a flexible axial support at the right end. The material properties are specified as: $E = 10^7$ psi, and $\alpha = 10^{-5}$ in./in.$^\circ$F, while the temperature distribution is

$$T = 2x + (0.4x^2 - 2x)\xi \qquad 0 < x < 10 \qquad \text{(IV-33)}$$

$$T = 20 + 20\xi \qquad 10 < x < 20 \qquad \text{(IV-34)}$$

(It is assumed that the temperature in the stress-free state, T_o, is 0°F). Thus, the temperatures vary both in the axial and depthwise directions. In the left span, the temperatures on each differential area of an element take on the value at the center of the element.

Results are presented in Figure IV-10. The support reactions are in close correspondence with the results of Reference 14 (see Figure IV-10a). The differences between the two sets of values are due to the fact that the Reference 14 results are obtained from an essentially "closed form" solution while the present values include discretization errors. The variation of extreme fiber stresses associated with these reaction forces is also shown in Figure IV-10a.

Figure IV-10b shows the displacement patterns due to temperature alone, temperature and applied load combined, and buckling.

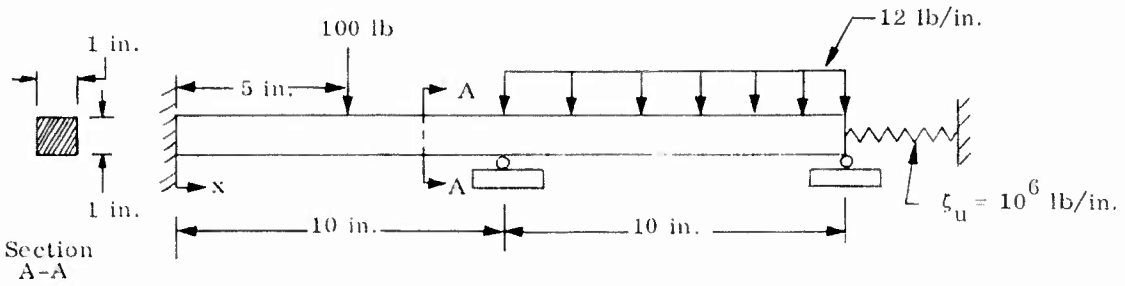

a. Given Conditions of Analysis

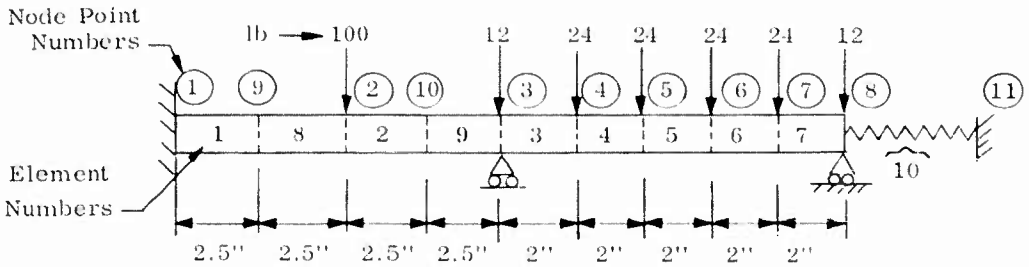

b. Element and Applied Load Idealization

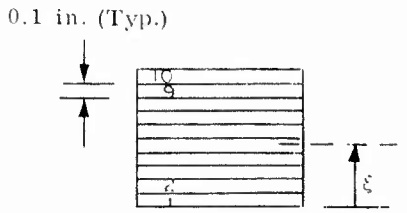

c. Idealization of Cross-Section (Typical)

Figure IV-9. Illustrative Complex Indeterminate Beam Problem

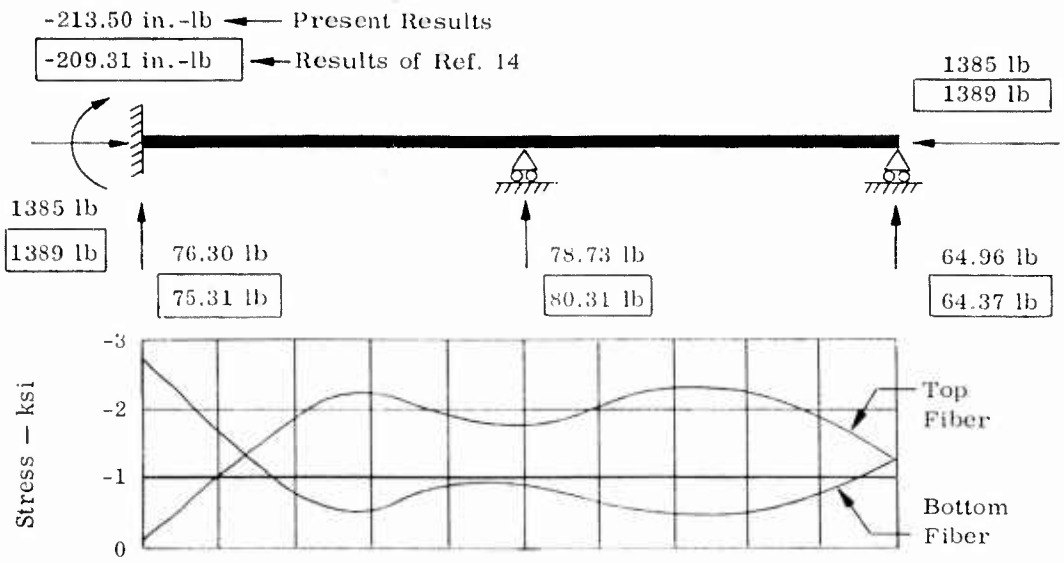

a. Predicted Stresses and Comparison of Predicted Support Reactions

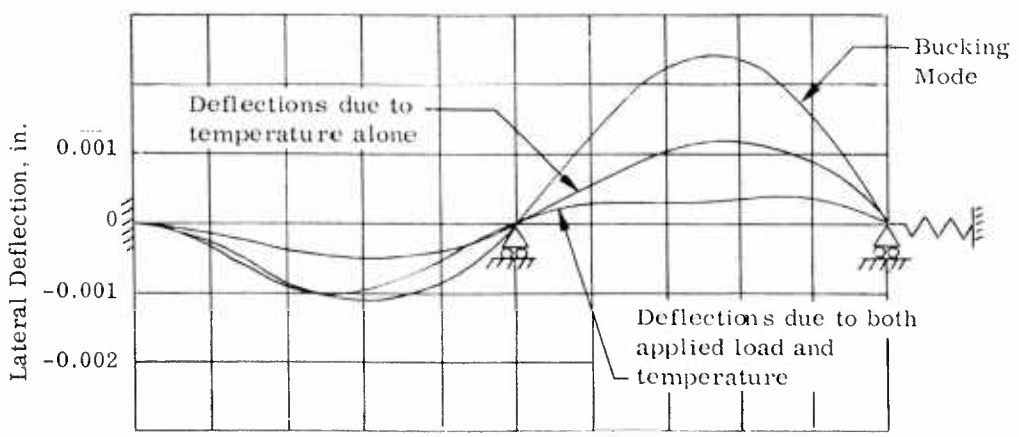

b. Predicted Lateral Deflections and Buckling Mode Shape

Figure IV-10. Results for Complex Indeterminate Beam Problem

CHAPTER V

PLATE ANALYSIS PROGRAM

A. SCOPE

The objective of the plate analysis program is to determine the structural behavior (i.e., stresses, displacements, and buckling stress) of flat plates of arbitrary planform and thickness variation subjected to nonuniformly distributed applied loads and temperatures. The plate material can be orthotropic but the principal directions of orthotropy and corresponding material properties must be the same at all points throughout the plate. Stiffening members can be accommodated; the program can in fact be used for truss or beam-gridwork analysis. The temperature dependence of material properties as well as inelastic behavior can be taken into account.

Three types of discrete elements are accommodated in the program:

(1) The beam segment (Fig. III-2).

(2) The triangular plate (Fig. III-6).

(3) The quadrilateral plate (Fig. III-7).

The behavior of each of these elements is segregated into "inplane" (or axial) behavior and "out-of-plane" (or flexural) behavior. Relationships were formulated in Chapter III for the beam segment. The bases for the derivation of the properites of plate elements are discussed in Chapter III; details are given in Reference 8.

Figure V-1 shows a typical plate structure whose behavior is to be predicted by the use of the program. Assume further that it possesses orthotropic material properties with the principal directions of orthotropy being parallel to the x and y axes. The reference axes for analysis must correspond to the principal directions of orthotropy.

Once the system axes have been established, an arrangement of discrete elements in idealization of the actual structure must be decided upon. Program capacity limits the scope of the idealization to a maximum of 80 node points.

If the thickness of the actual structure varies continuously, this variation must be represented in a stepped manner. With regard to the choice between the triangular and quadrilateral elements, it is believed that the quadrilateral is sufficiently versatile for most applications and, in addition, yields a solution for stress that is more easily interpreted than the solution for stress in a triangular plate. The triangular plate is indispensable, however, under certain geometric conditions.

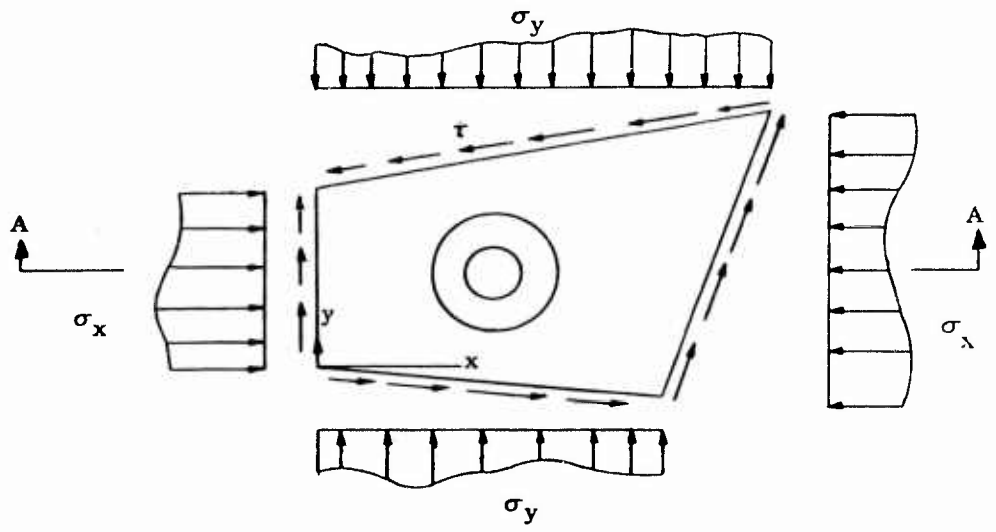

(a) Planform — Actual Structure

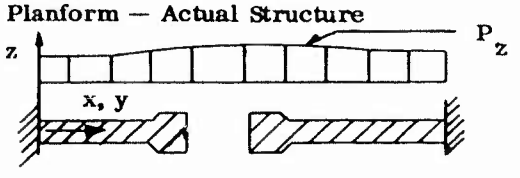

(b) Section A-A — Actual Structure

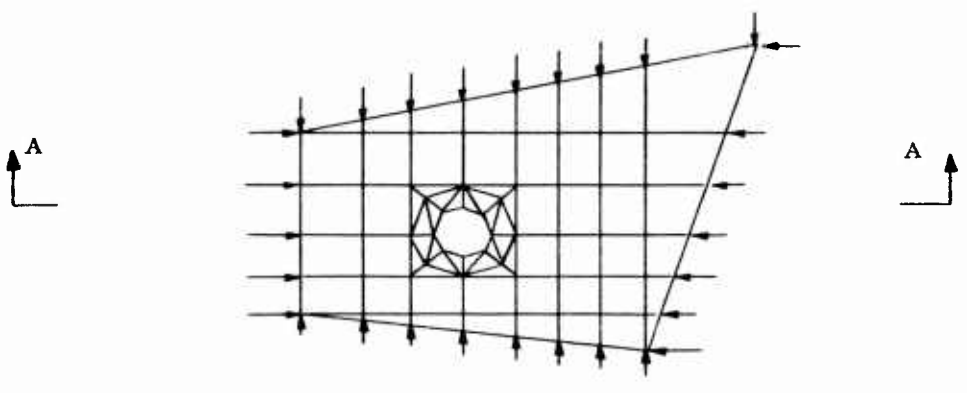

(c) Planform —Idealization

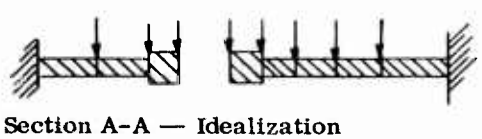

(d) Section A-A — Idealization

Figure V-1. Typical Plate Analysis Problem

Applied direct loads can exist in either the x, y, or z directions at each node point, and applied moments about the x and y axes can be present at each node. Normally, loads will exist only at the node points along the edges of the structure and they will likely be initially defined as distributed stresses. It is the responsibility of the analyst to transform the distributed applied stresses into equivalent concentrated forces at the affected node points. Subject to previously cited limitations, as many as 10 independent applied load conditions can be solved for in a single computational sequence.

The temperature distribution is assumed to be known at the start of the analysis. It must be emphasized that only one temperature condition per computational sequence is permissible since the stiffness properties of the system are dependent upon the material mechanical properties which, in turn, are allowed to be dependent upon temperature. In general, a change in temperature conditions requires a recalculation of the equations governing the elastic behavior of the structure.

The temperature state of the idealization for inplane analysis is initially defined by the temperatures of the node points. During the computational process each element is assigned a uniform temperature value which is the simple average of the temperatures at its corner points.

In the plate idealization for out-of-plane analysis, the input must define the "thermal moments" ($\bar{M}_x^{\alpha}, \bar{M}_y^{\alpha}$) at the node points. These are

$$\bar{M}_x^{\alpha} = \int_{-\frac{h}{2}}^{\frac{h}{2}} \frac{E_y(1+\mu_{xy})}{(1-\mu_{xy}\,\mu_{yx})}\,\alpha T\,\xi\,d\xi$$

$$\bar{M}_y^{\alpha} = \int_{-\frac{h}{2}}^{\frac{h}{2}} \frac{E_x(1+\mu_{yx})}{(1-\mu_{xy}\,\mu_{yx})}\,\alpha T\,\xi\,d\xi \qquad \text{(V-1)}$$

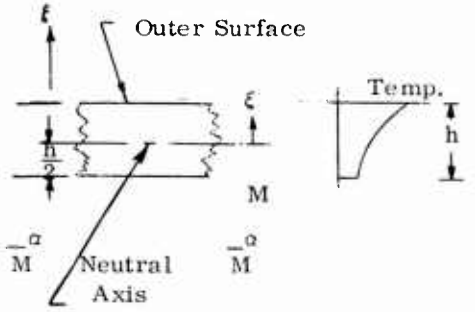

where ξ is a coordinate measured normal to the middle surface. For the particular case of an isotropic plate of thickness t with a linear temperature gradient through the thickness and constant material properties

$$\bar{M}^{\alpha} = \frac{E\,\alpha\,(T_1-T_2)h^2}{12(1-\mu)} \qquad \text{(V-2)}$$

where T_1 and T_2 are the outer and inner surface temperatures, respectively. During the computational process, each plate element is assigned a thermal moment which is the simple average of the thermal moments at its corner points.

For each flexural element, the thermal moment at each end (node point) must be included with the input. The formula for computing this value is:

$$\bar{M}_A^{\alpha} = \int_{\circ}^{A} E\,\alpha\,T\,\xi\,dA \qquad \text{(V-3)}$$

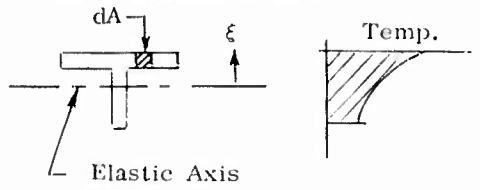

or, if the material properties are regarded as constant for the purpose of this determination and the cross-section is a solid rectangle, then

$$\bar{M}_A^{\alpha} = \frac{E\,\alpha\,(T_1-T_2)\,b\,d^2}{12} \qquad \text{(V-4)}$$

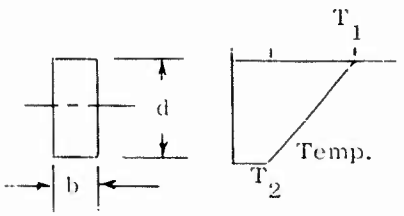

The material mechanical properties E_x, E_y, μ_{xy}, μ_{yx}, G_{xy}, and the coefficient of thermal expansion (α) are each permitted to sustain an independent variation with temperature, as represented by as many as five points on the material property versus temperature curve. This would appear to be a sufficient number of points for the common structural materials. If the true relationship is extremely complicated across the full range of temperatures it is likely that the problem involves only a restricted portion of this range, which in itself can be represented by five points. When evaluating the material properties for a given element the computer first selects the element temperature and then establishes the desired properties by linear interpolation of the material property versus temperature data.

Capabilities for inelastic analysis included in this program relate only to time independent behavior. The basic terms for inelastic analysis are included in the next section, which is a review of the computational process for elastic analysis. As in the case of the beam program (Chapter IV) inelastic analyses are performed as a series of elastic analyses. The incorporated rules for material inelastic behavior as well as the procedures which govern the series of analyses for such behavior are examined in a later section.

B. THEORETICAL BASIS

1. Elastic Analysis

The following discussion of the analysis procedure begins with a treatment of the inplane analysis sequence since these operations are always performed first by the program. The relationships between the inplane corner point

displacements (u, v) of each element and the corresponding corner point forces are expressed in the form:

$$\begin{Bmatrix} F_x \\ F_y \end{Bmatrix} = \begin{bmatrix} k_{xy} \end{bmatrix} \begin{Bmatrix} u \\ v \end{Bmatrix} - \begin{Bmatrix} F_x^{\alpha} \\ F_y^{\alpha} \end{Bmatrix} - \begin{Bmatrix} F_x^{p} \\ F_y^{p} \end{Bmatrix} \qquad (V-5)$$

where $\begin{bmatrix} K_{xy} \end{bmatrix}$ is the element "inplane" stiffness matrix, $\begin{Bmatrix} F_x^{\alpha}, F_y^{\alpha} \end{Bmatrix}$ are "thermal forces" at the node points and $\begin{Bmatrix} F_x^{p}, F_y^{p} \end{Bmatrix}$ are the node point plastic forces (assumed known in this discussion). The algebraic form of these relationships is detailed in Chapter III.

Based on the pertinent input data -- geometry, loads, temperatures, and material properties -- the computer first evaluates the inplane element relationships and constructs with them the system of equations that represent the analytical model of the complete structure for inplane analysis. These assembled equations are of the form

$$\begin{Bmatrix} P_x \\ P_y \end{Bmatrix} = \begin{bmatrix} K_{xy} \end{bmatrix} \begin{Bmatrix} u \\ v \end{Bmatrix} - \begin{Bmatrix} P_x^{\alpha} \\ P_y^{\alpha} \end{Bmatrix} - \begin{Bmatrix} P_x^{p} \\ P_y^{p} \end{Bmatrix} \qquad (V-6)$$

where $\begin{Bmatrix} P_x \\ P_y \end{Bmatrix}$ are applied loads at the node points, $\begin{bmatrix} K_{xy} \end{bmatrix}$ is the "master inplane stiffness matrix", and $\begin{Bmatrix} P_x^{\alpha} \\ P_y^{\alpha} \end{Bmatrix}$ and $\begin{Bmatrix} P_x^{p} \\ P_y^{p} \end{Bmatrix}$ are the "net" thermal and plastic forces at the node points. Although Equation V-6 indicates a single column of applied loads, as many as 10 different applied load conditions can be treated in an inplane analysis cycle for a given temperature distribution and in the absence of inelastic behavior. Only one temperature condition can be treated since the stiffness matrix $\begin{bmatrix} K_{xy} \end{bmatrix}$ is a function of the material properties and these in turn are a function of temperature.

For each designated support condition a column and the corresponding row are eliminated from the $\begin{bmatrix} K_{xy} \end{bmatrix}$ matrix and the affected rows are removed from the column matrices $\begin{Bmatrix} P_x \\ P_y \end{Bmatrix}$, $\begin{Bmatrix} u \\ v \end{Bmatrix}$, $\begin{Bmatrix} P_x^{\alpha} \\ P_y^{\alpha} \end{Bmatrix}$, and $\begin{Bmatrix} P_x^{p} \\ P_y^{p} \end{Bmatrix}$. Utilizing the subscript "R" to designate the thusly reduced matrices, one obtains

$$\begin{Bmatrix} P_x \\ P_y \end{Bmatrix}_R = \begin{bmatrix} K_{xy} \end{bmatrix}_R \begin{Bmatrix} u \\ v \end{Bmatrix}_R - \begin{Bmatrix} P_x^{\alpha} \\ P_y^{\alpha} \end{Bmatrix}_R - \begin{Bmatrix} P_x^{p} \\ P_y^{p} \end{Bmatrix}_R \qquad (V-6a)$$

The basic unknowns in Equation (V-6a) are the displacements $\begin{Bmatrix} u \\ v \end{Bmatrix}$ and these are solved for as follows:

$$\begin{Bmatrix} u \\ v \end{Bmatrix}_R = \left[K_{xy}\right]_R^{-1} \begin{Bmatrix} P_x \\ P_y \end{Bmatrix}_R + \left[K_{xy}\right]_R \left\{ \begin{Bmatrix} P_x^{\alpha} \\ P_y^{\alpha} \end{Bmatrix}_R + \begin{Bmatrix} P_x^{p} \\ P_y^{p} \end{Bmatrix}_R \right\} \qquad (V-7)$$

Once the solution for the displacements has been achieved, a "listing" is made of the displacements associated with the respective elements, so that they can be applied to the determination of the element stresses. Relationships between the stresses in the element and the element node point displacements are also stored in the program in the following form:

$$\begin{Bmatrix} \sigma_x \\ \tau_{xy} \\ \sigma_y \end{Bmatrix} = \left[S_{xy}\right] \begin{Bmatrix} u \\ v \end{Bmatrix} - \begin{Bmatrix} \sigma_x^{\alpha} \\ 0 \\ \sigma_y^{\alpha} \end{Bmatrix} - \begin{Bmatrix} \sigma_x^{p} \\ \tau_{xy}^{p} \\ \sigma_y^{p} \end{Bmatrix} \qquad (V-8)$$

$\{\sigma_x, \tau_{xy}, \sigma_y\}$ is a listing of the stresses at the corner points of the element, $\left[S_{xy}\right]$ is the "element stress matrix", and $\{\sigma_x^{\alpha}, 0, \sigma_y^{\alpha}\}$ represents the stresses developed on the basis of inducing the thermal expansion elastically. Equations V-8 are discussed in Chapter III.

The procedure employed for out-of-plane analysis is quite similar to that described above except that in the presence of instability effects an additional or "incremental" stiffness results from the presence of midplane forces. The element equation is now written as

$$\begin{Bmatrix} \bar{M}_x \\ \bar{M}_y \\ F_z \end{Bmatrix} = \left[\left[k_z\right] + \left[n\right]\right] \begin{Bmatrix} \theta_x \\ \theta_y \\ w \end{Bmatrix} - \begin{Bmatrix} \bar{M}_x^{\alpha} \\ \bar{M}_y^{\alpha} \\ F_z^{\alpha} \end{Bmatrix} - \begin{Bmatrix} \bar{M}_x^{p} \\ \bar{M}_y^{p} \\ F_z^{p} \end{Bmatrix} \qquad (V-9)$$

where $\left[n\right]$ is the incremental stiffness, the terms of which are functions of the midplane stresses determined through Equation (V-9). The detailed form of Equation (V-9) is examined in Chapter III. Again, the individual element stiffness matrices are evaluated and summed to form the stiffness matrix for the complete structure and the support conditions are applied, resulting in

$$\begin{Bmatrix} M_x \\ M_y \\ P_z \end{Bmatrix}_R = \left[\left[K_z \right] + \left[N \right] \right]_R \begin{Bmatrix} \theta_x \\ \theta_y \\ w \end{Bmatrix}_R - \begin{Bmatrix} M_x^{\alpha} \\ M_y^{\alpha} \\ P_z^{\alpha} \end{Bmatrix}_R - \begin{Bmatrix} M_x^{p} \\ M_y^{p} \\ P_z^{p} \end{Bmatrix}_R \qquad \text{(V-10)}$$

If the solution for the equilibrium displacements and stresses resulting from applied loads and temperature change is sought, one obtains:

$$\begin{Bmatrix} \theta_x \\ \theta_y \\ w \end{Bmatrix}_R = \left[\left[K_z \right] + \left[N \right] \right]_R^{-1} \left\{ \begin{Bmatrix} M_x \\ M_y \\ P_z \end{Bmatrix}_R + \begin{Bmatrix} M_x^{\alpha} \\ M_y^{\alpha} \\ P_z^{\alpha} \end{Bmatrix}_R + \begin{Bmatrix} M_x^{p} \\ M_y^{p} \\ P_z^{p} \end{Bmatrix}_R \right\} \qquad \text{(V-11)}$$

and, from the appropriate relationships

$$\begin{Bmatrix} M'_x \\ M'_y \\ M_{xy} \\ Q_x \\ Q_y \end{Bmatrix} = \left[S_z \right] \begin{Bmatrix} \theta_x \\ \theta_y \\ w \end{Bmatrix} - \begin{Bmatrix} M'^{\alpha}_x \\ M'^{\alpha}_y \\ 0 \\ 0 \\ 0 \end{Bmatrix} - \begin{Bmatrix} M'^{p}_x \\ M'^{p}_y \\ M^{p}_{xy} \\ Q^{p}_x \\ Q^{p}_y \end{Bmatrix} \qquad \text{(V-12)}$$

It is to be noted that moments and shears per linear inch, rather than stresses, are employed to define the internal distribution of load. (Such moments are "primed" rather than "barred" to indicate a distinction with the concentrated corner point moments).

If critical stresses are to be determined (i.e., if an elastic instability analysis is to be performed) $\left\{ M_x, M_y, P_z \right\}_R$ and $\left\{ M_x^{\alpha}, M_y^{\alpha}, P_z^{\alpha} \right\}_R$ are set equal to zero, the matrix $\left[N \right]$ is multiplied by the scalar λ, and Equation V-10 is rearranged as follows

$$\frac{1}{\lambda} \begin{Bmatrix} \theta_x \\ \theta_y \\ w \end{Bmatrix}_R = - \left[K_z \right]_R^{-1} \left[N \right]_R \begin{Bmatrix} \theta_x \\ \theta_y \\ w \end{Bmatrix}_R \qquad \text{(V-9)}$$

The scalar λ (which is the eigenvalue to be determined) as well as the relative magnitude of the displacements $\left\{ \theta_x, \theta_y, w \right\}$ (the eigenvector, which is the buckled shape) are then determined through matrix iteration as described in Chapter II. Note that λ represents a value by which all applied midplane loads are multiplied to achieve instability. Thus, if $\lambda = 1.0$, instability is reached and if $\lambda > 1.0$ the given midplane loads are not sufficient to produce instability.

The matrix $\left[N \right]$ is dependent upon the values of stress computed in the inplane analysis portion of the computational cycle. If many load conditions are

cited, the program will automatically utilize the inplane stresses due to the first inplane load condition in the formulation of the $[N]$ matrix.

An additional capability of the program is its ability to treat "oblique" support conditions. It sometimes occurs that a structure is constrained to displace in the direction of axes other than those employed in the definition of the behavior of the structure as a whole. (See sketch). Such conditions can

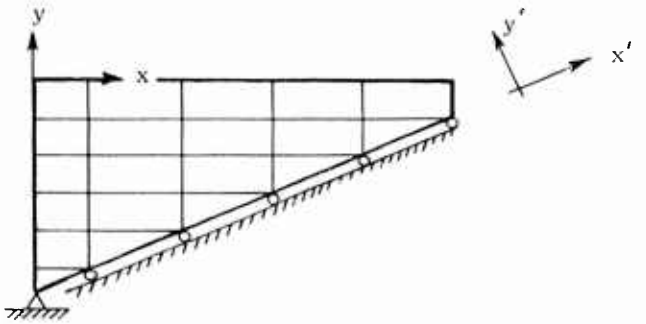

be accommodated simply by specifying for each affected point, the direction of the special x′ axis by means of node points. The program will then transform the relationships at all these points into equations referenced to the special axes, and boundary (support) conditions can be defined with respect to the latter.

2. Inelastic Analysis Procedure

An extension to the above-described plate analysis program permits analyses for time-independent plastic behavior under conditions of varying stress and temperature. This extension is limited to the use of the triangular plate element and excludes orthotropic behavior, i.e., only isotropic behavior can be treated.

Consider the typical triangular plate element sketched below. Since the stress, and therefore the plastic strain, varies across the thickness of the plate, it is necessary for purposes of plastic analysis to divide the thickness into laminae, or sub-elements, of thickness Δ t. The location of a given sub-element is specified by the ξ value to the center of the element, as shown. As many as 10 sub-elements can be employed in a given analysis.

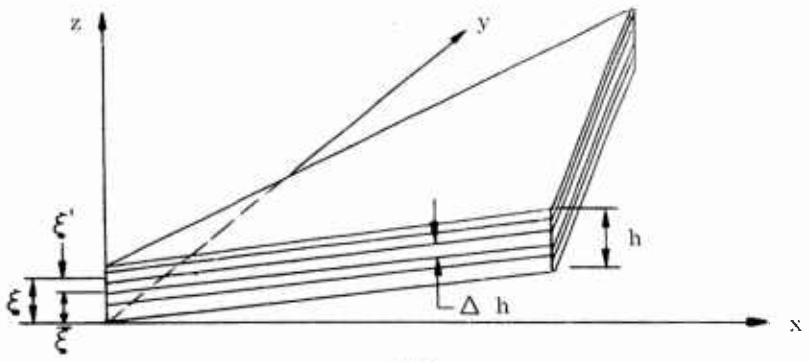

To define the temperature history of the structure it is necessary to specify the initial temperature of the entire plate and a temperature history for each lamina at every node point.

The effective temperature for each sub-element is then computed as the arithmetic mean of its three corner temperatures. These average temperatures are used to determine the pertinent material properties and the temperature differences ΔT.

At each specified time in the load-temperature history, equivalent thermal stress resultants for inplane and flexural behavior, as required for construction of the corner thermal forces and moments, are computed using the following equations

$$N^{\alpha} = \frac{1}{(1-\mu)} \sum E \alpha \Delta T \Delta h \qquad \text{(V-13)}$$

$$\bar{M}^{\alpha} = \frac{1}{(1-\mu)} \sum E \alpha \Delta T \xi' \Delta h \qquad \text{(V-14)}$$

Note that Equation (V-14) is a modification of Equation (V-1). Note also that in the inelastic analysis routine the thermal moments are evaluated by the computer, based on input data, while for elastic analyses these moments must be hand computed and entered with the input.

In addition, the inplane and flexural stiffnesses required in the determination of the elastic neutral axis $\bar{\xi}$ and in the construction of the stiffness matrices are given by

$$\overline{Eh} = \sum E \Delta h \qquad \text{(V-15)}$$

$$\overline{EI} = \sum E (\xi')^2 \Delta h \qquad \text{(V-16)}$$

where

$$\xi' = \xi - \bar{\xi} \quad \text{and} \quad \bar{\xi} = \frac{\sum E \xi \Delta h}{Eh}$$

The various inelastic column force matrices present in the general force displacement relationships are composed of the following inelastic stress resultants.

$$N_x^p = \frac{1}{(1-\mu^2)} \sum E(\epsilon_{x_T}^p + \mu \epsilon_{y_T}^p) \Delta h \qquad \bar{M}_x^p = \frac{1}{(1-\mu^2)} \sum E(\epsilon_{x_T}^p + \mu \epsilon_{y_T}^p) \xi' \Delta h$$

$$N_y^p = \frac{1}{(1-\mu^2)} \sum E(\epsilon_{y_T}^p + \mu \epsilon_{x_T}^p) \Delta h \qquad \bar{M}_y^p = \frac{1}{(1-\mu^2)} \sum E(\epsilon_{y_T}^p + \mu \epsilon_{x_T}^p) \xi' \Delta h$$

$$N_{xy}^p = \frac{1}{2(1+\mu)} \sum E \gamma_{x_{y_T}}^p \Delta h \qquad M_{xy}^p = \frac{1}{2(1+\mu)} \sum E \gamma_{xy_T}^p \xi' \Delta h$$

(V-17)

The symbols $\epsilon_{x_T}^{p}$, $\epsilon_{y_T}^{p}$ and $\gamma_{xy_T}^{p}$ represent the total plastic strains for the biaxial stress case and are computed with the aid of plastic analysis Method A discussed in Chapter IV for the uniaxial stress case. By consideration of the uniaxial stresses and strains employed in Method A as effective stresses and strains, and adopting the biaxial inelastic stress-strain relationships consistent with the incremental theory of plastic flow, plastic strain increments $\Delta\epsilon_{x_T}^{p}$, $\Delta\epsilon_{y_T}^{p}$, $\gamma_{xy_T}^{p}$ are computed and accumulated for a given load-temperature history. Details of this portion of the procedure are delineated in Reference 9.

The extension of the plate program requires the detailed computation of the stresses for each area from the following expression

$$\begin{Bmatrix} \sigma_x \\ \sigma_y \\ \tau_{xy} \end{Bmatrix} = \frac{E}{(1-\mu^2)} \begin{bmatrix} 1 & \mu & 0 \\ \mu & 1 & 0 \\ 0 & 0 & \frac{(1+\mu)}{2} \end{bmatrix} \begin{Bmatrix} \alpha\Delta T \\ \alpha\Delta T \\ 0 \end{Bmatrix} + \begin{Bmatrix} \epsilon_{x_T}^{p} \\ \epsilon_{y_T}^{p} \\ \gamma_{xy_T}^{p} \end{Bmatrix} + \begin{bmatrix} S_{xy} \end{bmatrix} \begin{Bmatrix} u \\ v \end{Bmatrix} + \xi' \begin{bmatrix} S_z \end{bmatrix} \begin{Bmatrix} \theta_x \\ \theta_y \\ w \end{Bmatrix} \qquad \text{(V-18)}$$

The general computational procedure parallels that of the one-dimensional program. First, the load-temperature history is divided into time intervals and each of these is in turn subdivided into time increments. Consider, for example, the computation of the stresses at time t_i. At this time the elements of the plate may have experienced prior biaxial plastic straining. Node point deformations are computed for the imposed loading and net plastic forces and are then employed in the computation of the biaxial stresses from the element stress equations. These stresses are used to evaluate effective stresses which are used to compute the change in effective strains required subsequently in the determination of the change in biaxial plastic strains. The latter are added to the prior total plastic strains to establish new values for the total plastic strains. Stresses are then computed and the process continued until successive stresses are reproduced in satisfaction of a convergence criteria.

C. ILLUSTRATIVE EXAMPLES

1. Comparison with Alternate Solutions

As in the case of the one-dimensional structure program, the objectives in presenting the following illustrative examples are to provide an outline of the results to be obtained through exercising the various program options and to demonstrate the level of accuracy that can be achieved with use of the program. To accomplish the second objective it is again necessary to compare results with solutions for relatively simple conditions. For the present program, the comparisons are further limited in versatility by the relatively few available alternate solutions for orthotropic plate problems. Although the theoretical formulation of the governing differential equations for orthotropic behavior are well established, there are few numerical solutions to such problems. No significant solutions for thermal stress conditions in orthotropic plates have been found by the authors. Hence, in what follows, the thermal stress problems are concerned only with isotropic plates.

The following types of analyses are performed in this section;

(a) Stress and Deflection Analyses

(1) Isotropic Rectangular Plate - Thermal stress analysis

(2) Orthotropic Rectangular Plate - Plane stress analysis

(3) Isotropic Triangular Plate - Thermal stress and flexure

(b) Instability Analyses

(1) Isotropic Rectangular Plate - Thermal buckling

(2) Orthotropic Rectangular Plate - Flexure and Instability Analyses

The analysis of a problem involving geometric irregularities and more practical circumstances than the above problems will be described in the next section.

a. Stress and Deflection Analyses

(1) Isotropic Rectangular Plate - Thermal Stress Analysis

The rectangular plate shown in Figure V-2a has a length that is twice its width and has a thickness variation in the width direction given by $h = \left[1 - 0.9 \left(\frac{y}{c}\right)^2\right] h_o$. The temperature varies in the width direction, $T = \left[\left(\frac{y}{c}\right)^2 - \frac{1}{3}\right] T_o$, producing midplane elastic thermal stresses. A solution for these thermal stresses was advanced by Mendelson and Hirschberg in Reference 15.

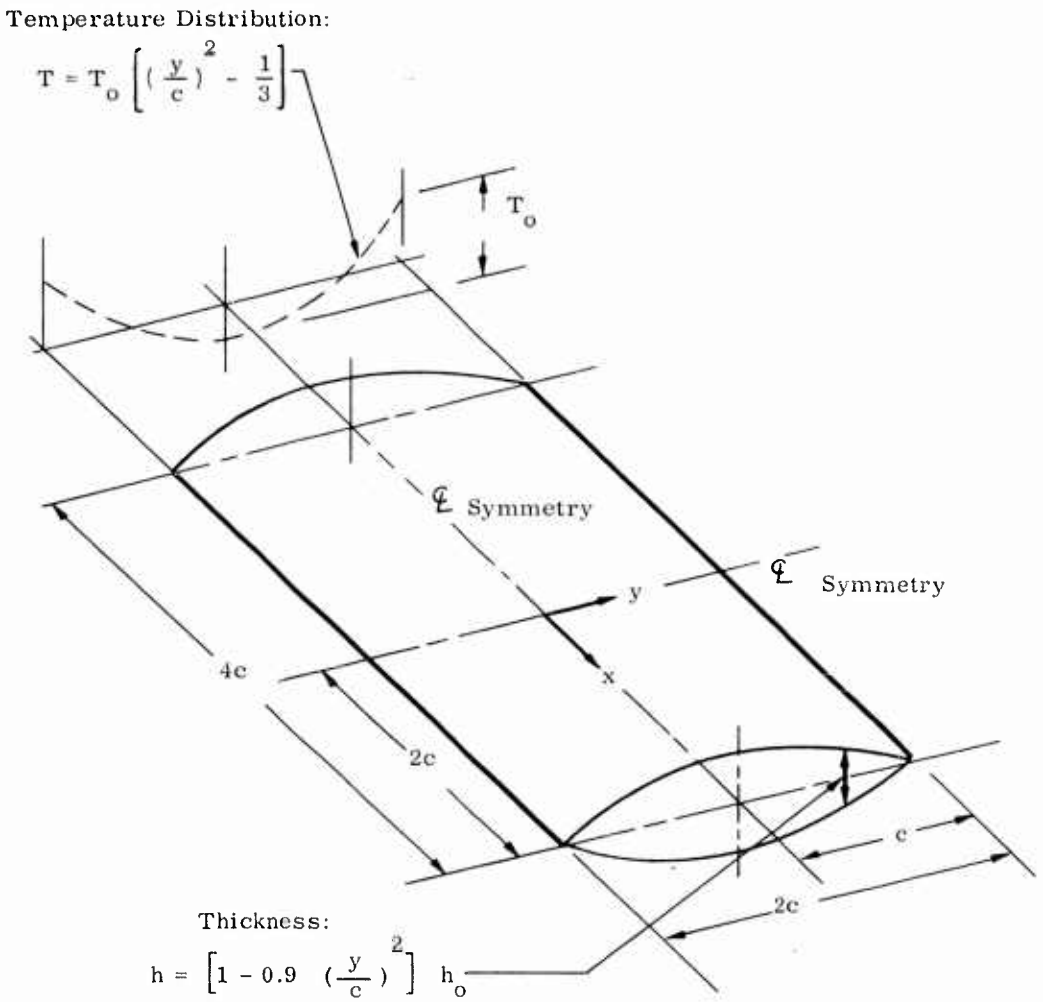

a. Actual Plate

Figure V-2. Isotropic Rectangular Plate for Thermal Stress Analysis

(1) Discrete Elements

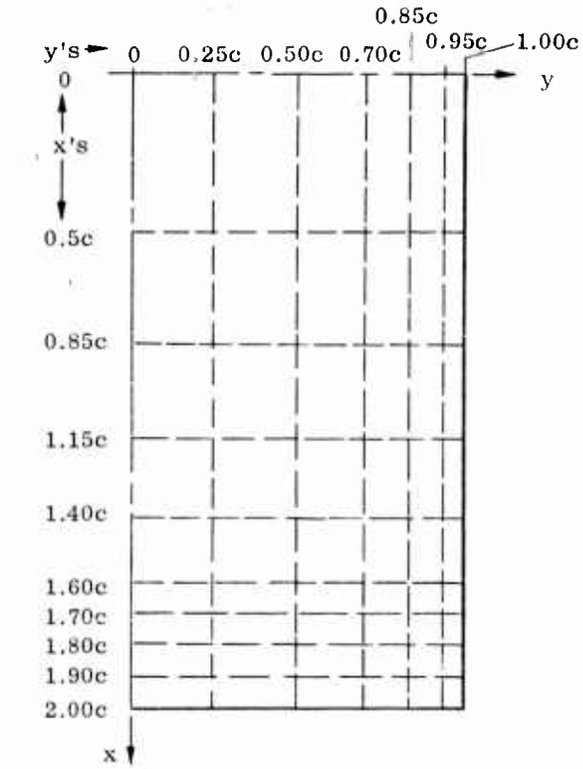

(2) Thickness Variation

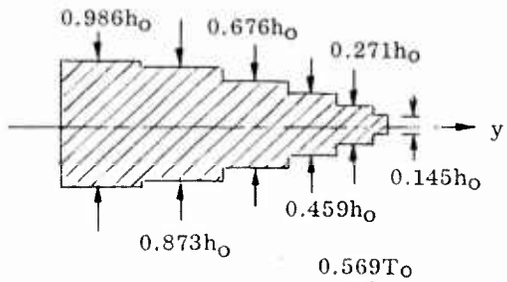

(3) Temperature Variation

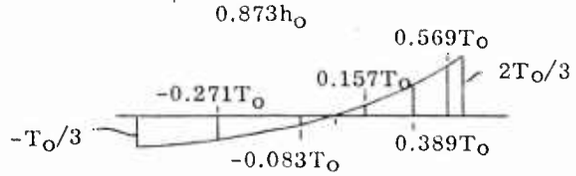

b. Idealization of Heated Plate - One Quadrant

Figure V-2. (Concl'd) Isotropic Rectangular Plate for Thermal Stress Analysis

From symmetry it is only necessary to consider a quadrant of the plate. The idealization for analysis consists in dividing the plate quadrant into 54 quadrilateral plate elements as illustrated in Figure V-2b. Judgement dictates the placement of small elements at the tip and side where stresses change rapidly in consequence of edge effects and the temperature gradient and thickness changes are most severe.

Selected results from the present analysis and from Reference 15 are plotted in Figure V-3. All results are expressed in nondimensional form. The distribution of longitudinal thermal stress (σ_x) is given on a cross-section located 0.25c from the end (x = 1.75c), where this component of stress is significantly influenced by "end effects". The chordwise stress (σ_y), which is entirely due to end effects, is plotted for the tip chord (x = 2.00c) while the chordwise variation of shear stress (τ_{xy}) is shown for x = 1.60c. The dotted lines represent the computer program solution; the solution from Reference 15is shown by solid lines. As seen from this figure, there is close agreement between the two solutions.

(2) Orthotropic Rectangular Plate – Plane Stress Analysis

For plane stress, one of the most interesting orthotropic plate problems to have been solved is illustrated in Figure V-4a. An orthotropic plate, E_{y/E_x} = 0.17 and $\frac{G}{E_y}$ = 0.134, of aspect ratio 4.0, is loaded by equal and opposite concentrated forces P in the manner indicated. The plate thickness is h.

The idealization for discrete element analysis consists of the 36 rectangular plate elements shown in Figure V-4b (due to symmetry, only a quadrant of the plate need be treated). Again, smaller elements are utilized in the vicinity of the concentrated load. The discrete element analysis results are presented in Figure V-4c, where they are compared with the results derived by Conway (Reference 16) by use of a classical type of approach. It is seen that there is an extremely close agreement between the two solutions.

(3) Isotropic Triangular Plate - Thermal Stress and Flexure

To illustrate the accuracy of the program in the analysis of plates subjected to temperature gradients across the thickness, the equilateral triangular plate shown in Figure V-5a has been analyzed. The linear 450°F temperature gradient through the thickness is assumed to be constant throughout the plate. An analytical solution for this type of problem was obtained by Maulbetsch (Reference 17).

Since the plate is symmetric about the x-axis it was necessary to consider only one half of the plate. The idealization was achieved by means of 21 quadrilateral plate elements and 7 triangular elements as shown in Figure V-5b.

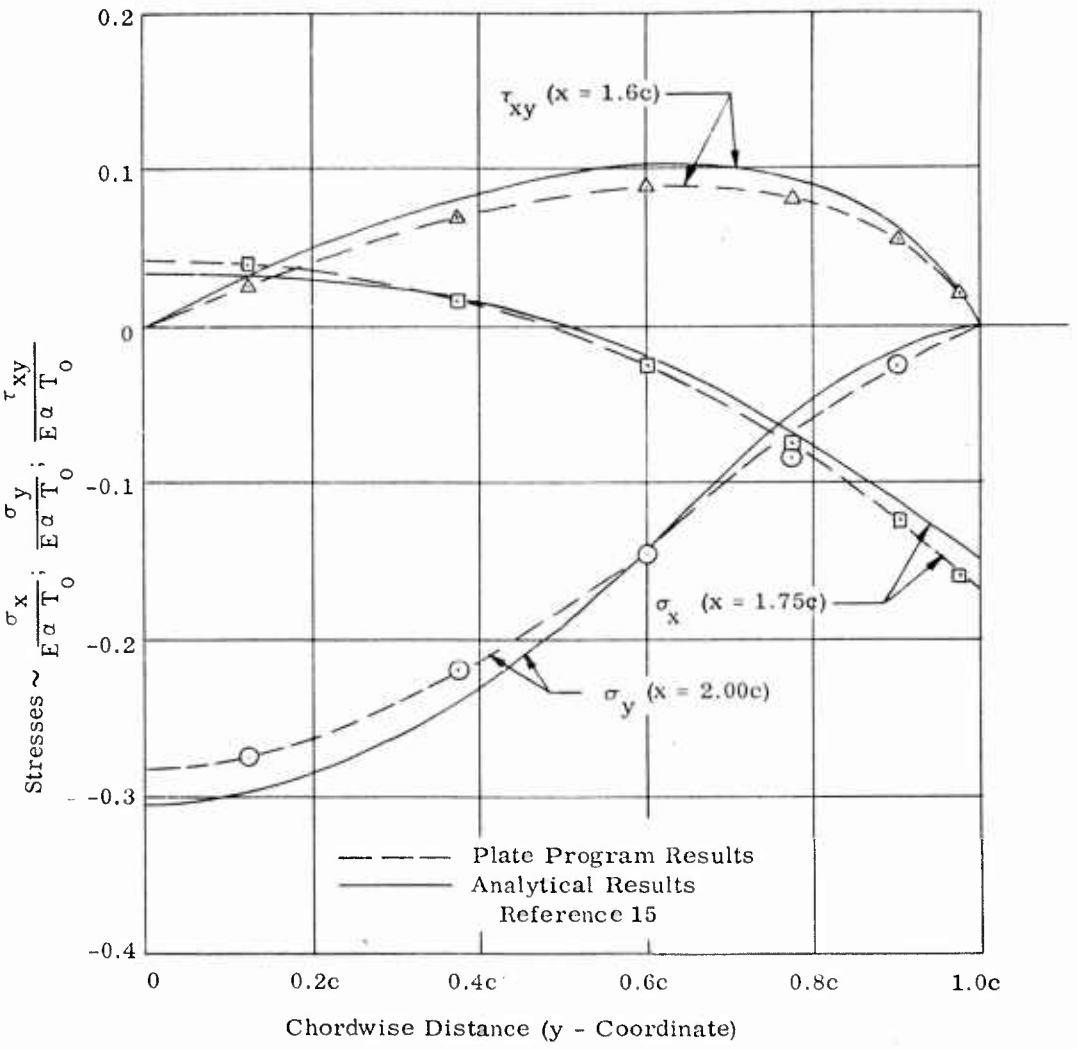

Figure V-3. Comparison of Results - Isotropic Plate Thermal Stress Analysis

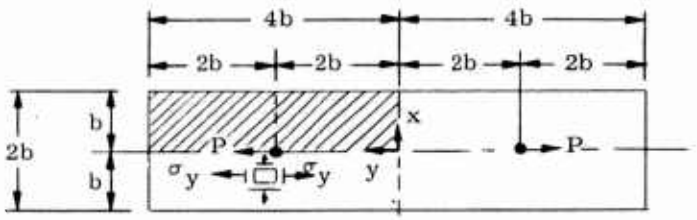

(a) Actual Plate

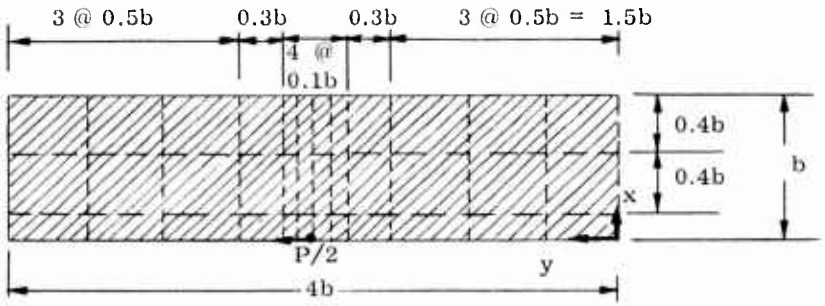

(b) Analytical Idealization — One Quadrant

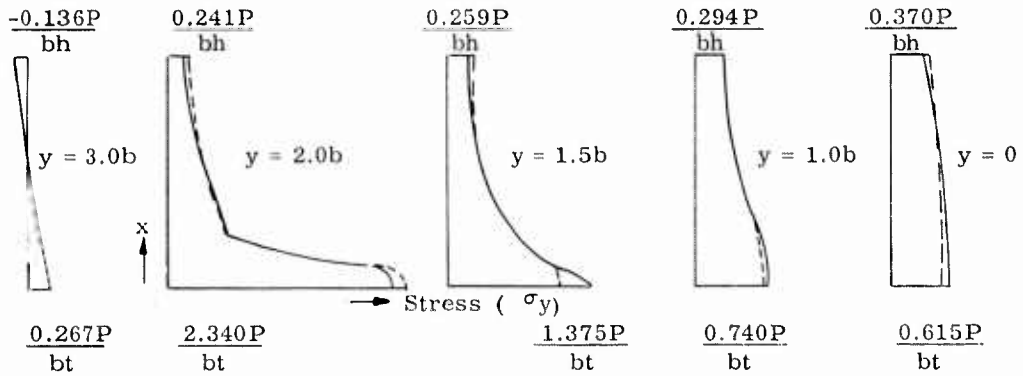

(c) Comparison of Solutions for Longitudinal Stress

——— Discrete Element Idealization Results

– – – – Alternate Analytical Approach

Figure V-4. Inplane Stress Analysis — Rectangular Orthotropic Plate

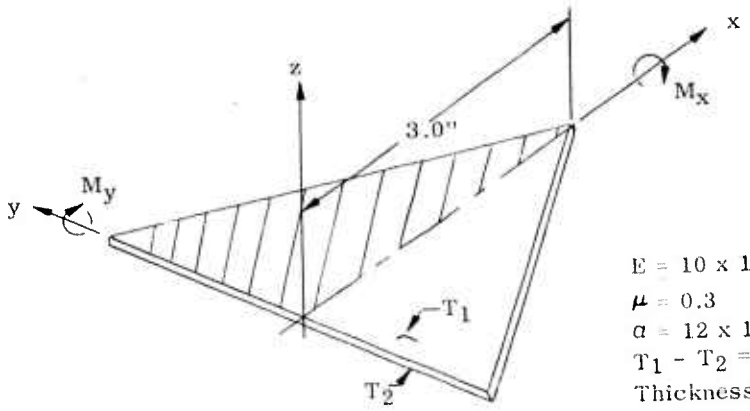

$E = 10 \times 10^6$ lb/in.^{2}
$\mu = 0.3$
$\alpha = 12 \times 10^{-6}$ in/in.-°F
$T_1 - T_2 = 450$°F
Thickness = 0.1 in.
All edges simply supported

(a) Equilateral Triangular Plate

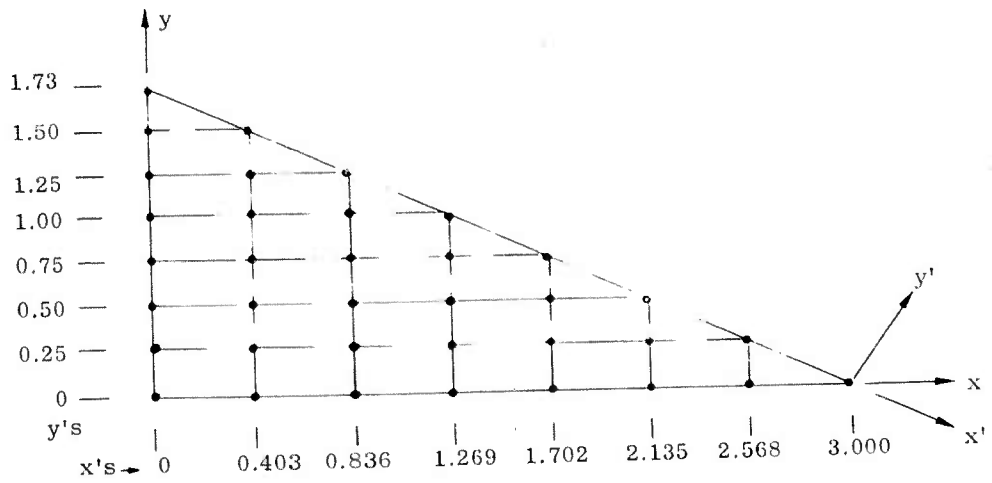

(b) Idealization of One-Half of Triangular Plate

Figure V-5. Isotropic Triangular Plate for Thermal and Flexural Analysis

To satisfy the support conditions along the swept edge, it was convenient to apply "oblique" coordinates along this edge.

The results of the discrete element analysis are compared to the results of Reference 17 in Figure V-6. The deflection of the plate along the x-axis is plotted in Figure V-6a. An almost exact agreement exists between the deflections obtained from the program and the analytical results of Reference 17.

The thermal moments M_x and M_y (moments about the x-axis and y-axis respectively) are independent of the y-coordinate. The distribution of these moments in the x-direction are shown in Figure V-6b. The symbolized points for the program results correspond to the elements adjacent to the x-axis. With the exception of two elements, the results are in very good agreement.

Figure V-6c compares the thermal twisting moments M_{xy} by plotting their distribution in the y-direction (the twisting moments are independent of the x-coordinate). The discrete element results given in Figure V-6c correspond to the elements adjacent to the y-axis. The results are again in very good agreement except for the triangular and adjacent rectangular element which are in fair agreement.

b. Instability Analyses

(1) Isotropic Rectangular Plate - Thermal Buckling

As an illustration of buckling caused by temperature change, the problem of a uniformly heated rectangular plate, simply supported along two parallel edges and restrained against rotation and normal expansion along the other two edges, is analyzed. The conditions of analysis are as shown in Figure V-7 where 4 rectangular elements have been employed in the idealization of a quadrant of the plate.

The theoretical buckling stress in the x-direction for this plate is determined by the expression

$$\sigma_{x_{cr}} = \frac{k_c \quad {}^2E}{12(1- \quad \mu^2)} \quad \left(\frac{t}{b}\right)^2 \qquad \sigma_x = \frac{\pi^2 c}{12(1- \mu^2)} \left(\frac{b}{h}\right) \tag{V-19}$$

Using the value of the buckling coefficient k_c as 6.65 (from Reference 10), the critical stress is computed to be 4050 lb/in.^{2}.

A temperature rise of 15.9°F, corresponding to a thermal stress of 2000 lb/in.^{2}, was imposed on the plate and an inplane and instability analysis

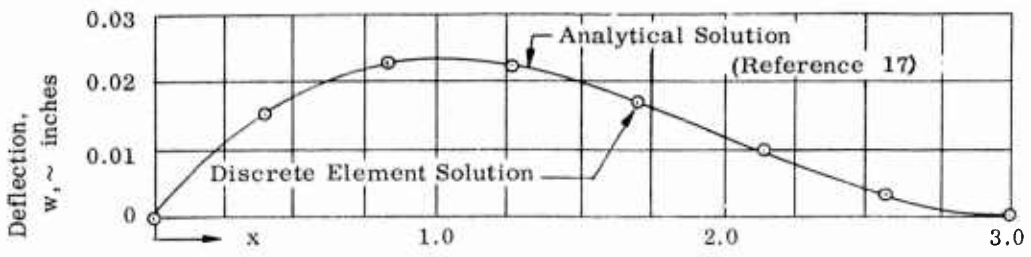

(a) Deflection Along x-Axis

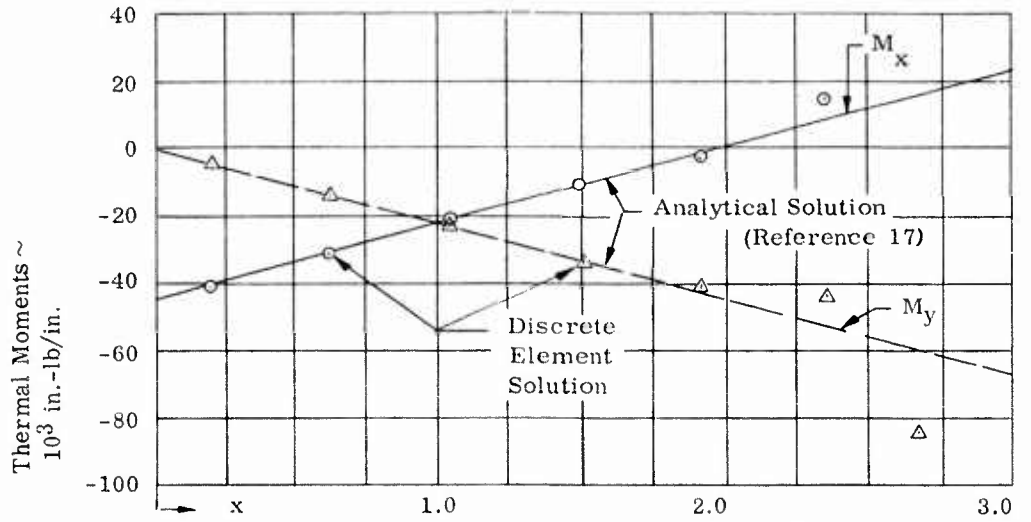

(b) Thermal Moments M_x^α and M_y^α

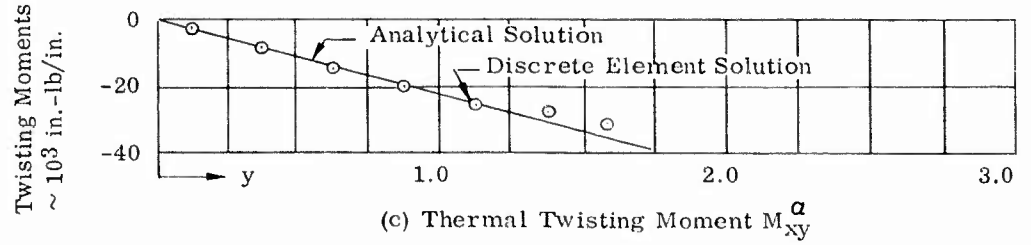

(c) Thermal Twisting Moment M_{xy}^α

Figure V-6. Comparison of Results - Isotropic Triangular Plate

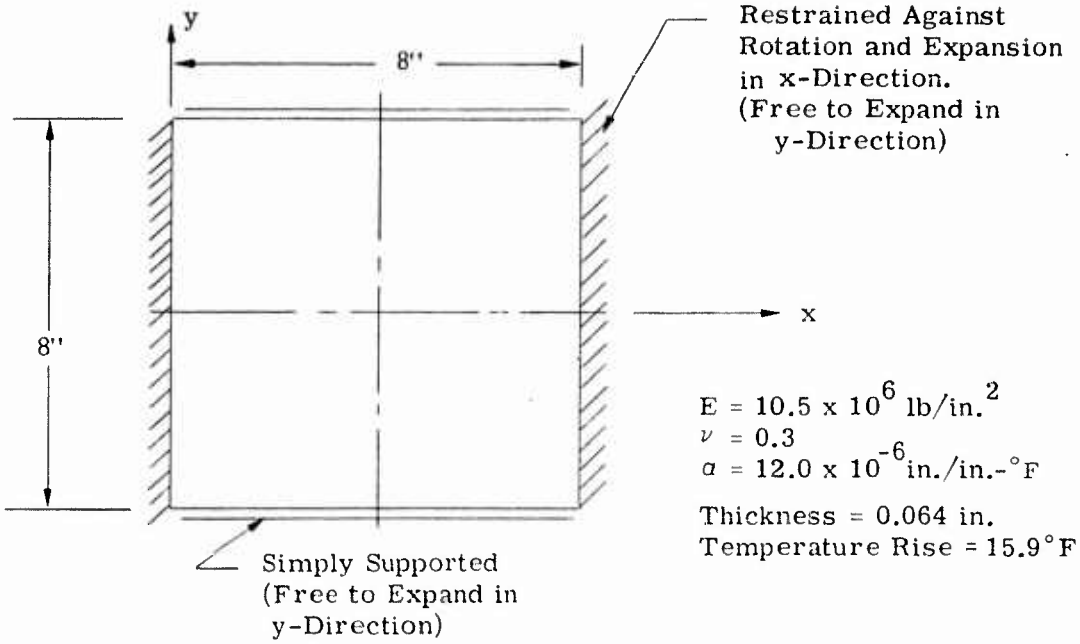

(a) Plate Planform and Support Conditions

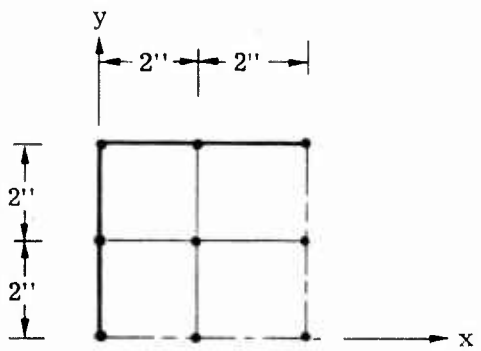

(b) Idealization of Plate Quadrant

Figure V-7. Isotropic Plate for Thermal Buckling Analysis

performed by the subject computational program. The results of the inplane analysis indicated a compressive stress of 2003 lb/in.^{2} in the x-direction and the instability analysis showed a critical inplane load factor ($\frac{1}{\lambda}$) of 1.9015. The program, therefore, predicted a buckling stress of 1.9015(2003) = 3860 lb/in.^{2} which agrees within 5 percent of the theoretical value of 4050 lb/in.^{2}. The accuracy of the predicted buckling stress may be improved by utilizing a larger number of elements in the idealization.

(3) Orthotropic Rectangular Plate - Flexure and Instability Analysis

Formulas for the deflection of rectangular orthotropic plates subjected to a concentrated lateral center load and uniform lateral pressure have been published by Hearmon (Reference 18), and formulas for the instability of orthotropic plates under various support conditions are presented in Reference 19. The following is a comparison of certain of these formulas with results obtained by discrete element analysis for the particular conditions illustrated in Figure V-8a. Two cases are examined:

(1) The deflection of the center of the plate under a concentrated center load of 35.5 pounds.

(2) Instability analysis under uniform compression stress in the x-direction.

For the deflection analysis a quadrant of the plate was idealized by 36 elements as shown in Figure V-8b. The discrete element analysis resulted in a center deflection of 0.0208 inches corresponding to a center concentrated load of 35.5 pounds. From Reference 18 the center deflection is determined by the formula

$$w = \frac{P_c}{24.8\left(\frac{D_x b}{a^3} + \frac{D_y a}{b^3} + \frac{2D_Q}{ab}\right)} \qquad (V-20)$$

where

$$D_x = \frac{E_x t^3}{12(1-\mu_{xy}\,\mu_{yx})} \qquad (V-21)$$

$$D_y = \frac{E_y t^3}{12(1-\mu_{xy}\,\mu_{yx})} \qquad (V-22)$$

$$D_Q = \mu_{yx} D_x + 2 D_{xy} \qquad (V-23)$$

$$D_{xy} = \frac{G_{xy} h^3}{12} \qquad (V-24)$$

$E_x = 30 \times 10^6$ lb/in.^{2}

$E_y = 5 \times 10^6$ lb/in.^{2}

$G_{xy} = 10 \times 10^6$ lb/in.^{2}

$\mu_{xy} = 0.3, \mu_{yx} = 0.05$

Thickness = 0.1 in.

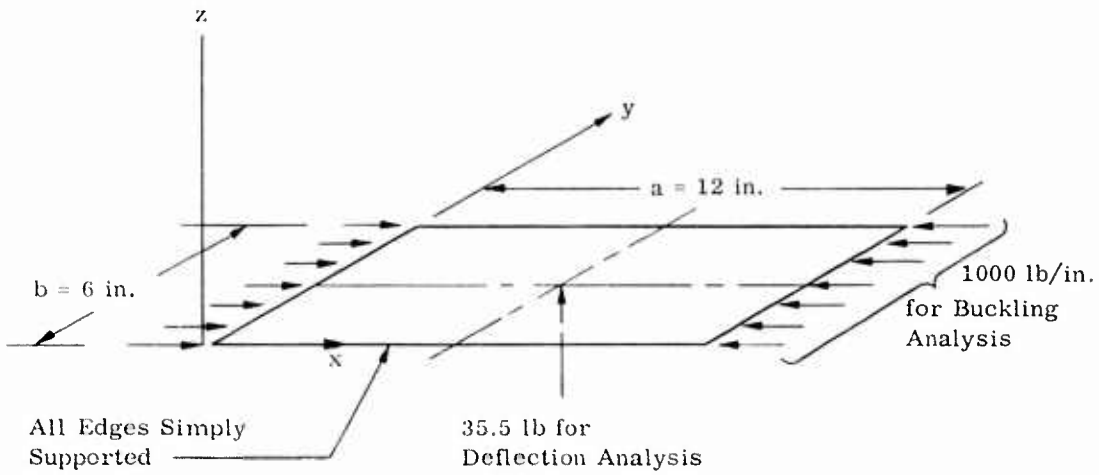

(a) Conditions of Analysis

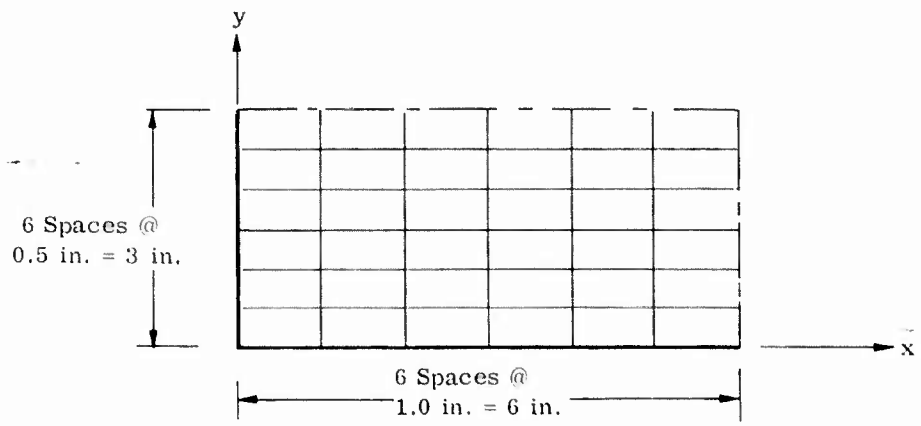

(b) Idealization of Plate Quadrant

Figure V-8. Orthotropic Rectangular Plate

which results in a deflection of 0.025 inch. It is noted that the discrete element approach gives a stiffer solution. In view of the fact that the Hearmon formula is in itself an approximation, the agreement between the two solutions is considered to be satisfactory.

The buckling stress of the orthotropic, simply supported plate was determined by the expression

$$\sigma_{x_{cr}} = \frac{\pi^2}{h_o^2}\sqrt{D_x D_y} \qquad \text{(V-26)}$$

From Reference 19 the valve of c is given as

$$c = \left(2.0 + 2\frac{D_Q}{\sqrt{D_x D_y}}\right) \qquad \text{(V-27)}$$

which results in a computed buckling stress of $\sigma_{x_{cr}} = 10{,}160$ lb/in.^{2}.

For the discrete element instability analysis the buckling mode is assumed to be a double buckle, i.e., the aspect ratio 2 plate will buckle like two square plates. By considering antisymmetry in the x-direction and symmetry in the y-direction it is only necessary to analyze a quadrant of the plate. The idealization is the same as for the deflection analysis (Figure V-8b) and compressive edge forces of 1000 lbs/in. are imposed in the x-direction. Analysis by the subject program resulted in inplane stresses of 10,000 lb/in.^{2} in the x-direction and a critical inplane load factor $(1/\lambda)$ of 1.781. The predicted buckling stress is therefore 17,810 lb/in.^{2} which is considerably larger than the 10,160 lb/in.^{2} from Reference 19. This difference is consistent with the deflection analysis in that the discrete element analysis again gave a stiffer result than the alternate analytical solution.

2. Analysis of Practical Complex Conditions

The trapezoidal plate shown in Figure V-9 furnishes a more practical problem involving geometric irregularities. The plate contains a centrally located reinforced hole and is assumed to be simply supported on all edges. The mechanical loading consists of a uniform lateral pressure, inplane loads in both the x and y directions, and balancing shear flows along the edges. The σ_x stresses are uniform and the σ_y stresses vary linearly as indicated in Figure V-9. In addition the plate is subjected to linear temperature gradients through the thickness which produce thermal moments.

Since the plate and loading conditions are symmetric about the x-axis, only a half of the plate is treated in the analysis. Figure V-10 shows the half-plate idealization consisting of 43 elements and utilizing both quadrilateral and triangular plates. Oblique coordinates (x', y') were used along the tapered edge. The distributed edge loads and shear forces were transformed into equivalent concentrated x and y forces at the edge node points, and the lateral pressure was prorated as concentrated z forces to the node points. The thermal moments were hand computed from Equation V-2.

The assumed material properties E and α as functions of temperature are shown in the following table:

Temp °F	E 10^6 lb/in.^{2}	α 10^{-6} in./in.-°F
100	10.65	12.6
200	10.25	12.86
300	9.82	13.09
400	9.35	13.32
500	8.73	13.54

Poisson's Ratio was assumed constant at 0.3.

A complete analysis was performed including inplane, out-of-plane, and instability analyses. The inplane direct stresses are shown in Figure V-11 for several rows of elements. The stresses for the elements along the x-axis are plotted in Figure V-11a and the stresses corresponding to elements along the sides parallel to the y-axis are given in Figures V-11b and V-11c. The results show that the direct stresses are tension for all the elements in the reinforcement around the hole. Since the reinforcement is the cooler portion of the plate, the tension stresses are reasonable.

The out-of-plane displacements along the ordinates y = 0 (x-axis) and y=7 inches are plotted in Figure V-12.

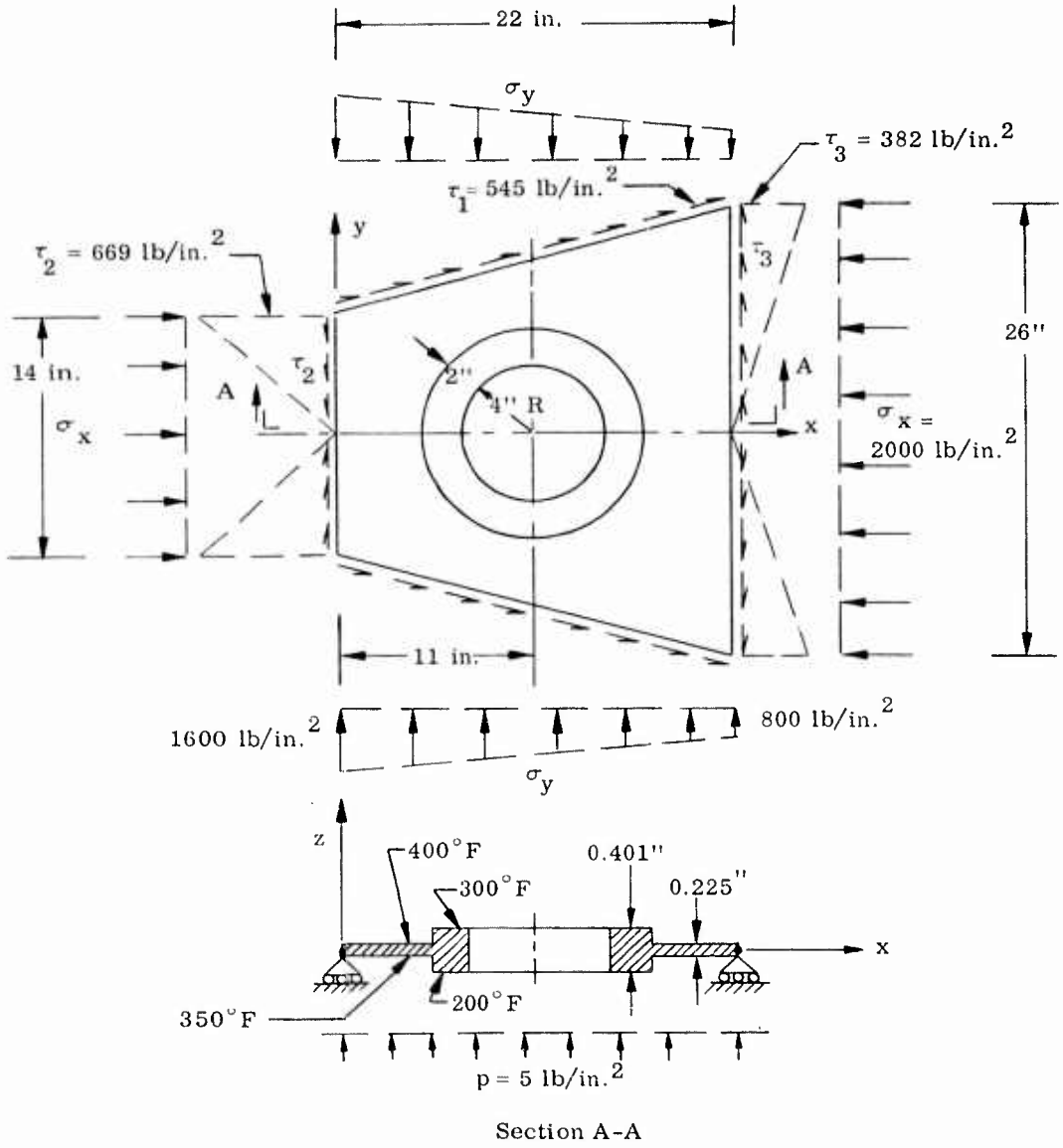

Section A-A

Figure V-9. Complex Trapezoidal Plate

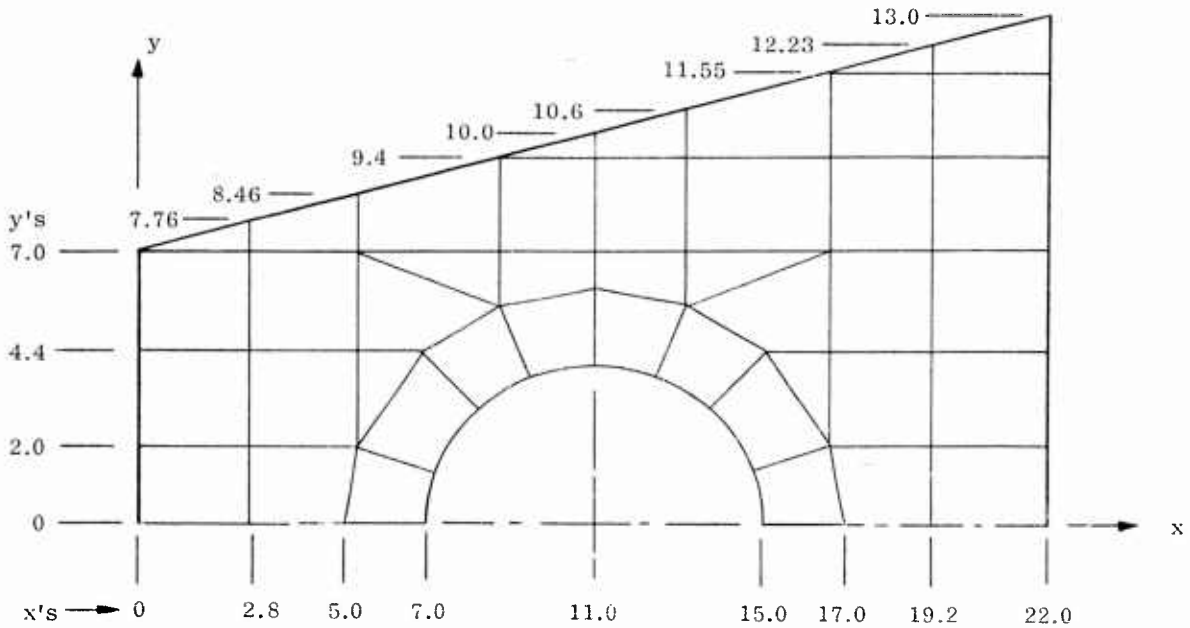

Figure V-10. Idealization of Trapezoidal Plate

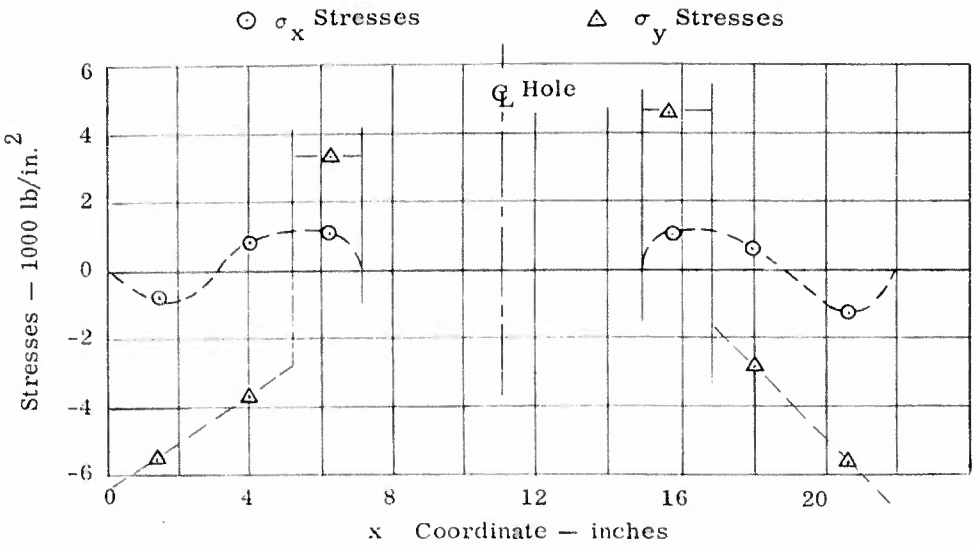

(a) Inplane Stresses at y = 1.0

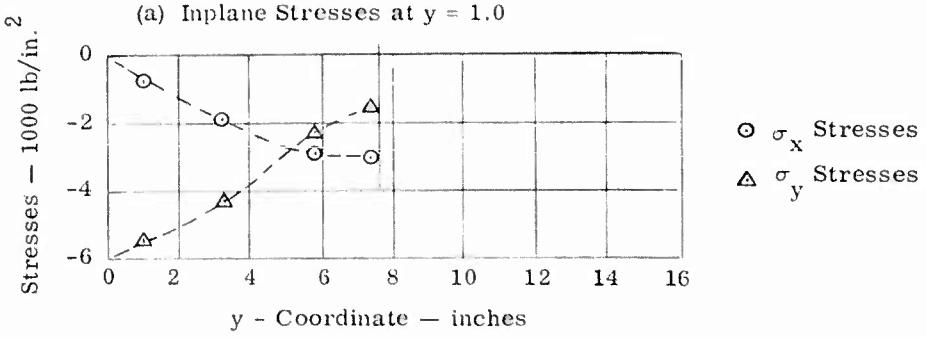

(b) Inplane Stresses at x = 1.4

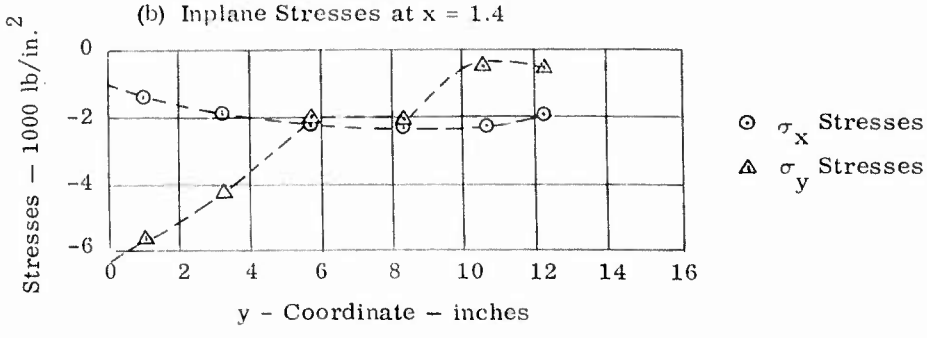

(c) Inplane Stresses at x = 20.6

Figure V-11. Inplane Stresses for Trapezoidal Plate

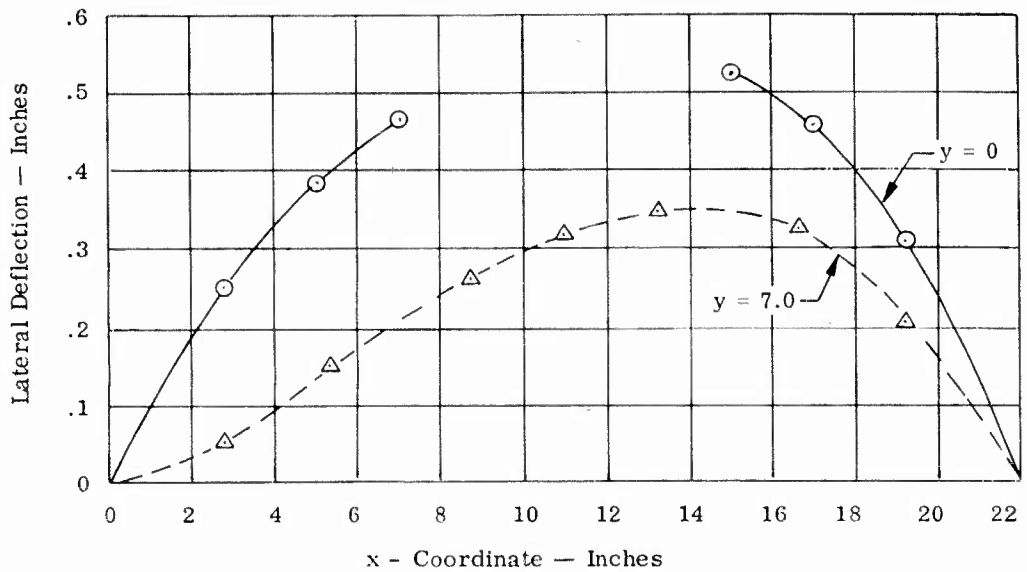

Figure V-12. Lateral Deflection of Trapezoidal Plate

The inplane load factor $(1/\lambda)$ determined from the instability analysis is 1.3 which gives critical stresses of $\sigma_{x_{cr}} = 1.3(2000) = 2600$ and $\sigma_{y_{cr}} = 1.3$ (1600) to 1.3(800) = 2080 to 1040 or an average $\sigma_{y_{cr}}$ of 1560 lb/in.^{2}.

Since no test data or alternate analytical solution for this plate is available, it is not possible to make a comparison of the discrete element solutions with other results. Approximate buckling stresses can be obtained, however, by assuming a 20 x 22 inch simply supported rectangular plate without a hole and loaded by uniform x and y edge forces. On this basis the critical σ_x and σ_y stresses, assuming $\sigma_y = 0.6\ \sigma_x$, are determined from Reference 20 to be 2420 lb/in.^{2} and 1450 lb/in.^{2} respectively. These critical stresses are in agreement with the results from the discrete element analysis.

CHAPTER VI

CYLINDER ANALYSIS PROGRAM

A. SCOPE

The cylinder program can be used to analyze the structural behavior, i.e., displacements and stresses, for heated stiffened and unstiffened fuselage segments and cylinders. The skin material may be either orthotropic or isotropic for an untapered structure (a body of revolution with the generatrix parallel to the longitudinal axis). For a tapered section, however, the skin material must be isotropic. The internal members (stiffeners and frames) are permitted to be composed of an isotropic material which need not be the same as the skin material. The temperature dependence of the material properties is taken into account.

For illustration a simplified fuselage section is shown in Figure VI-1a. In Figure VI-1b is shown an idealization scheme which contains most of the permissible elements. For use in idealizing the structure, the cylinder program accommodates the following types of elements:

(1) Axial force elements, for idealization of longerons or longitudinal stiffeners.

(2) Axial-flexural element, employed in the representation of frame elements.

(3) Triangular plate element, used to represent either the skin or the plate portions of a stiffened bulkhead.

(4) Quadrilaterial plate element, for idealization of portions of the skin and bulkheads.

The force-displacement relationships for these elements were discussed in Chapter III.

The existing capabilities of the program with respect to the size of the problem which can be handled are limited to the inversion of a 150th order stiffness matrix. This limitation cannot be precisely defined in terms of the permissable number of node points or elements; it can only be stated that no more than 150 displacement degrees of freedom can remain after application of the displacement boundary conditions.

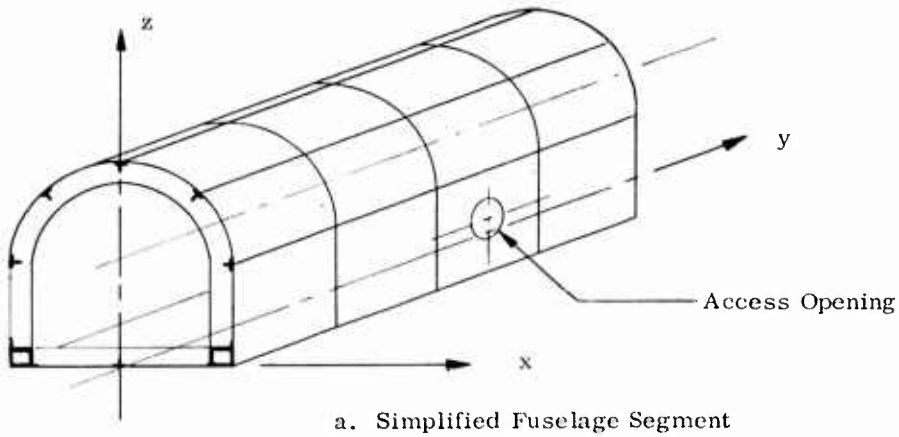

a. Simplified Fuselage Segment

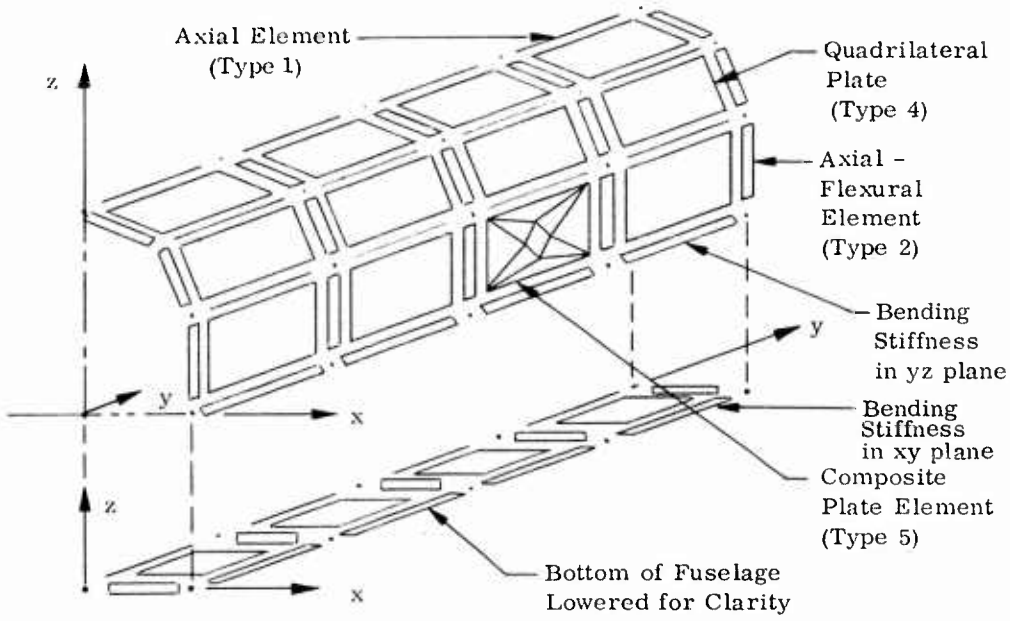

b. Idealization of Fuselage Segment

Figure VI-1. Fuselage Segment

The applied loads consist of concentrated forces in the x, y, z directions and moments about the x, y, z axes at each reference point. If a pressure load is exerted on the shell then it is necessary for the analyst to redistribute the pressure load in the form of concentrated loads at the reference points. The program can accommodate up to 10 applied load conditions per structural problem.

The relationships for computing the axial, or inplane, thermal forces are coded in the program. The computation of these thermal forces utilizes the elemental geometric, temperature, and material properties which are input quantities. A single average temperature is assigned to the axial and axial-flexural elements. For the skin elements (triangular and quadrilateral plates) the temperatures are specified at each reference point. The temperature of a given skin element is computed as the simple average of its corner point temperatures.

The out-of-plane thermal moments must be hand computed and entered as input to the program. For the axial-flexural element an average thermal moment is entered as part of the element input data. For the skin elements the hand computed distributed thermal moments about the local x and y axes are stated at each reference point. In computing the concentrated corner thermal moments for a given element, the distributed moments along the edges are assumed to be the average of the distributed moments at the corners.

As in the Plate Analysis Program, the Cylinder Program is capable of accommodating "oblique" support conditions. In some problems the fuselage segment may be constrained to displace in the direction of axes other than those employed in the definition of the behavior of the structure as a whole. Such conditions can be handled simply by specifying the coordinates of three points which define the special axes. The program transforms the elemental relationships at all the affected reference points into equations referenced to the special axes, and boundary conditions can be defined with respect to the latter.

In addition to possessing the capabilities described above, the program has been designed to accommodate relationships for instability analysis, two additional types of elements, and the capability to deal with systems of approximately 480th order. To a limited extent, these additional capabilities are coded or contained in the existing program but were not checked out as to operational correctness as of the conclusion of the subject study.

The two above-cited elements, which were intended to complement elements (1)-(4), are the following:

(5) Composite plate element of arbitrary planform, used in idealizing skin and bulkhead panels.

(6) Composite axial-flexural element, representive of longerons, stiffeners, and frames.

These composite elements, are assembled from more basic elements in the Plate Analysis Program and the One-Dimensional Element Analysis Program, respectively. By incorporating into the present program the appropriate parts of these two programs, the elemental matrices for the composite elements are computed. Essentially, this process consists of assembling the complete matrices for the composite elements and reducing out the equations pertaining to the intermediate points which are not reference points on the fuselage structure. This produces the element matrices referenced to the attachment points between the composite element and fuselage structure.

With regard to planned capabilities for larger order systems, the program has been designed to accommodate a maximum of 80 reference points per idealization. Since there can be six degrees of freedom (3 linear and 3 angular displacements) at each point, a total of 480 degrees of freedom can exist in an idealization. An important limitation is that sufficient "displacement" and "force" boundary conditions must be applied so that no more than 238 degrees of freedom remains in the problem. A "displacement" boundary condition represents restraint against a given displacement component. A "force" boundary condition exists when a force component at a given point is known to have zero value under all load and temperature conditions. In either case, the effect of applying such a condition is to remove one equation and the corresponding unknown from the problem.

B. THEORETICAL BASIS

The theoretical basis of this program parallels, for the most part, the approach taken in the plate program (Chapter IV). The differences lie mainly in the use of three, rather than two, coordinate dimensions for each element and the fact that in the cylinder analysis the membrane and bending behaviors are incorporated in a single computational process.

It is of interest, however, to describe the analytical procedures involved in the reduction of the governing stiffness equations by virture of geometric and force boundary conditions. These procedures provide the theoretical basis for the planned extension of the program to accommodate larger order problems . In accordance with the displacement approach to matrix structural analysis, the complete set of

analysis, the complete set of force displacement equations are in general given by:

$$\left\{\begin{array}{c} P_1 \\ \hline P_2 \\ \hline P_3 \end{array}\right\} = \left[\begin{array}{c|c|c} K_{11} & K_{12} & K_{13} \\ \hline K_{21} & K_{22} & K_{23} \\ \hline K_{31} & K_{32} & K_{33} \end{array}\right] + \left[\begin{array}{c|c|c} N_{11} & N_{12} & N_{13} \\ \hline N_{21} & N_{22} & N_{23} \\ \hline N_{31} & N_{32} & N_{33} \end{array}\right] \left\{\begin{array}{c} \Delta_1 \\ \hline \Delta_2 \\ \hline \Delta_3 \end{array}\right\} - \left\{\begin{array}{c} P_1^{\alpha} \\ \hline P_2^{\alpha} \\ \hline P_3^{\alpha} \end{array}\right\} \qquad \text{(VI-1)}$$

Equation (VI-1) has been arranged and partitioned as follows:

The first partition refers to forces and displacements affected by force boundary conditions, thus $\{P_1\} = 0$.
The second partition refers to forces and displacements unaffected by either force boundary conditions or displacement boundary conditions.
The third partition contains the forces and displacements affected by displacement boundary conditions thus $\{\Delta_3\} = 0$ and $\{P_3\} =$ the reaction forces at the support points.

It is possible to reduce Equation (VI-1) so that only the unaffected applied forces and moments $\{P_2\}$, and displacements ($\{\Delta_2\}$) appear in the relationship. This is accomplished by simply removing the third partition and operating upon the remaining $[K]$ and $[N]$ matrices and thermal forces $\{P^{\alpha}\}$ as follows: The $[K]$ matrix is reduced by:

$$[K]_{RF} = [K_{22}] - [K_{21}][R_{11}]^{-1}[R_{12}] \qquad \text{(VI-2)}$$

where $[R_{11}] = [K_{11}] + [N_{11}]$

$[R_{12}] = [K_{12}] + [N_{12}]$

Similar to the reduction of the $[K]$ matrix, the $[N]$ matrix is reduced by:

$$[N]_{RF} = [N_{22}] - [N_{21}][R_{11}]^{-1}[R_{12}] \qquad \text{(VI-3)}$$

The reduction of the thermal force column is accomplished by:

$$\{P^{\alpha}\}_{RF} = \{P_2^{\alpha}\} - \left[[K_{21}] + [N_{21}]\right][R_{11}]^{-1}\{P_1^{\alpha}\} \qquad \text{(VI-4)}$$

The reduced form of Equation (VI-1) can now be written as

$$\{P_2\} = [K]_{RFT}\{\Delta_2\} - \{P^{\alpha}\}_{RF} \qquad \text{(VI-5)}$$

where $[K]_{RFT} = [K]_{RF} + [N]_{RF}$

The displacements $\{\Delta_2\}$, which are unaffected by boundary conditions, can be solved for by the expression:

$$\{\Delta_2\} = [K]^{-1}_{RFT} \left\{ \{P_2\} + \{P^{\alpha}\}_{RF} \right\} \tag{VI-6}$$

Utilizing the known $\{\Delta_2\}$ displacements, the displacements, $\{\Delta_1\}$, associated with the force boundary conditions, can be determined by :

$$\{\Delta_1\} = -[R_{11}]^{-1}[R_{12}] \quad \{\Delta_2\} + [R_{11}]^{-1} \{P_1^{\alpha}\} \tag{VI-7}$$

Having determined all the displacements, the displacements of the individual elements are established and the elemental stresses, or stress resultant forces, are computed.

If critical stresses are to be determined (i.e., if an elastic instability analysis is to be performed) $\{P_2\}$ and $\{P^{\alpha}\}_{RF}$ are set equal to zero, the $[K]_{RF}$ matrix is reduced, and an equivalent reduced $[N_{RF}]$ matrix is derived. The $[K]_{RF}$ matrix is reduced by partitioning it as follows:

$$\{P_2\} = \begin{Bmatrix} F_y \\ M_x \\ M_y \\ M_z \\ \hline F_x \\ F_z \end{Bmatrix} = \left[\begin{array}{c|c} K_{RF_{11}} & K_{RF_{12}} \\ \hline K_{RF_{21}} & K_{RF_{22}} \end{array}\right] \begin{Bmatrix} v \\ \theta_x \\ \theta_y \\ \theta_z \\ \hline u \\ w \end{Bmatrix} \tag{VI-8}$$

and,

$$[K]_{RFR} = [K_{RF_{22}}] - [K_{RF_{21}}][K_{RF_{11}}]^{-1} [K_{RF_{12}}] \tag{VI-9}$$

An equivalent reduced $[N_{RF}]$ matrix is obtained by subtracting $[K]_{RFR}$ from the reduced $[K]_{RFT}$ matrix which is obtained in a similar manner to $[K]_{RFR}$. That is, first the $[K]_{RFT}$ matrix is partitioned as shown:

$$\left\{\begin{array}{c} F_y \\ M_x \\ M_y \\ M_z \\ \hline F_x \\ F_z \end{array}\right\} = \left[\begin{array}{c|c} K_{RFT_{11}} & K_{RFT_{12}} \\ \hline K_{RFT_{21}} & K_{RFT_{22}} \end{array}\right] \left\{\begin{array}{c} v \\ \theta_x \\ \theta_y \\ \theta_z \\ \hline u \\ w \end{array}\right\} \qquad \text{(VI-10)}$$

and then reduced by the expression:

$$\left[K\right]_{RFTR} = \left[K_{RFT_{22}}\right] - \left[K_{RFT_{21}}\right]\left[K_{RFT_{11}}\right]^{-1}\left[K_{RFT_{12}}\right] \qquad \text{(VI-11)}$$

The equivalent reduced incremental matrix is obtained by

$$\left[N_{RFR}\right]_{Eq.} = \left[K\right]_{RFTR} - \left[K\right]_{RFR} \qquad \text{(VI-12)}$$

For the purpose of an elastic stability analysis, Equation (VI-1) may be restated in the reduced form as:

$$\left\{\begin{array}{c} F_x \\ F_z \end{array}\right\} = \left[\left[K\right]_{RFR} + \left[N_{RFR}\right]_{Eq.}\right]\left\{\begin{array}{c} u \\ w \end{array}\right\} - \left\{\begin{array}{c} F_x^{\alpha} \\ F_z^{\alpha} \end{array}\right\} \qquad \text{(VI-13)}$$

Setting $\left\{\begin{array}{c} F_x \\ F_z \end{array}\right\}$ and $\left\{\begin{array}{c} F_x^{\alpha} \\ F_z^{\alpha} \end{array}\right\}$ equal to zero, the matrix $\left[N_{RFR}\right]_{Eq.}$ is multiplied by the scalar λ, and Equation (VI-13) is rearranged as follows:

$$\frac{1}{\lambda}\left\{\begin{array}{c} u \\ w \end{array}\right\} = -\left[K\right]_{RFR}^{-1}\left[N_{RFR}\right]_{Eq.}\left\{\begin{array}{c} u \\ w \end{array}\right\} \qquad \text{(VI-14)}$$

The scalar λ, which is the eigenvalue, and the eigenvector, $\left\{\begin{array}{c} u \\ w \end{array}\right\}$, (which is the relative magnitude of the displacements and thus represents the buckled shape) are determined through matrix iteration.

C. ILLUSTRATIVE EXAMPLE

1. Stress Analysis for Unheated Conditions

Figure VI-2a illustrates the conditions of analysis for a ring-stiffened cylinder. The cylinder is cantilevered and subjected to an applied concentrated load at the free end. The conditions shown were duplicated in a test performed at the NACA Structures Laboratory; results of the test were described in Reference 21.

Due to symmetry, only one half the structure need be considered in analysis. The analytical idealization appears in Figure VI-2a. Rectangular plates in plane stress (Element 4) are employed in representation of the skin; the flexural stiffness of these plates has been neglected. The ring segments are axial-flexural elements (Element 2); their behavior is limited to flexure in the plane of the ring, shear, and direct axial loading. The middle line of these elements coincides with the middle surface of the skins so that the "eccentricity" is zero.

Results of the discrete element analysis, the solution obtained from beam theory, and the test data appear in Figure VI-2c. Only the longitudinal stresses in the skin are compared but comparisons of other stress components can be shown to follow the same trends and lead to identical conclusions. The beam theory results are grossly in error at all points and, in certain locations, even fail to predict the correct sign (tension or compression) of the resulting stress. The accuracy of the discrete element solution, on the other hand, is excellent at all points. Discrete element solutions to this problem have been published by other investigators (see References 22 and 23). Generally, the latter have utilized shear panels in idealization of the skins, but their results agree closely with the discrete element solution of Figure VI-2c.

2. Cylinder Thermal Stress Analysis

Anderson and Card (Reference 24) have recently described elevated temperature tests of ring-stiffened cylinders. One such test specimen is shown in Figure VI-3. Due to the imposition of heat the cylinder skin assumes the longitudinal and circumferential temperature profiles shown in Figure VI-4, resulting in a state of thermal stress. Only one-half the length of the specimen is shown since the temperatures are symmetric about ring number 5. Also, there is symmetry about the z-axis so that only one-quarter of the complete cylinder need be considered in analysis.

The analytical idealization is shown in Figure VI-5. As in the previous example, the skins are idealized with use of Element 4 while Element 2 is employed in idealization of the ring segments. In the present case, however, there is an eccentricity between the middle line of the rings and the middle surface of the skin and this was taken into account in the analysis performed. Pertinent material properties, as given in Reference 24, are listed in Figure IV-6.

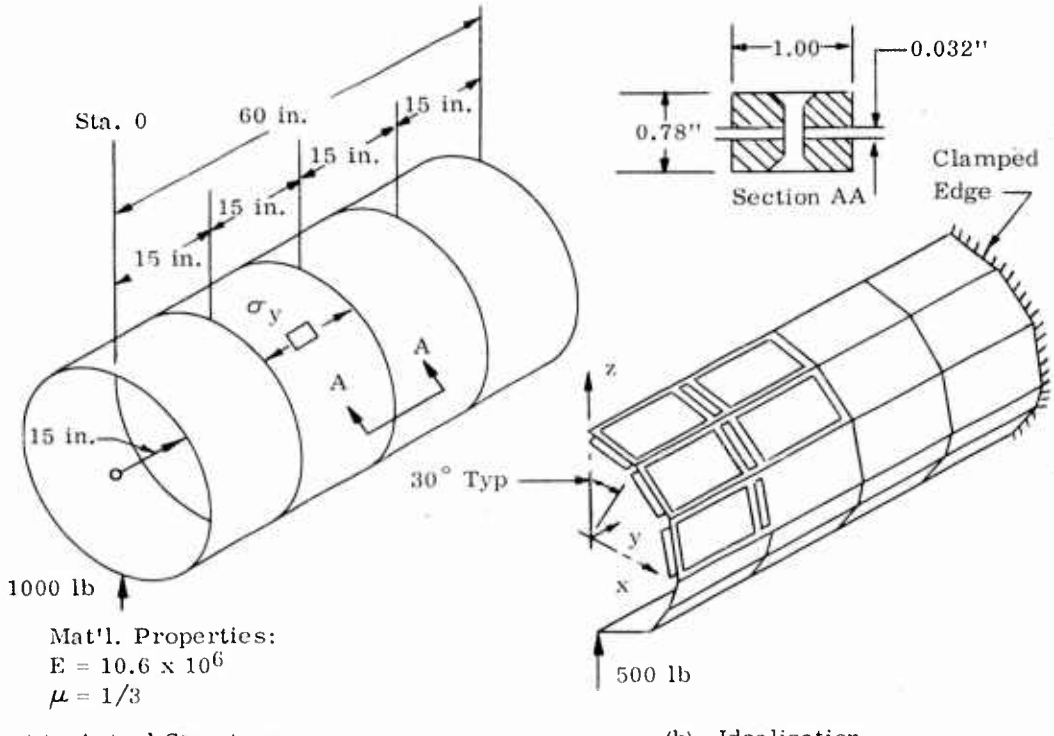

(a) Actual Structure

(b) Idealization

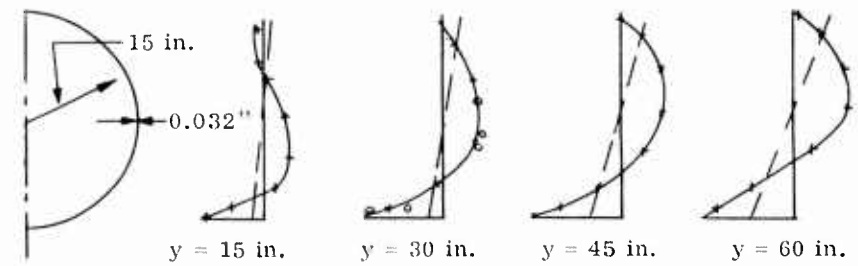

——— Discrete Element Diealization Results

- - - - - - Beam Theory

° Test Data - NACA ARR L5H23

(c) Comparison of Longitudinal Stress (σ_y) Profiles (Test versus Beam Theory versus Matrix Analysis)

Figure VI-2. Analysis of Ring-Stiffened Cylinder

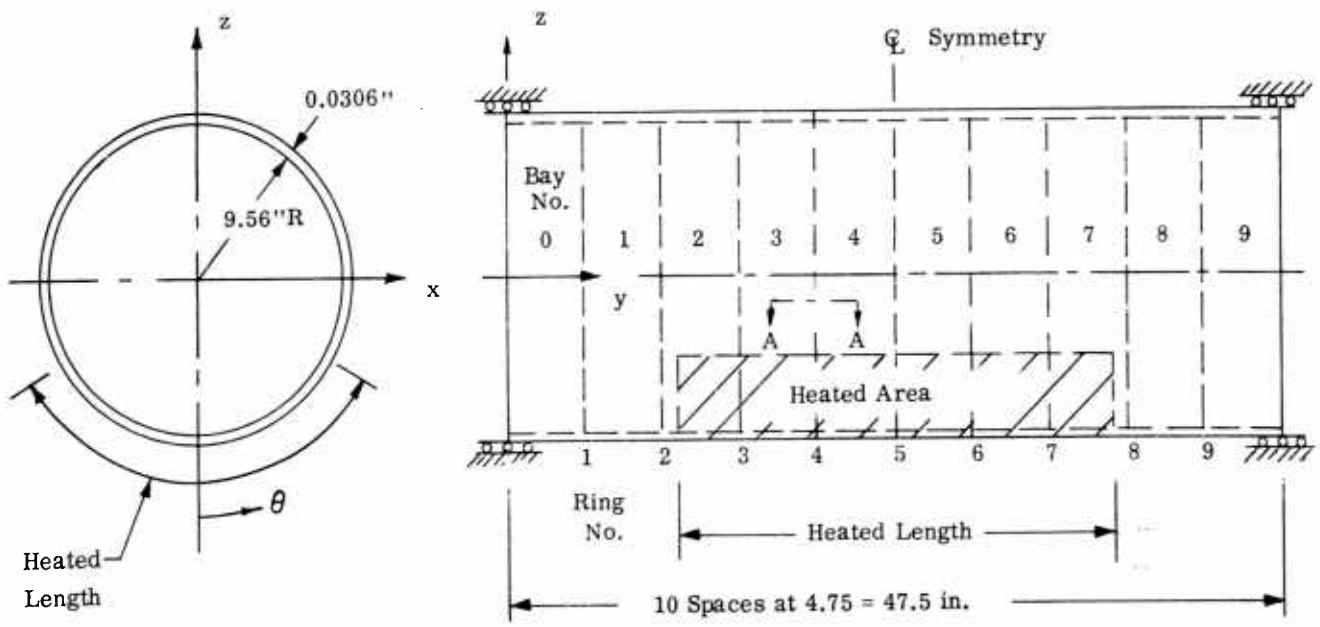

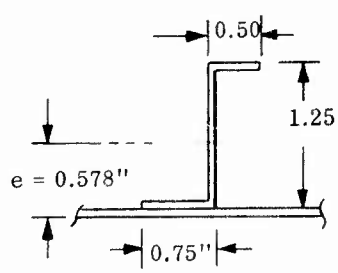

Section A-A

$I = 0.0295 \text{ in.}^4$

$A = 0.18 \text{ in.}^2$

Figure VI-3. Heated Cylinder Test Specimen

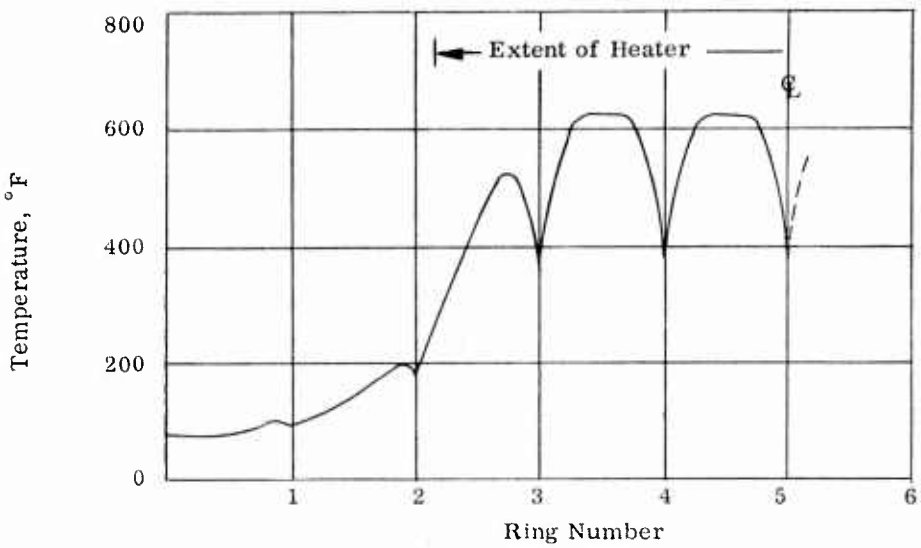

(a) Longitudinal Temperature Distribution at $\theta = 0$

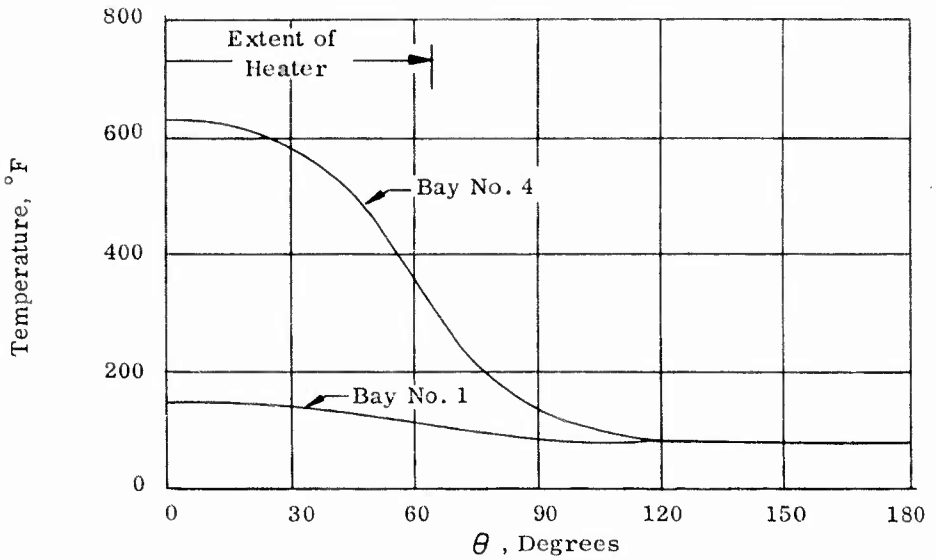

(b) Circumferential Temperature Distribution at Midbay

Figure VI-4. Heated Cylinder Temperature Distribution

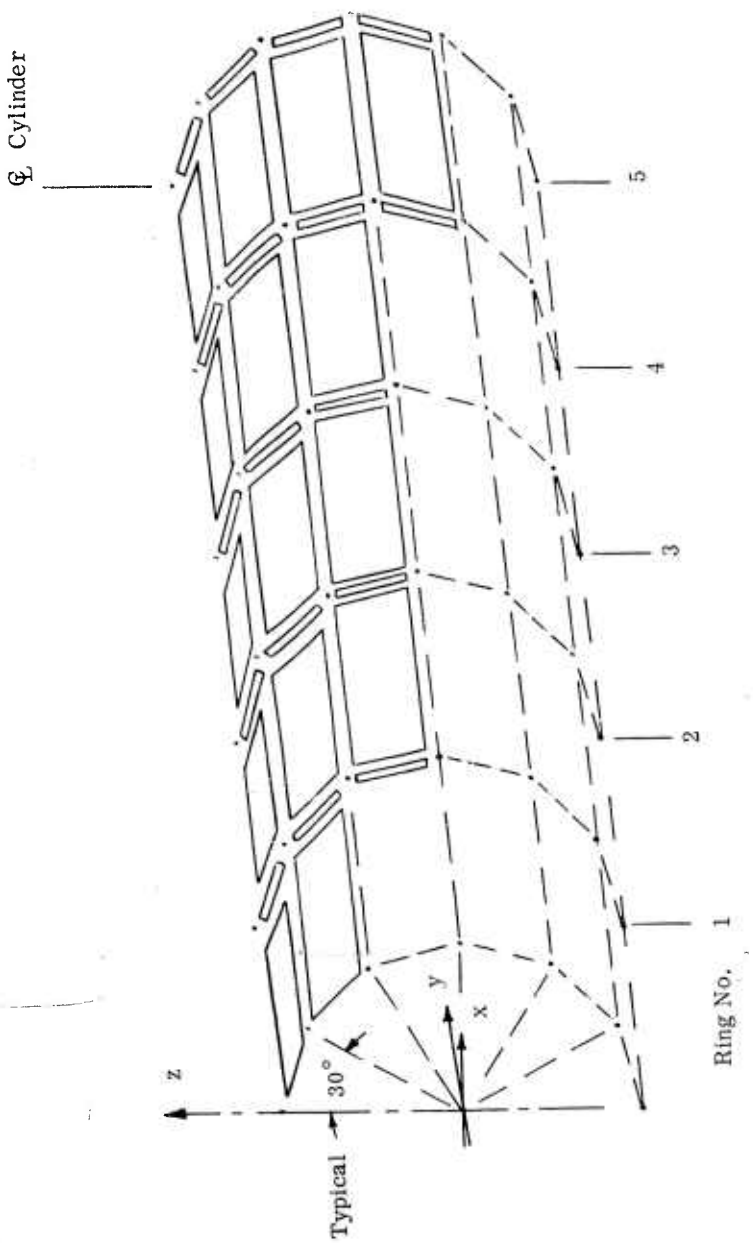

Figure VI-5. Idealization of Heated Cylinder

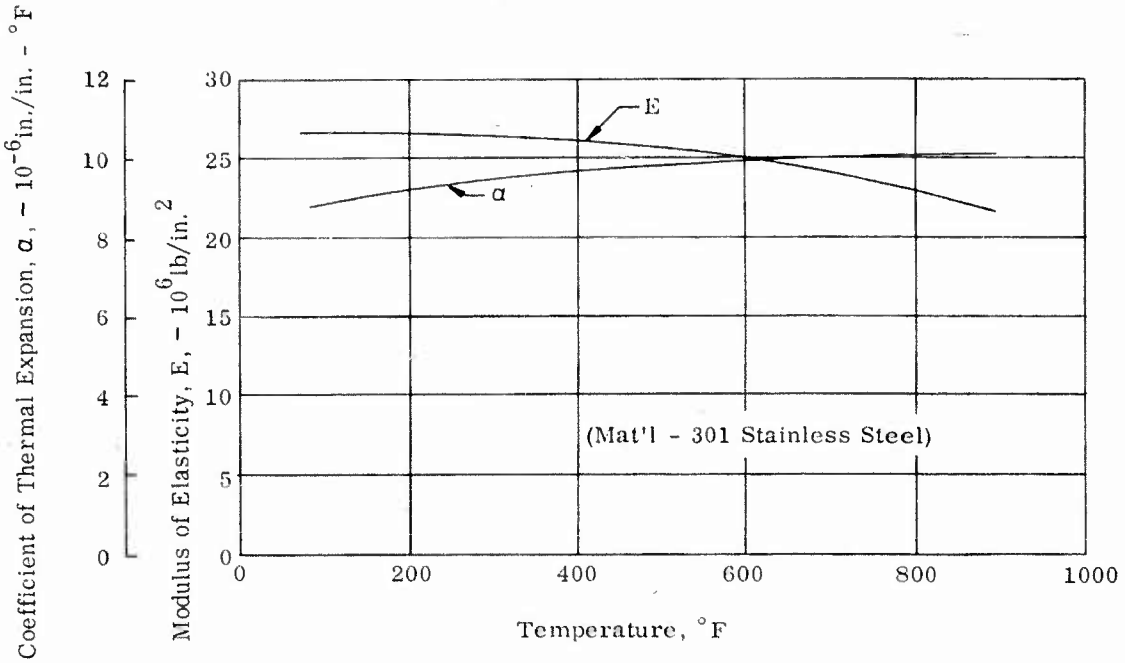

Figure VI-6. Material Properties for Heated Cylinder

The results of analysis are shown in Figure VI-7. This figure is a reproduction of the one shown in Reference 24 with the present results being given by the heavily dashed lines. As indicated the discrete element solution corresponds with test data to approximately the same extent as the analytical approach proposed in Reference 24. Elementary theory is seen to be entirely inadequate for prediction of the correct results.

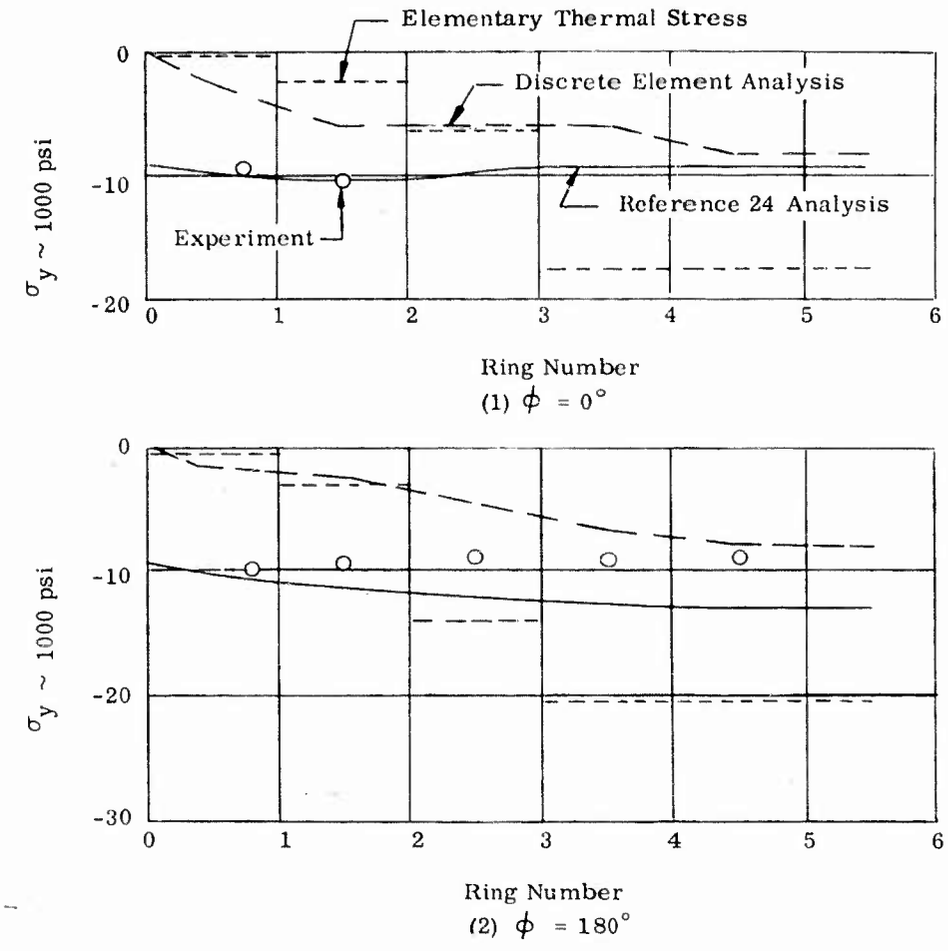

(a) Variation of axial thermal stress in longitudinal direction.

Figure VI-7. Comparison of Theoretical and Experimental Thermal Stresses

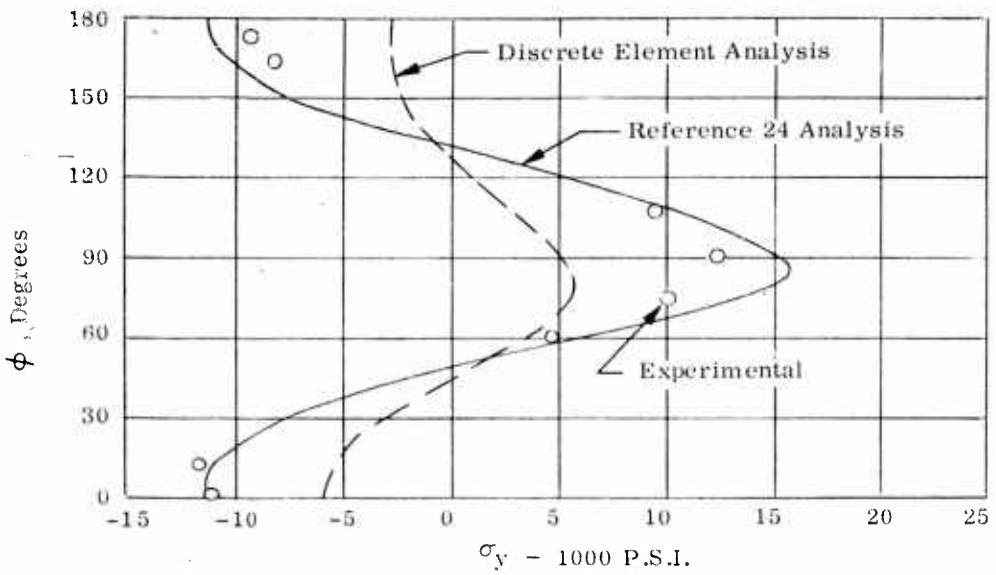

(1) Bay 1

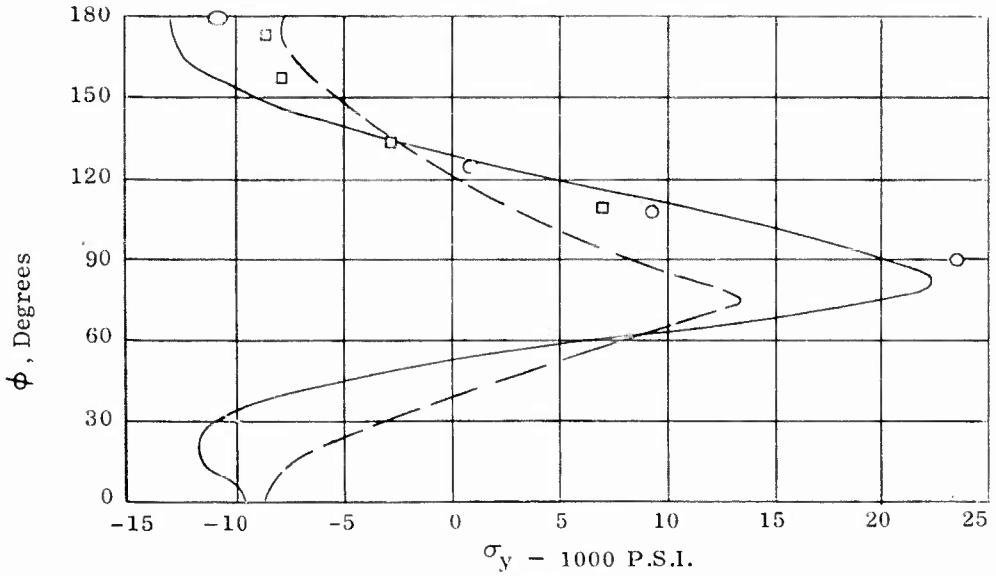

(2) Bay 4

(b) Variation of Axial Thermal Stress in Circumferential Direction

Figure VI-7. (Concl'd) Comparison of Theoretical and Experimental Thermal Stresses

CHAPTER VII

REFERENCES

1. Gallagher, R. H., and Huff, R. D., "Thermal Stress Determination Techniques for Supersonic Transport Aircraft Structures. Part I. A Bibliography of Thermal Stress Analysis References, 1955-1962" ASD TDR 63-783, Jan. 1964

2. Gellatly, R. A., and Gallagher, R. H., "Thermal Stress Determination Techniques for Supersonic Transport Aircraft Structures. Part II - Design Data for Sandwich Plates and Cylinders Under Applied Loads and Thermal Gradients," ASD TDR 63-783, Part II, Jan. 1964.

3. Turner, M. J., Clough, R. W., Martin, H. C., and Topp, L. J., "Stiffness and Deflection Analysis of Complex Structures" Journal of the Aeronautical Sciences, Vol. 23 Sept., 1956.

4. Samson, C. H., and Bergmann, H.W., "Analysis of Low-Aspect-Ratio Aircraft Structures," Journal of the Aerospace Sciences, Vol. 21, Sept. 1960.

5. Gallagher, R. H., "A Correlation Study of Methods of Matrix Structural Analysis," AGARDograph 69, Pergamon Press, Oxford. 1964.

6. Gallagher, R. H., and Padlog, J., "A Discrete Element Approach to Structural Instability Analysis," AIAA Journal, Vol. 1, June, 1963.

7. Gallagher, R. H., "Techniques for the Derivation of Element Stiffness Matrices," AIAA Journal, Vol. 1, June 1963.

8. Gallagher, R. H., and Huff, R. D., "Derivation of the Force-Displacement Properties of Triangular and Quadrilateral Orthotropic Plates in Plane Stress and Bending," Bell Aerosystems Company Report No. D2114-950005, November 1963.

9. Padlog, J., Huff, R. D., and Holloway, G., "Inelastic Behavior of Structures Subjected to Cyclic Thermal and Mechanical Stressing Conditions," WADD TR 60-271, April 1960.

10. Timoshenko, S., "Theory of Elastic Instability," McGraw-Hill Book Co., New York, 1936.

11. Hoff, N. J., "The Effects of Temperature and Time on Aircraft and Missile Structures," AFOSR TN 61-646, January 1961.

12. Scalzo, A. J., "Critical Buckling Load of Elastically Restrained Slender Struts," Machine Design, Dec. 20, 1962.

13. Klemperer, W., and Gibbons, H. B., "On Buckling Strength of Beams Under Axial Compression Bridging Elastic Intermediate Supports," ASME National Applied Mechanics Meeting, New Haven, Conn., June 1932.

14. Switzky, H., Newman, M., and Forray, M., "Thermo-Structural Analysis Manual - Volume I," ASD TR 60-517, Sept. 1960.

15. Mendelson, A., and Hirschberg, M., "Analysis of Elastic Thermal Stresses in Thin Plate with Spanwise and Chordwise Variations of Temperature and Thickness," NACA TN 3778, Nov. 1956.

16. Conway, H. D., "Stress Distributions in Orthotropic Strips," Journal of Applied Mechanics, Vol. 22, No. 3, Sept. 1955.

17. Maulbetsch, J. L., "Thermal Stresses in Plates," Journal of Applied Mechanics, Vol. 2, No. 2, June 1935.

18. Hearmon, R. F. S., "An Introduction to Applied Anistropic Elasticity," Oxford Press, 1961.

19. Krivetsky, A., "Buckling of Orthotropic Plates," Bell Aerosystems Company Report No. 7-60-941001; Dec. 1960.

20. Libove, C., and Stein, M., "Charts for Critical Combinations of Longitudinal and Transverse Direct Stress for Flat Rectangular Plates," NACA ARR L6A05, March 1946.

21. Kuhn, P., Duberg, J, and Griffith, G., "Effect of Concentrated Loads on Flexible Rings in Circular Shells," NACA ARR No. L5H 23, 1945.

22. Jensen, W. R., "On Simplified Fuselage Structures Stress Analysis," Journal of the Aeronautical Sciences, Oct. 1958.

23 Denke, P., "A General Digital Computer Analysis of Statically Indeterminate Structures," NASA TN D-1666, 1962.

24. Anderson, M. S., and Card, M. F., "Buckling of Ring-Stiffened Cylinders Under a Pure Bending Moment and a Nonuniform Temperature Distribution," NASA TN D-1513, Nov. 1962.

Aeronautical Systems Division, Flight Dynamics Lab., Wright-Patterson AFB, Ohio
Rpt. No. ASD-TDR-63-783, Part III, THERMAL STRESS DETERMINATION TECHNIQUES FOR SUPERSONIC TRANSPORT AIRCRAFT STRUCTURES. PART III - COMPUTER PROGRAMS FOR BEAM, PLATE, AND CYLINDRICAL SHELL ANALYSIS. Technical Documentary Rpt., Jan., 1964, 125 pp., incl illus., tables.

Unclassified Report

UNCLASSIFIED

1. Supersonic planes
2. Transport planes
3. Stresses
4. Thermal stresses

I AFSC Project 9056
II Contract AF33(657)-8936
III Textron's Bell Aerosystems Company, Buffalo, N.Y.
IV Gallagher, R. H.
Padlog, J.
Huff, R. D.
V ASD-TDR-63-783, Part III

This report describes computer programs developed for the analysis of heated beams, plates, and stiffened cylindrical shells. The matrix displacement approach to structural analysis, which forms the theoretical basis of these programs, is developed in detail. Derivation of new relationships employed in these programs is also detailed. The capabilities and limitations of the respective programs are outlined and illustrative applications are presented.

VI Avail. fr. DDC
VII Not Avail. fr. OTS

Aeronautical Systems Division, Flight Dynamics Lab., Wright-Patterson AFB, Ohio
Rpt. No. ASD-TDR-63-783, Part III, THERMAL STRESS DETERMINATION TECHNIQUES FOR SUPERSONIC TRANSPORT AIRCRAFT STRUCTURES. PART III - COMPUTER PROGRAMS FOR BEAM, PLATE, AND CYLINDRICAL SHELL ANALYSIS. Technical Documentary Rpt., Jan., 1964, 125 pp., incl illus., tables.

Unclassified Report

UNCLASSIFIED

1. Supersonic planes
2. Transport planes
3. Stresses
4. Thermal stresses

I AFSC Project 9056
II Contract AF33(657)-8936
III Textron's Bell Aerosystems Company, Buffalo, N.Y.
IV Gallagher, R. H.
Padlog, J.
Huff, R. D.
V ASD-TDR-63-783, Part III

This report describes computer programs developed for the analysis of heated beams, plates, and stiffened cylindrical shells. The matrix displacement approach to structural analysis, which forms the theoretical basis of these programs, is developed in detail. Derivation of new relationships employed in these programs is also detailed. The capabilities and limitations of the respective programs are outlined and illustrative applications are presented.

VI Avail. fr. DDC
VII Not Avail. fr. OTS

Aeronautical Systems Division, Flight Dynamics Lab., Wright-Patterson AFB, Ohio
Rpt. No. ASD-TDR-63-783, Part III, THERMAL STRESS DETERMINATION TECHNIQUES FOR SUPERSONIC TRANSPORT AIRCRAFT STRUCTURES. PART III - COMPUTER PROGRAMS FOR BEAM, PLATE, AND CYLINDRICAL SHELL ANALYSIS. Technical Documentary Rpt., Jan., 1964, 125 pp., incl illus., tables.

Unclassified Report

(over)

UNCLASSIFIED

1. Supersonic planes
2. Transport planes
3. Stresses
4. Thermal stresses

I AFSC Project 9056
II Contract AF33(657)-8936
III Textron's Bell Aerosystems Company, Buffalo, N.Y.
IV Gallagher, R. H.
Padlog, J.
Huff, R. D.
V ASD-TDR-63-783, Part III

This report describes computer programs developed for the analysis of heated beams, plates, and stiffened cylindrical shells. The matrix displacement approach to structural analysis, which forms the theoretical basis of these programs, is developed in detail. Derivation of new relationships employed in these programs is also detailed. The capabilities and limitations of the respective programs are outlined and illustrative applications are presented.

VI Avail. fr. DDC
VII Not Avail. fr. OTS

Aeronautical Systems Division, Flight Dynamics Lab., Wright-Patterson AFB, Ohio
Rpt. No. ASD-TDR-63-783, Part III, THERMAL STRESS DETERMINATION TECHNIQUES FOR SUPERSONIC TRANSPORT AIRCRAFT STRUCTURES. PART III - COMPUTER PROGRAMS FOR BEAM, PLATE, AND CYLINDRICAL SHELL ANALYSIS. Technical Documentary Rpt., Jan., 1964, 125 pp., incl illus., tables.

Unclassified Report

(over)

UNCLASSIFIED

1. Supersonic planes
2. Transport planes
3. Stresses
4. Thermal stresses

I AFSC Project 9056
II Contract AF33(657)-8936
III Textron's Bell Aerosystems Company, Buffalo, N.Y.
IV Gallagher, R. H.
Padlog, J.
Huff, R. D.
V ASD-TDR-63-783, Part III

This report describes computer programs developed for the analysis of heated beams, plates, and stiffened cylindrical shells. The matrix displacement approach to structural analysis, which forms the theoretical basis of these programs, is developed in detail. Derivation of new relationships employed in these programs is also detailed. The capabilities and limitations of the respective programs are outlined and illustrative applications are presented.

VI Avail. fr. DDC
VII Not Avail. fr. OTS

Aeronautical Systems Division, Flight Dynamics Lab., Wright-Patterson AFB, Ohio
Rpt. No. ASD-TDR-63-783, Part III, THERMAL STRESS DETERMINATION TECHNIQUES FOR SUPERSONIC TRANSPORT AIRCRAFT STRUCTURES. PART III - COMPUTER PROGRAMS FOR BEAM, PLATE, AND CYLINDRICAL SHELL ANALYSIS. Technical Documentary Rpt., Jan., 1964, 125 pp., incl illus., tables.

Unclassified Report

(over)

UNCLASSIFIED

1. Supersonic planes
2. Transport planes
3. Stresses
4. Thermal stresses

I AFSC Project 9056
II Contract AF33(657)-8936
III Textron's Bell Aerosystems Company, Buffalo, N.Y.
IV Gallagher, R. H.
Padlog, J.
Huff, R. D.
V ASD-TDR-63-783, Part III

VI Avail. fr. DDC
VII Not Avail. fr. OTS

This report describes computer programs developed for the analysis of heated beams, plates, and stiffened cylindrical shells. The matrix displacement approach to structural analysis, which forms the theoretical basis of these programs, is developed in detail. Derivation of new relationships employed in these programs is also detailed. The capabilities and limitations of the respective programs are outlined and illustrative applications are presented.

Aeronautical Systems Division, Flight Dynamics Lab., Wright-Patterson AFB, Ohio
Rpt. No. ASD-TDR-63-783, Part III, THERMAL STRESS DETERMINATION TECHNIQUES FOR SUPERSONIC TRANSPORT AIRCRAFT STRUCTURES. PART III - COMPUTER PROGRAMS FOR BEAM, PLATE, AND CYLINDRICAL SHELL ANALYSIS. Technical Documentary Rpt., Jan., 1964, 125 pp., incl illus., tables.

Unclassified Report

(over)

UNCLASSIFIED

1. Supersonic planes
2. Transport planes
3. Stresses
4. Thermal stresses

I AFSC Project 9056
II Contract AF33(657)-8936
III Textron's Bell Aerosystems Company, Buffalo, N.Y.
IV Gallagher, R. H.
Padlog, J.
Huff, R. D.
V ASD-TDR-63-783, Part III

VI Avail. fr. DDC
VII Not Avail. fr. OTS

This report describes computer programs developed for the analysis of heated beams, plates, and stiffened cylindrical shells. The matrix displacement approach to structural analysis, which forms the theoretical basis of these programs, is developed in detail. Derivation of new relationships employed in these programs is also detailed. The capabilities and limitations of the respective programs are outlined and illustrative applications are presented.

Aeronautical Systems Division, Flight Dynamics Lab., Wright-Patterson AFB, Ohio
Rpt. No. ASD-TDR-63-783, Part III, THERMAL STRESS DETERMINATION TECHNIQUES FOR SUPERSONIC TRANSPORT AIRCRAFT STRUCTURES. PART III - COMPUTER PROGRAMS FOR BEAM, PLATE, AND CYLINDRICAL SHELL ANALYSIS. Technical Documentary Rpt., Jan., 1964, 125 pp., incl illus., tables.

Unclassified Report

(over)

UNCLASSIFIED

1. Supersonic planes
2. Transport planes
3. Stresses
4. Thermal stresses

I AFSC Project 9056
II Contract AF33(657)-8936
III Textron's Bell Aerosystems Company, Buffalo, N.Y.
IV Gallagher, R. H.
Padlog, J.
Huff, R. D.
V ASD-TDR-63-783, Part III

VI Avail. fr. DDC
VII Not Avail. fr. OTS

This report describes computer programs developed for the analysis of heated beams, plates, and stiffened cylindrical shells. The matrix displacement approach to structural analysis, which forms the theoretical basis of these programs, is developed in detail. Derivation of new relationships employed in these programs is also detailed. The capabilities and limitations of the respective programs are outlined and illustrative applications are presented.

Aeronautical Systems Division, Flight Dynamics Lab., Wright-Patterson AFB, Ohio
Rpt. No. ASD-TDR-63-783, Part III, THERMAL STRESS DETERMINATION TECHNIQUES FOR SUPERSONIC TRANSPORT AIRCRAFT STRUCTURES. PART III - COMPUTER PROGRAMS FOR BEAM, PLATE, AND CYLINDRICAL SHELL ANALYSIS. Technical Documentary Rpt., Jan., 1964, 125 pp., incl illus., tables.

Unclassified Report

(over)

UNCLASSIFIED

1. Supersonic planes
2. Transport planes
3. Stresses
4. Thermal stresses

I AFSC Project 9056
II Contract AF33(657)-8936
III Textron's Bell Aerosystems Company, Buffalo, N.Y.
IV Gallagher, R. H.
Padlog, J.
Huff, R. D.
V ASD-TDR-63-783, Part III

VI Avail. fr. DDC
VII Not Avail. fr. OTS

This report describes computer programs developed for the analysis of heated beams, plates, and stiffened cylindrical shells. The matrix displacement approach to structural analysis, which forms the theoretical basis of these programs, is developed in detail. Derivation of new relationships employed in these programs is also detailed. The capabilities and limitations of the respective programs are outlined and illustrative applications are presented.

UNCLASSIFIED